

Significant Advances in C1 Catalysis: Highly Efficient Catalysts and Catalytic Reactions

Jun Bao*,†^{ID} Guohui Yang‡ Yoshiharu Yoneyama§ and Noritatsu Tsubaki*,§^{ID}

†National Synchrotron Radiation Laboratory, Key Laboratory of Surface and Interface Chemistry and Energy Catalysis of Anhui Higher Education Institutes, University of Science and Technology of China, Hefei 230029, P.R. China

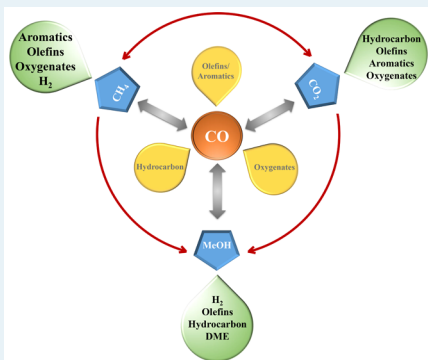
‡Institute of Coal Chemistry, Chinese Academy of Sciences, Taiyuan, P.R. China

§Department of Applied Chemistry, School of Engineering, University of Toyama, Gofuku 3190, Toyama 930-8555, Japan

Supporting Information

ABSTRACT: C1 catalysis refers to the conversion of simple carbon-containing compounds, such as carbon monoxide, carbon dioxide, methane, and methanol into high-value-added chemicals, petrochemical intermediates, and clean fuels. Because of the rising oil price and the apprehension of fossil fuel depletion in the future, C1 catalysis has been attracting widespread academic and industrial interest and became one of the most attractive research fields in heterogeneous catalysis. Especially in recent years, benefiting from advanced technology development, precise and controllable material synthesis methods, and powerful computational simulation capabilities, C1 catalysis has achieved remarkable progress in many aspects, including insights into the reaction mechanism, identification of active-site structures, highly efficient catalysts and reaction process, and the reactor designs. This Review highlights the latest developments (from 2012 to 2018) in highly efficient catalyst systems and reaction processes in this field. The content covers the catalytic utilization of the four molecules including carbon monoxide, carbon dioxide, methane, and methanol. The catalytic performances of these highly efficient systems, including activity, selectivity, and stability, are introduced in detail and compared to previously reported catalysts. Furthermore, the established relationships between reactivity and active-site structure are clarified. Finally, current challenges and perspectives for future research are discussed.

KEYWORDS: C1 catalysis, valuable chemicals, highly efficient catalysts, catalytic performance, active site



1. INTRODUCTION

C1 catalysis mainly addresses the conversion of simple molecules with one carbon atom (prominent examples are carbon monoxide, carbon dioxide, methane, and methanol) into various high-value-added liquid fuels and chemicals. The most important resources for C1 compounds are coal, natural gas, organic waste, and biomass. With strongly fluctuating prices and decreasing reserves of crude oil, C1 catalysis has been attracting widespread academic and industrial attention over the past century and has become one of the most active fields in the modern coal chemical industry and the natural gas chemical industry. Particularly in recent years, benefiting from the rapid developments of advanced analytic technologies, precise and controllable synthesis methods, and powerful computational simulation capabilities, C1 catalysis has achieved remarkable progress from fundamental studies to industrial application. Research activities related to C1 catalysis have experienced significant intensification, and the number of related publications has tremendously increased, as illustrated in Figure 1. Catalysts are the key to C1 catalysis. The development of highly efficient, low-cost catalyst systems for

the targeted synthesis of desired products under mild conditions has always been the core issue in C1 catalysis.

The conversion of syngas ($\text{CO} + \text{H}_2$) is the most important and fundamental part in C1 catalysis. Best known are the Fischer–Tropsch synthesis (FTS) and methanol synthesis, both of which are extensively applied industrially. The FTS reaction produces mixtures of hydrocarbons and oxygenated products.^{1,2} Among these, the linear paraffins and α -olefins are the main products. FTS mechanism can be described as the reductive oligomerization of CO with an exponentially decreasing total product yield with chain length, following a so-called Anderson–Schulz–Flory (ASF) distribution.^{3–6} Selectivity regulation and catalyst deactivation caused by particle sintering or coke deposition are the main challenges. Typical active metals for FTS are Fe,^{7–10} Co,^{11–13} and Ru-based catalysts; however, only Fe and Co-based catalysts are economically viable long-term. Fe-based FT catalysts can be operated in a wide temperatures range and H_2/CO ratios,¹⁴

Received: September 29, 2018

Revised: February 19, 2019

Published: February 22, 2019



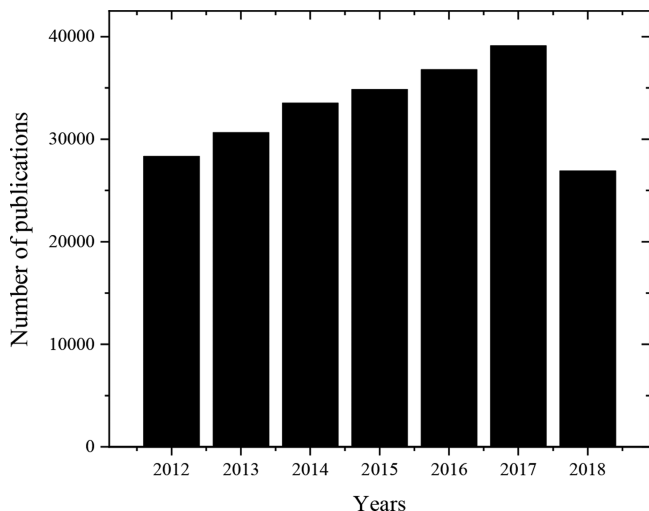


Figure 1. Increasing trend and number of publications on C1 catalysis versus years (2012–2018) extracted from the Web of Science database retrieved using the keywords “CO or syngas or CO₂ or methane or methanol”.

while Co-based FT catalysts are more efficient for the production of linear long-chain hydrocarbons.¹⁵ Synthesis of oxygenates (mainly methanol and higher alcohols) from syngas is economically favorable. Methanol synthesis from syngas has been widely commercialized and hundreds of plants are distributed around the world,¹⁶ which generally run with classic Cu/ZnO/Al₂O₃ at 493–573 K and 5–10 MPa.¹⁷ Higher alcohols (HA) can be produced directly from syngas over many different catalysts, such as Cu,^{18–21} Co,^{22,23} Mo,^{24,25} and Rh-based²⁶ systems. Despite considerable efforts on this subject, the progress achieved so far did not translate into highly efficient catalyst systems or processes that have achieved large-scale industrial application.

Methane is one of the most abundant carbon resources in the world. Over the past decades, with the discovery of more reserves of methane hydrate, shale gas, and coalbed methane, the development of highly efficient catalysts and processes for methane conversion to high-value-added chemicals and fuels has become critical. The methane molecule is thermodynamically very stable, and a high energy input is required for the activation of the C–H bond. Currently utilized commercial routes for methane activation involve the methane conversion into syngas via a reforming reaction, and the subsequent conversion into fuels or chemicals.²⁷ Methane reforming to syngas is strongly endothermic and requires temperatures above 600 °C.²⁸ The most widely used technologies include steam reforming (SRM),^{29–31} dry reforming (DRM),^{32,33} partial oxidation (POM),^{34,35} and autothermal reforming (ARM).^{36,37} The used catalysts, oxidants, H₂/CO ratio, and energetics differ between these processes.³⁸ Methane pyrolysis, nonoxidative methane dehydroaromatization (MDA), and oxidative coupling methane (OCM) are promising approaches for the direct methane conversion. However, these processes require high operation temperature and generally suffer from rapid catalyst deactivation and low product yields. The low-temperature methane conversion largely focuses on the partial oxidation of methane into valuable chemicals or fuels. The main challenge is that the selectivity for desirable products is limited because most of the products or intermediates are more reactive and more easily oxidized than methane. Despite

the numerous efforts for improving the catalysts performance and reactor design, the one-step methane conversion into chemicals and fuels is still far from the industrially required standard.

CO₂ is the most important anthropogenic greenhouse gas. In 2016, the atmospheric CO₂ level exceeded 400 ppm. Therefore, the formulation of strategies and technologies to effectively reduce CO₂ emissions has attracted great attention in the past decades. In addition to capture and sequestering, the chemical conversion and utilization of CO₂ into high-value chemicals and fuels seems to be a more attractive and promising solution toward fulfilling the requirements of sustainable processes and renewable carbon sources. CO₂ is a thermodynamically stable molecule with low reactivity. Therefore, CO₂ activation has to overcome a high barrier, and the chemical utilization of CO₂ constitutes a significant challenge. To date, very few industrial processes use CO₂ as chemical feedstock (e.g., synthesis of methanol, salicylic acid, carbonates, and urea and its derivatives).^{39–41} Methanol synthesis from CO₂ hydrogenation has attracted great attention since it is a useful strategy for CO₂ utilization and a practical approach toward a sustainable development. Several relevant catalysts have been studied, including Cu-based^{42–45} and Pd-based^{46–48} systems, which are commonly used to minimize the formation of byproducts and maximize both methanol yield and selectivity. Among these, the Cu/ZnO catalysts are well-known because of their high activity and selectivity. A recent review described the general aspects of CO₂ hydrogenation to methanol, covering catalyst performance, both reaction mechanism and kinetic, and technological advances.⁴⁹ CO₂ methanation represents a further promising route for the utilization of CO₂, which shows several advantages over other chemicals. The formed methane can be directly injected into the pipelines of natural gas and can be used as feedstock to make various chemicals. In addition, CO₂ methanation can be operated under atmospheric pressure and relatively low reaction temperature. Supported Ni-based and noble metal catalysts have been widely employed for CO₂ methanation.^{50–52} Their catalytic performances depend on various parameters, such as the effects of supports and promoters, the nature of the active phase, and synthesis methods.⁵³

Methanol is an important raw material for the synthesis of various chemicals such as acetic acid, dimethyl ether, formaldehyde, and hydrocarbons (gasoline or olefins/propylene). Among these, methanol to olefins (MTO) has attracted particular interest as lower olefins, such as propylene and ethylene, which are key reaction intermediates for the production of many useful chemicals and polymers. Since MTO was first proposed by the Mobil Corporation in 1977,⁵⁴ significant progress has been made in the catalyst synthesis, reaction mechanism, process research, reactor design, and commercialization development. The world's first 600 000 ton/year MTO unit was started in 2010 by the Dalian Institute of Chemical Physics (DICP), which represented a milestone and a crucial step toward the production of lower olefins from coal. Recently, a thorough review summarized the general aspects of MTO technology from fundamentals to commercialization.⁵⁵ Methanol steam reforming (MSR) is a further important application in the context of methanol-based energy-storage systems, which can provide high-pure hydrogen for fuel cells. The suppression of CO and the improvement of low-temperature activity remain major challenges.^{56,57} A number of

promising MSR catalysts are currently available. The most common catalysts are Cu-based systems due to their high activity and selectivity.^{58–60} However, these catalysts suffer from deactivation due to the change of oxidation state, catalyst sintering, and coke deposition. In contrast, group 8–10 transition metal catalysts are more stable and offer similar selectivity.^{61–64} However, their activities are generally lower than those of Cu-based catalysts.

A schematic diagram of C1 catalysis is shown in Figure 2. In the framework of C1 catalysis, syngas conversion forms the

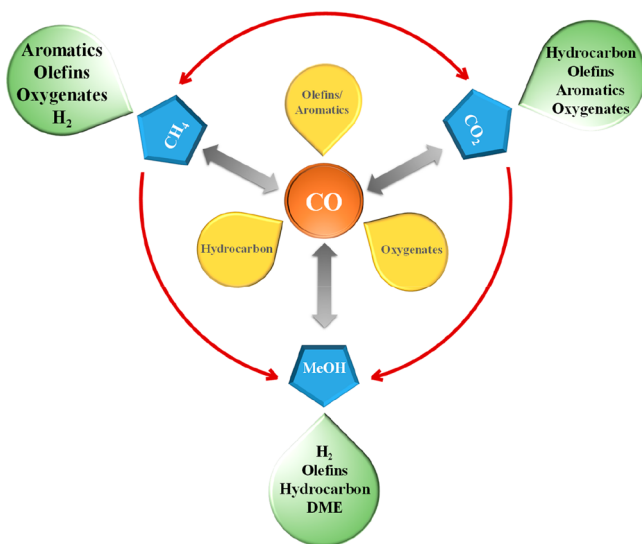


Figure 2. A schematic diagram of C1 catalysis.

basis and has achieved great success from fundamental studies to commercial application. Methanol is an important building block and represents the indirect conversion route. The conversions of CH_4 and CO_2 have attracted great attention over the past decades. However, only few of these processes have been commercialized. CO and methanol act as important intermediates in the conversion of CO_2 and CH_4 . Over the past decades, numerous reviews have been published on various aspects of C1 catalysis, covering the reaction mechanism, the type of catalyst and its synthesis, reactor selection and design, process demonstration, and commercialization. In general, these reviews have only focused on a specific C1 molecule or a specific type of catalytic reaction; however, few reviews provided a comprehensive overview of C1 catalysis as a whole. In contrast to the perspectives of previous reviews, this Review highlights the latest developments in highly efficient catalyst systems and new reaction processes in C1 catalysis. The content covers the catalytic utilization of four C1 molecules (CO , CH_4 , CO_2 , and CH_3OH) and provides an overview of the latest developments of catalysts throughout the whole C1 field. This Review is mainly based on several considerations. New catalyst systems trigger intensive research on the synthesis-structure–function relationship that enables an in-depth understanding of the reaction mechanism, which is essential for the design of next-generation catalysts. Furthermore, highly efficient catalysts or reaction processes are of great interest for potential industrial application. In addition, many reactions in C1 catalysis are closely related and often have similar elemental components and active-site structures. As an instance, the widely used Cu-based catalysts for CO hydrogenation have also been applied

to the activation of CO_2 . Therefore, a comprehensive understanding of the whole picture of the field may be helpful. The catalytic performances and established structure–performance relationship of new systems have been introduced in detail and compared to previously reported catalysts. The challenges faced and future prospects have also been discussed. Not all reactions are introduced in this Review, such as the syngas to methanol and MTO. The former has achieved important progress for the establishment of the exact nature of active sites in the past few years;^{65–67} however, no substantial improvement has been reported in the catalyst. For MTO reaction, the present and most active catalyst is still SAPO zeolite, the general aspect of which has already been summarized by several reviews.^{55,68} In addition, the photoelectric reduction of CO_2 is also not addressed, which is a very active field and numerous relevant reviews have been published recently.

2. CO CONVERSION

2.1. Syngas to Hydrocarbons via FTS. FTS is a commercially proven and economically viable approach to convert low-value biomass, coal, and natural gas into high-value chemicals and fuels.^{69–71} It has been developed for more than 80 years and is the core reaction of C1 catalysis. Co, Fe, Ni, and Ru are all active in FTS, but only Co and Fe are used in industry. An overly broad product distribution due to the ASF law and catalyst deactivation are the two main issues with the FTS. In recent studies, much attention has been paid to the development of various novel synthesis methods to obtain desired structural properties. A successful example has been reported by Hutchings et al.⁷² They first used gas antisolvent precipitation (GAS) to prepare a common $\text{Co}-\text{Ru}/\text{TiO}_2$ catalyst with high Co loading (20 wt %), high Co dispersion (3.9%), good Co reducibility, and intimate contact between Co and Ru. The technique uses dense gases near or above their critical point as antisolvents to precipitate a substrate that is insoluble in supercritical fluid from the solvent-miscible solution. Since it enhanced the ability of Ru to catalyze the hydrogenolysis of carbonaceous deposits, while reducing surface oxygen, the catalyst achieved a promising selectivity (>85%) for C_{5+} products with a CO turnover of ca. 4.5×10^{-5} mol $\text{CO g}^{-1}\text{s}^{-1}$ at 210 °C and 20 bar, which is much higher than comparable catalysts prepared via wet impregnation. In addition to its relationship with the supercritical deposition technique, the main advantage of GAS is to enable higher metal loadings, lower operating pressures and temperatures, as well as less complex and cheaper metal salts.

The direct synthesis of gasoline-range isoparaffin (C_5 – C_{11}) via FTS is a typical tandem reaction. An active catalyst has two types of active sites: FTS sites and acidic sites.⁷³ The FTS sites convert syngas to linear hydrocarbons, which then migrate to acidic sites for further hydrocracking/isomerization to branched hydrocarbons. The most-used bifunctional catalysts are prepared via simple mixing of the FTS catalyst and the zeolite catalyst. The randomly distributed active sites on the surface generate a large amount of reaction intermediates (i.e., linear hydrocarbons), which may leave the catalyst directly without further reaction at the acidic site and consequently decrease the selectivity of target products. To overcome this challenge, Tsubaki et al.⁷⁴ proposed the novel concept of the bifunctional capsule catalyst. Here, the catalyst has a specific core–shell structure, in which the core and shell are FTS catalysts and zeolite membrane, respectively. As illustrated in

Figure 3, syngas first passes through the zeolite shell to reach the core, where it forms linear paraffins via FTS. All

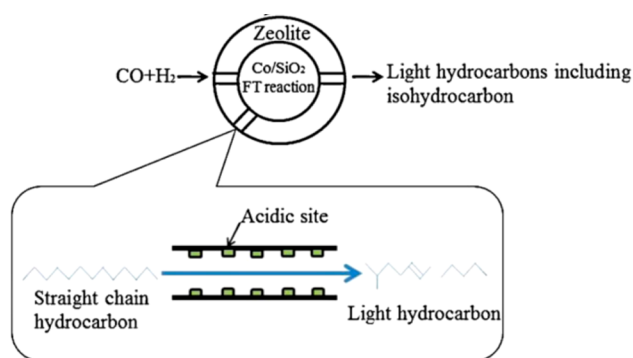


Figure 3. Schematic image of the actions of a capsule-like catalyst in the FTS reaction

hydrocarbons must diffuse through the zeolite pores before leaving the catalyst, all of which have a very good chance to be cracked and isomerized at the acidic sites of zeolite. The synthesized catalyst based on this strategy showed high selectivity toward isoparaffins compared to a conventional hybrid catalyst (Figure 4). The formation of C_{12+} hydrocarbons was completely suppressed and the middle isoparaffins became the major products. Furthermore, a desirably low selectivity for methane was also realized. Khodakov et al.⁷⁵ reported a nanosized Co@SiO₂ with a similar capsule-like structure (a so-called nanoreactor), which consists of Co

nano-particles (2–4 nm) encapsulated by nanosized porous silica spheres. Because of the high cobalt loading (50 wt %) and limited nanoreactor diameter, the nanoreactor exhibited a several times higher FT reaction rate and much narrower hydrocarbon distribution than that of the Co/SiO₂ catalyst synthesized via impregnation. The encapsulation of cobalt nanoparticles into nanosized porous silica nanoreactors also prevented the aggregation of cobalt nanoparticles, thus improving their stability. This new concept provides a tailored and confined reaction environment that offers spatial confinement effects and shape selectivity. It can be extended to various catalytic reactions with desired product distribution by varying both shell and core components.

Hierarchical zeolites, which contain both micropores and mesopores, have received strong attention in recent years because they combine the advantages of crystalline zeolites (strong acidity and high stability) with those of amorphous mesoporous materials (high mass transfer efficiency). Wang et al.^{76–78} reported a series of studies on mesoporous-zeolite-supported catalysts for FTS. Recently, the authors demonstrated that the use of mesoporous H-ZSM-5, instead of the microporous H-ZSM-5, can suppress the production of lighter hydrocarbons (CH_4 and C_{2-4}) and significantly increased the selectivity to C_{5-11} hydrocarbons.⁷⁹ The fabricated Co/H-meso-ZSM-5-0.5 m catalyst exhibited a 70% selectivity to C_{5-11} hydrocarbons and achieved a C_{iso}/C_n ratio of 2.3 under mild conditions (513 K, 2.0 MPa, $F = 20$ mL/min and $H_2/CO = 1$). The selectivity to C_{5-11} hydrocarbons was about 50% higher than the maximum expected by the ASF law (ca. 45%). The mesoporosity and Brønsted acidity are the key factors in controlling the hydrocracking reactions and determining product selectivity in FTS.

More recently, a significant discovery reported by Li et al.⁸⁰ indicated that the selectivity of FTS products can be tuned by only varying the crystallite sizes of confined cobalt nanoparticles without any other modification. The authors synthesized uniformly sized cobalt nanocrystals that were embedded into mesoporous SiO₂. By enlarging cobalt crystallites from 7.2 to 11.4 nm, the TOF value increased from 3.9×10^{-2} to $6.4 \times 10^{-2} s^{-1}$, and the major product changed from diesel-range hydrocarbons (66.2% selectivity) to gasoline-range hydrocarbons (62.4% selectivity). This phenomenon differs from previous reports: that is, larger Co nanoparticles generally promote the carbon-chain growth and thus contribute to the formation of heavier hydrocarbons.^{81,82} Detailed characterizations showed that the cobalt nanocrystals with small size are conducive to the adsorption of active C* species. The confined mesoporous structure inhibited the aggregation of cobalt nanocrystals and the escape of reaction intermediates, enabling higher selectivity toward heavier hydrocarbons. The discovery provides new understanding of the structure–activity relationship for FTS and also suggests a very simple approach for tuning the complex FTS product selectivity.

In a very recent work, Tsubaki and Wang et al.⁸³ achieved a breakthrough in FTS. The authors developed an integrated catalytic system that only uses mesoporous Y-type zeolite-supported cobalt catalysts and selectively synthesized three distinct types of liquid fuels (gasoline, jet fuel, and diesel fuel) without subsequent hydrorefining post-treatments of Fischer–Tropsch waxes. By tuning the acid properties and porosity of zeolites, the selectivities for gasoline, jet fuel, and diesel fuel reached 74, 72, and 58%, respectively, at 2.0 MPa, 523 K, $H_2/F = 10$ g·h·mol⁻¹.

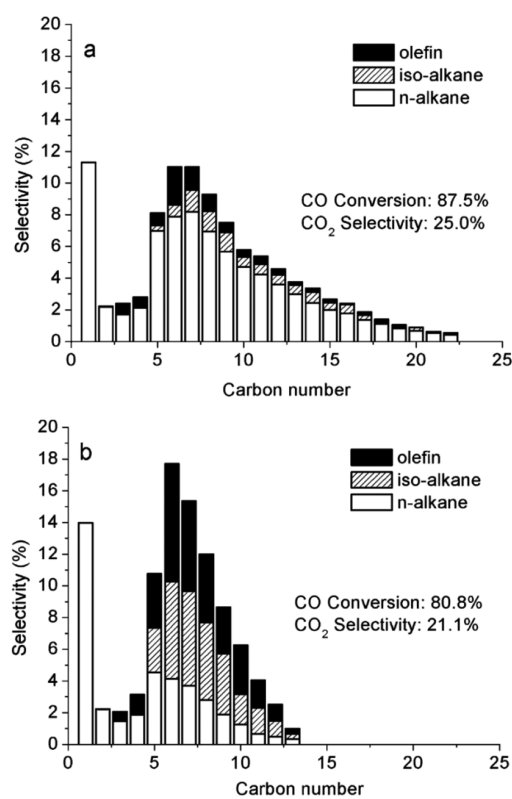


Figure 4. Product distributions of FTS over (a) Co/SiO₂ and (b) a capsule catalyst with an H- β shell (10 wt % H- β). Reaction conditions: $T = 538$ K, $P = 1.0$ MPa, molar ratio of $H_2/CO = 2.2$, $W_{core\ catalyst}/F = 10$ g·h·mol⁻¹.

$\text{CO} = 1.0$ and $W_{\text{cat}}/F = 10 \text{ g h}^{-1} \text{ mol}^{-1}$. The obtained fuels can meet strict criteria (such as the octane number or cetane number) for the corresponding combustion engines. The authors also built a new product-distribution model for bifunctional catalysts. They proposed that the chain growth probability and cracking contribution degree are the two central parameters and should be rationally controlled to enhance the specific-range products.

Compared with Co-based catalysts, Fe-based FT catalysts exhibit some superior properties, such as low price, wide availability, and suitability for CO-rich syngas derived from biomass or coal. The main challenge for Fe-based catalysts is to overcome the high deactivation rates caused by carbon deposition, catalyst sintering, and Fe phase changes due to the transformation of Hägg carbide phase into oxides and/or inactive carbides during activation and/or reaction.^{84–87} Unsupported Fe catalysts, in some cases, exhibit high FT performance;⁸⁸ however, they are generally mechanically unstable. Supported Fe catalysts have a high dispersion of the active phase and resist mechanical degradation. However, research with regard to supported Fe catalysts has had limited success, because the strong Fe oxide-support interactions impede the conversion of Fe oxide into the active Fe carbide phase.⁸⁹ To minimize the support interaction with metal oxides, Hecker et al.⁹⁰ used Si-doped $\gamma\text{-Al}_2\text{O}_3$ (AlSi) materials with superior thermal stability but weak interactions with metal oxides. The strategy has been successfully applied for the development of highly efficient supported Fe catalysts for the production of lower olefins from syngas⁹¹ (this will be introduced further below). The obtained Fe/Cu/K catalyst (100Fe/7.5Cu/4K/150Al₂O₃) displayed very active and stable FT performance under typical FTS conditions (2.1 MPa, 260 °C, and H₂/CO = 1). The reaction rate constants k_{cat} and k_{Fe} (based on per gram Fe) reached up to 350 mmol (H₂+CO)/g_{cat}/MPa/h and 878 mmol (H₂+CO)/g_{Fe}/MPa/h, respectively, which is about 2–7 times higher than any previously reported supported Fe catalyst and is consequently comparable to the best unsupported Fe catalysts. More importantly, the catalyst was extremely stable, and its activity and productivity increased up to 700 h. This excellent performance is a result of using the AlSi support. Its large pore diameter and high pore volume facilitated a high loading of Fe (40%), and its unusually high thermal stability (pretreated at 1100 °C) supplied the material with a small number of acid sites and weak interactions between metal oxide and support, which are desirable properties for Fe-based FT catalysts.

Oxide supports, such as ZnO, SiO₂, $\gamma\text{-Al}_2\text{O}_3$, and TiO₂, help to form mixed oxides that are difficult to be reduced and therefore inactive for FTS.^{92,93} Alternatively, carbon materials, such as carbon nanotubes, carbon nanofibers, and carbon sphere, have been used as supports for FTS catalysts.^{85,94} In general, carbon-supported catalysts are prepared by a multistep process that includes the precursor carbonization, the support activation, the deposition of active components, and thermal treatment. This process is usually discontinuous, and the dispersion of the active species is often compromised, especially at high loading. Gascon et al.⁹⁵ described a simple, tunable, and scalable MOF-mediated synthesis method for the production of highly dispersed Fe carbides embedded in porous carbon material. The intimate contact between C and Fe enabled a very high carbidization degree of Fe. Furthermore, high Fe loading (>40 wt %) can be realized via optimal dispersion of Fe active phase ($d_{\text{p,Fe}} < 4 \text{ nm}$). The

spatial confinement caused by encapsulation minimized the aggregation and oxidation of the active Hägg Fe carbide phase. These features resulted in high activity and superior stability. The reported Fe time yield (FTY, mol of CO converted to hydrocarbons, excluding CO₂) and catalyst productivity (volume of CO converted per mass of catalyst) for FTS reached $4.38 \times 10^{-4} \text{ mol}\cdot\text{g}_{\text{Fe}}^{-1} \text{ s}^{-1}$ and $6.9 \text{ L}\cdot\text{kg}^{-1} \text{ s}^{-1}$, respectively, at 20 bar, 613 K, H₂/CO = 1 and 30 000 h⁻¹ GHSV. This is about 1–2 orders of magnitude higher than commercial benchmark catalysts (i.e., the well-known Sasol and Ruhrchemie catalysts). The catalyst was also very stable after more than 200 h reaction even at a high space velocity of 70 000 h⁻¹ and low conversion levels.

2.2. Syngas to Olefins via FTS. Lower olefins (C₂–C₄) are key chemical feedstock for the synthesis of various products such as solvents, polymers, cosmetics, detergents, and drugs. FTS is the only effective technology to date that offers a direct route (i.e., without intermediate steps) for the conversion of syngas into lower olefins, the so-called Fischer–Tropsch to olefins (FTO).^{96,97} For industrial application, this technology remains limited due to the low olefin selectivity, high methane selectivity, and serious carbon deposition. These drawbacks are a result of the FTS reaction mechanism. Due to the limitation of the ASF law, the maximum selectivity to C₂–C₄ (including olefins and paraffins) reaches only 58%.⁹⁶ The key challenge for the FTO reaction is to precisely control the C–C coupling while inhibiting both methane formation and over hydrogenation. Recently, Bao et al.⁷⁰ achieved a landmark breakthrough in this field. The authors reported a bifunctional catalyst named Oxide-Zeolite (OX-ZEO), which contained an oxide (ZnCrO_x) and a mesoporous SAPO zeolite (MSAPO). ZnCrO_x activates the CO and H₂, forming the CH₂ species, and subsequent ketene (CH₂CO). The ketene diffuses to the MSAPO zeolite where it is converted to lower olefins through C–C coupling within the confined environment. The catalyst exhibited very good selectivities to C₂–C₄ (80%) and C₂–C₄ (94%) with only 2% methane at a CO conversion of 17% under industrial conditions (400 °C, 25 bar) and catalyst lifetime exceeding 110 h (Figure 5). The use of metal oxide, instead of metal catalysts for CO activation, prevents the polymerization of CH_x species by forming ketene via CO

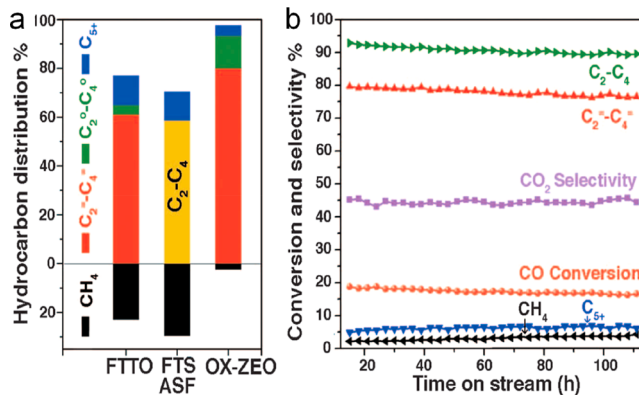


Figure 5. (a) Hydrocarbon distribution in OX-ZEO compared to that reported for FTTO (4) and that in FTS predicted by the ASF model for a chain growth probability of 0.46. The yellow bar represents the selectivity of C₂–C₄ hydrocarbons. (b) Stability test of a composite catalyst with ZnCrO_x/MSAPO ratio = 0.9 at 6828 mL/h·g_{cat} and H₂/CO of 2.5.

insertion. Most importantly, by separating the CO activation and C–C bond coupling, the ASF distribution in the FTO could be successfully circumvented. This led to the surprisingly high selectivity of 80% for lower olefins. The new process enables a new avenue for the development of FTO technologies, which is of great interest to both academia and industry. Consequently, it became a serious competitor for other industrial processes such as MTO.^{55,98} According to published reports (http://www.sohu.com/a/77368775_131990), the relevant industrialization research has already made important progress.

Based on the above, Bao et al.^{70,99} further improved the selectivity for ethylene by employing a ZnCrOx-mordenite (MOR) OX-ZEO catalyst. The ethylene selectivity alone reached up to 73% among other hydrocarbons at a CO conversion of 26% under 360 °C and 2.5 MPa, which far exceeds those obtained by any other direct conversion of syngas or multistep conversion of methanol-to-olefin. Mechanistic studies indicated that the highly selective pathway for the syngas-to-ethylene conversion was realized via a ketene intermediate rather than methanol over the active sites within the 8-membered ring (8MR) side pockets of MOR. This work provides substantial evidence for a new syngas chemistry via ketene as the key intermediate, which enables a very high ethylene selectivity. The design concept, catalyst, and reaction mechanism of the novel OX-ZEO differ from conventional FTS. This process can be extended to produce C₅₊ hydrocarbons and aromatics.^{100,101}

In addition to the OX-ZEO process, the combination of methanol-synthesis and MTO process using a bifunctional catalyst has also been reported. Wang et al.¹⁰² suggested this as an effective approach to realize the direct and highly selective synthesis of olefin from syngas. The authors integrated the methanol synthesis catalyst Zr–Zn oxide and the MTO catalyst H-SAPO-34, and achieved a promising 74% selectivity toward C₂–C₄ lower olefins at a CO conversion of 11% under typical MTO conditions (400 °C and 10 bar, with H₂/CO = 2:1). The catalyst stability was maintained after 100 h of reaction. The control of the hydrogenation ability and the micro- to nanoscale proximity between the two components in the bifunctional catalyst are crucial for obtaining high C₂–C₄ olefin selectivity. Although in the combined processes the presented single-pass CO conversion to olefins (~10%) is insufficient to compare to the two-stage MTO reaction, the work demonstrates the feasibility and potential of the combined processes for industrial application.

In addition to novel bifunctional catalysts, recent studies on conventional cobalt- and iron-based catalysts have also achieved important progress. Cobalt-based FT catalysts preferably produce C₅₊ linear alkanes and the formation of Co₂C is known to cause the catalyst deactivation in FTS.^{103–106} However, recent work by Sun et al.¹⁰⁷ challenged this assumption. The authors reported that a Co₂C quadrangular nanoprism catalyst displayed an unusual catalytic performance for the FTO reaction. The selectivity for lower olefins reached 60.8% C with only 5.0% methane selectivity at a CO conversion of 31.8% and under very mild reaction conditions (1 bar, 250 °C, H₂/CO ratio of 2). The ratio of desired unsaturated hydrocarbons to low-valued saturated hydrocarbons in the C₂–C₄ products reached as high as 30. The catalyst enabled the use of biomass- or coal-derived syngas with low H₂/CO ratios. As the H₂/CO ratio decreased from 2 to 0.5, methane selectivity further decreased to 2.4% C, and the

olefin/paraffin ratio in the C₂–C₄ increased to 51; however, the selectivity of lower olefins remained unchanged (45.1% C). Detailed characterization results and DFT calculations indicated that the preferentially exposed {020} and {101} facets played a key role for the synthesis of olefin and the inhibition of methane formation. This finding indicates Co₂C nanoprisms as a promising new catalyst system for the direct conversion of syngas to lower olefins.

In contrast to cobalt catalysts, iron FT catalysts disfavor the competing methane formation, and catalyze the water–gas shift (WGS) reaction, which enable the use of CO-rich syngas. Unsupported bulk Fe and supported Fe catalysts have both advantages and disadvantages, as discussed above. In most cases, supported Fe catalysts show an inverse relationship between activity and selectivity.¹⁰⁸ The reason could be attributed to the fact that the supports favor the strong interaction between Fe oxide and support, and associated low reducibility to active Fe carbides. De Jong et al.¹⁰⁹ first introduced the idea to use support materials that are weakly interactive toward Fe. α -Alumina (α -Al₂O₃) and carbon nanofiber (CNF) were used as supports to prepare supported Fe oxide catalysts using ammonium iron citrate as precursor. The catalysts showed a high selectivity for lower olefins (~60% C), while methane selectivity is <25% C. The catalyst was stable after a 60 h reaction, which fully meets the requirements for the application of these catalysts in fluidized-bed reactors; this method therefore shows industrial potential.

2.3. Syngas to C₂₊ Oxygenates via FTS. C₂₊ oxygenates, represented by higher alcohols (C₂–C₅), have numerous applications as hydrogen carriers, fuels, precursors for important platform chemicals, and reagents for the synthesis of plasticizers and detergents.^{110–112} The direct synthesis of C₂₊ oxygenates from syngas is a prime example for the required synergy between proximate catalytic sites with different functionality. Moreover, it shows a more complex reaction mechanism than FTS as both dissociative activation and nondissociative insertion of CO are required to produce C₂₊ oxygenates.^{16,113} Unlike for Cu-catalyzed methanol synthesis or for FTS of hydrocarbons with Co- or Fe-based catalysts, because of the complexity of the reaction, none of the catalysts or processes developed for higher alcohol synthesis (HAS) to date feature sufficient performance to justify their industrial commercialization. Consequently, relevant research experienced an intensification over the last decades. Developing solid catalysts with sufficient selectivity and yields to realize the commercial-scale synthesis of HAS remains a major challenge.

Generally, monometallic catalysts have a high atom utilization efficiency. However, this kind of catalyst is not attractive because of the bifunctionality requirement for HAS reaction. Four different metals (including Mo, Rh, Co, and Fe) have been described as monometallic HAS catalysts.^{16,113} These transition metals typically have two or more oxidation states, thus forming a dual active site (i.e., metal–oxide) for HAS. Among these, the Co-based metal-oxide pair (Co⁰–Co²⁺) recently attracted wide attention. Li et al.²² synthesized a highly active and stable Co–Co₂C catalysts for the synthesis of high alpha-alcohols. The CO conversion was 25.3% with an alcohol selectivity of 37.0% at 3.0 MPa, 493 K, H₂/CO = 2.0, and a total flow rate of 33.6 mL min^{−1}. More importantly, among the alcohol products, the fractions of ethanol, C₂–C₅ linear alpha-alcohols, and C₆–C₁₈ linear alpha-alcohols reached 13.0, 60.9 and 26.1%, respectively. The Co₂C and the interface between Co metal and Co₂C are essential for the

synthesis of high alpha-alcohols from syngas. The Co metal is responsible for the dissociative adsorption of CO and subsequent carbon-chain growth, whereas the noble-metal-like Co_2C is efficient for the nondissociative adsorption of CO. Their synergistic effects are responsible for the synthesis of alcohols. Similar conclusions were drawn by Ding and Sun et al.^{114,115} In addition, it has been proposed that the Co_2C nanocrystals with specific exposed facets may also act as a new type of active dual-sites for the synthesis of oxygenates.²³

Compared with monometallic catalysts, the widely reported bimetallic catalysts show significantly higher performance for HAS due to the required synergism effect.¹¹³ Among the reported systems, Co–Mo and Co–Cu bimetallic catalysts offer the best potential.^{116–123} Although it has been reported that intimate contact between metal components is important to achieve satisfactory selectivity, catalyst preparation methods generally result in metal segregation and typically form copper oxide during activation treatment, which limits metal intimacy. De Jongh et al.¹²⁴ adopted a combined approach, informed by computational design and controlled synthesis, and developed a highly efficient bimetallic Co–Cu catalyst for HAS. The DFT coupled to a microkinetic model predicted that the ideal catalyst surface for the synthesis of C_{2+} alcohols is a CuCo alloy phase with Co-rich compositions, in which no segregated Cu atoms exist. Based on this prediction, a novel synthesis route for CuCo catalysts aimed to achieve superior alloy formation was developed, which is based on the exsolution of metal nanoparticle from a molybdate precursor compound. The crystalline structure of the alloy phase can accommodate Cu^{2+} and Co^{2+} cations in a wide range of compositions. The obtained Cu–Co catalysts showed superior performance for high alcohols. At a Cu/(Cu+Co) ratio of 0.3, the selectivities for total alcohol and C_{2+} alcohols were maximum (47% and 58%, respectively), far exceeding that of the K-CuCoCr reference catalyst (22% and 44%, respectively). In particular, the yield of C_{2+} alcohols reached 27 mmol $\text{g}_{\text{Cu+Co}}^{-1}\cdot\text{h}^{-1}$, which is about 2 orders of magnitude higher than that of the reference catalyst. Interestingly, the optimal catalyst composition matches the maximum occurrence of the nanosized CuCo alloy phase. This is a successful example for the perfect combination of theoretical prediction and experimental verification for the development of highly efficient catalysts.

Kruse et al.¹²⁵ reported an intriguing observation, namely that the CO hydrogenation can be tuned to produce 1-alcohols, long-chain *n*-aldehydes, *n*-paraffins, and olefins over K-promoted Co–Mn bimetallic catalysts by varying the H_2/CO pressure ratios at constant total pressure. At $\text{H}_2/\text{CO} = 0.5$, the product contains about 60% *n*-aldehydes. With an increase of H_2/CO ratio, the alcohol fraction increases and reaches a maximum value of ~45% at H_2/CO ratio of 5. The product distribution at H_2/CO ratio of 9 consists of 35% terminal alcohols and 65% straight-chain hydrocarbons. No other products including CO_2 are detected. Physico-chemical characterization indicated that the synergistic interaction between the Co_2C phase and Mn_3O_8 is responsible for this unique product spectra. The distribution of C_{4+} products follows a linear ASF law and is independent of the H_2/CO ratio, which agrees with a unique carbon-chain growth mechanism.

Over the past decade, trimetallic/multimetallic catalysts have caused rapidly growing interest because there are more variables that can be tuned to meet the requirement of the particular HAS reaction.^{126–133} Kruse et al.¹³⁴ introduced

reducible Nb oxides into the Co–Cu system via oxalate coprecipitation. The ternary “CoCuNb” catalyst had a bimodal nanosized particle distribution consisting of both large Co–Cu (25–40 nm) and small NbO_2 nanoparticles (4–8 nm). Nb oxides acted as a structural dispersant for Co–Cu particles and as promoter for the production of 1-alcohol/1-olefin. Bimodal catalysts favored the alcohol distribution from C_{2+} to C_{7+} . The total selectivity toward alcohol (including CO_2) reached ~50 wt % with a 1-alcohol/1-alkene selectivity as high as ~73 wt % under relatively mild conditions (200 °C, $\text{H}_2/\text{CO} = 1.5$, 60 bar, and total gas flow 40 mL/min). The fraction of $\text{C}_2\text{--C}_5$ primary alcohols in the total alcohols was up to 75%, with negligible CO_2 and little methanol production. Therefore, the HAS catalyst has great potential for an industrial application.

Mo-based HAS catalysts have also received specific interest due to their excellent sulfur tolerance.^{135,136} Bao et al.¹³⁷ reported the highly efficient multimetallic Mo-based catalyst Mn-K-Co-Mo for HAS. A Mn oxide was introduced to tune the interaction between Co and Mo particles, the reducibility of components, and dispersion of Mo particles. The sol–gel preparation method enabled a highly homogeneous component distribution, ensuring intimate and sufficient contact between promoters and Mo species. Before the reaction, a two-step activation strategy was used to tune and match the valence state of active Co and Mo species to a large extent. These structural properties promoted the formation of active sites and ensured good synergy between different active sites with different functionality. Benefiting from properties, the catalyst exhibited very high selectivity for C_{2+} alcohol synthesis. The mass fraction of C_{2+}OH in total alcohols was as high as 80 wt % and the yield and selectivity of total alcohol reached 148.3 g· $\text{kg}^{-1}\cdot\text{h}^{-1}$ and 58.6% C at a CO conversion of 23.9 at 5.0 MPa, 320 °C, GHSV = 6000 h^{-1} , $\text{H}_2/\text{CO} = 2$. An in-depth understanding of the structure–activity relationship remains obscure due to the complexity of this particular catalyst system.

The number of studies on other C_{2+} oxygenates apart from higher alcohols are limited. For the first time, Wang et al.¹³⁸ presented a new reaction-coupling strategy, the so-called relay catalysis, for the selective conversion of syngas into acetic acid (AA) and methyl acetate (MA) by both integrating syngas-to-methanol/DME and methanol/DME-to-AA/MA reactions. Figure 6 shows the target product selectivity and reaction pathways. The authors designed several different combinations of catalysts in one reactor. The combination of DME synthesis catalyst Cu-Zn-Al/H-ZSM-5 and carbonylation catalyst H-MOR achieved a selectivity (MA + AA) of 97% at a CO conversion of 4.5% at 473 K. No significant catalyst deactivation was observed during 100 h reaction by removing the acid sites in 12-MR channels of H-MOR. The intimate contact between Cu-Zn-Al and H-ZSM-5 removed most of the H_2O by WGS reaction, thus favoring the subsequent DME carbonylation. Using a combination of spinel-structured ZnAl_2O_4 and H-MOR, the selectivity of (MA + AA) reached 85% at a CO conversion of 11% and at 643 K without significant deactivation. DME is the key reaction intermediate. The precise C–C bond coupling via the carbonylation of DME led to the highly selective production of MA and AA at both lower and higher temperatures. Furthermore, the direct conversion of syngas into ethylene and ethanol can be realized by using ZnAl_2O_4 and H-MOR combinations at different arrangements. $\text{ZnAl}_2\text{O}_4 \mid \text{H-MOR} \mid \text{ZnAl}_2\text{O}_4$ provides an ethanol selectivity of 52%, while $\text{ZnAl}_2\text{O}_4 \mid \text{H-MOR} \mid \text{ZnAl}_2\text{O}_4$

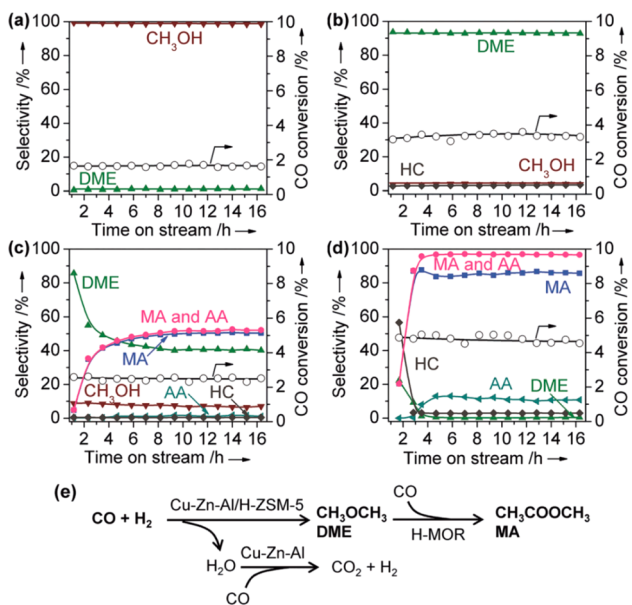


Figure 6. Catalytic performances and reaction pathways for syngas conversions at 473 K. (a) Cu-Zn-Al oxide. (b) Cu-Zn-Al/H-ZSM-5. (c) Cu-Zn-Al + H-MOR. (d) CuZn-Al/H-ZSM-5 + H-MOR. (e) Scheme for MA formation. Reaction conditions: H₂/CO = 1; P = 3 MPa; F = 25 mL·min⁻¹; weights of Cu-Zn-Al, H-ZSM-5, HMOR = 0.33, 0.17, 0.50 g.

| H-MOR provides ethylene. The close proximity between ZnAl₂O₄ and H-MOR increased ethylene selectivity to 65%.

3. METHANE CONVERSION

3.1. Methane Reforming to Syngas/Hydrogen. Currently utilized methane reforming processes include steam reforming (SRM),^{29–31} dry reforming (DRM),^{32,33} autothermal reforming (ARM),^{34,35} and partial oxidation (POM).^{36,37} The final H₂/CO ratio, used oxidants, and energetics differ in these processes.³⁸ SRM is the most widely used technology for methane reforming, which produces about 98% of the world's hydrogen gas supply.¹³⁹ This reaction consists of several steps, including the activation of methane and water, and the production of CO, H₂, and CO₂. DRM has the lowest operation cost in all these reforming processes and is an environmentally friendly process that converts two major greenhouse gases to syngas for the production of chemicals and fuels.¹⁴⁰ Methane reforming reaction is highly endothermic and therefore requires high temperatures (>640 °C).³⁶ In addition to noble metals, Ni-based catalysts have received increasing attention in methane reforming due to high activity and low price, making them more desirable for industrial applications. However, they easily deactivate because of carbon deposition or sintering.^{141–143} Highly dispersed Ni particles can inhibit such carbon deposition; however, they easily agglomerate during the reaction. To inhibit the carbon deposition while maintaining high performance and stability, Kawi et al.¹⁴⁴ designed and synthesized a Ni-yolk@Ni@SiO₂ catalyst with yolk-satellite-shell structure, which contains a cavity between the metal core and the silica shell. The catalyst showed stable and near equilibrium conversion for the DRM reaction due to the combination of advantages of the yolk shell structure and high activity and carbon resistance ability of small Ni particles. Compared to Ni@SiO₂ core–shell nanoparticles, the Ni-yolk@Ni@SiO₂ with a shell thickness of 11.2

nm showed much higher CH₄ conversion (90% vs 60%) and CO₂ conversion (95% vs 75%) during 90 h with negligible carbon deposition at 800 °C, GHSV = 36000 mL·g⁻¹cat·h⁻¹, CO₂:CH₄:N₂ = 1:1:1. The H₂/CO ratio was approximately ~0.82. The dual effects of Ni phyllosilicate formation due to the strong Ni-SiO₂ interaction and the small Ni particles dispersed in the silica contributed to the improved performance. The evolution of core–shell structure to yolk–shell structure during calcination further enhanced the catalytic performance due to the confinement effect.

Sorbent enhanced steam methane reforming (SE-SMR) is an efficient approach to produce the high-purity hydrogen.¹⁴⁵ In this process, the SRM is simultaneously run with the WGS and a CO₂ abstraction reaction (a typical carbonation of CaO). One of the important advantages of SE-SMR process is the possible operation at lower temperatures, thus suppressing the deactivation of catalyst due to coking and sintering. In addition, it is feasible to reduce both the investment and operation costs of a hydrogen plant. A bifunctional catalyst (Ca-Ni-ex-Htcl) containing the Ca-based CO₂ sorbent and Ni reforming catalyst has been reported to be very efficient for the SE-SMR reaction.¹⁴⁶ The catalyst was synthesized via a coprecipitation technique, which used a hydrotalcite precursor to ensure that CaO and Ni particles were embedded in the thermally stable Mg_xAl_yO_z matrix. The mole fraction of hydrogen in the effluent stream over the material was 99 vol % at 550 °C with a steam-to-methane ratio of 4, which reached the thermodynamic equilibrium of the methane conversion. The yield of high-purity H₂ far exceeded the commercial Ni-SiO₂ catalyst mixed with limestone or a Ca-free, Ni hydrotalcite-derived catalyst. The catalytic performance remained stable over 10 reaction cycles. The hydrotalcite-based matrix can effectively stabilize the Ni particles even at 750 °C for the recalcination of CaCO₃. In addition, the catalyst possessed a high CO₂ absorption capacity, which was significantly more stable than that of natural limestone during the repeated carbonation/decarbonation cycles. This could be attributed to the fact that the highly stable and porous (Al:Mg:Ca)O_x structure stabilized the CaO grains and reduced their sintering.

The water that forms during the DRM process, via WGS reaction, can cause an unwanted back-reaction to CO₂, thus decreasing the CO yield. To overcome this, Marin et al.¹⁴⁷ proposed an original “super-dry” CH₄ reforming route for improving the production of CO from CO₂ and CH₄. The process used 10NiO/MgAl₂O₄ as CH₄ reforming catalyst, 50Fe₂O₃/MgAl₂O₄ as solid oxygen carrier, and earth-abundant materials 90CaO/Al₂O₃ as CO₂ sorbent, with a CO₂/CH₄ ratio of 3:1. The process contained two reaction steps operated at 1023 K, and the schematic representation is shown in Figure 7. In the oxidation step of CH₄, Ni catalyzed the CO₂-reforming of CH₄ to produce syngas, then Fe₃O₄ was reduced by syngas while producing H₂O and CO₂, finally the CO₂ was removed in situ by CaO carbonation. Overall, CH₄ was oxidized to H₂O and CO₂, Fe₃O₄ was reduced to Fe, and CaCO₃ was obtained by CO₂ and CaO. By switching the feed to an inert gas in the next reduction step of CO₂, CaCO₃ decomposed into CO₂ and CaO, and Fe was oxidized to Fe₃O₄ by reducing CO₂ to CO. The configuration of two steps removed the formed H₂O during the CH₄ oxidation and avoided the production of an equilibrium mixture of CO, CO₂, H₂O, and H₂. The process avoided the loss of CO yield caused by WGS reaction and was therefore termed “super-dry

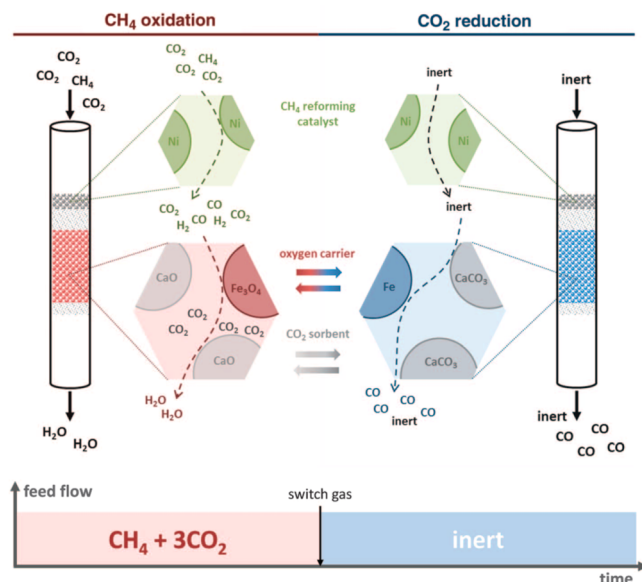


Figure 7. Schematic representation of the proposed process.

reforming of CH_4 ". Moreover, by improving the CO_2 utilization efficiency via Le Chatelier's principle, the process can use a feed gas with a CO_2/CH_4 ratio up to 3:1 and yielded a higher CO production and purity than a conventional CH_4 reformer. The space-time yield of CO reached 7.5 mmol $\text{CO s}^{-1}\text{kg}^{-1}$ of iron at 1023 K. Furthermore, although the process proceeded at a high reaction temperature of 1023 K, the carbon deposition could be avoided.

For methanol synthesis, the optimal H_2/CO ratio of syngas is 2:1. CO_2 DRM produces syngas with a H_2/CO ratio of about 1:1,¹⁴⁸ while SRM produces syngas with a H_2/CO ratio of approximately 3:1.¹⁴⁹ Both approaches require additional steps to adjust the H_2/CO ratio so that it meets the methanol synthesis requirements. The combination of dry reforming and steam reforming processes in a single step is a potential option for producing syngas with an optimal H_2/CO ratio of 2:1, but is generally considered difficult and had very limited success.¹⁵⁰ Recent work by Prakash et al.¹⁵¹ has achieved significant progress. The authors successfully developed a one-step bireforming process, combining both the dry and steam reforming of pure methane or natural gas exclusively to metgas (methanol syngas with a H_2/CO ratio of 2:1) using a cheap and abundant NiO/MgO catalyst. At 830 °C and 7 bar with a $\text{CH}_4/\text{CO}_2/\text{H}_2\text{O}$ ratio of ~3:2:1, the catalyst showed a stable CO_2 and CH_4 conversions of 62% and 71%, respectively, over a 320 h reaction. The selectivities for CO and H_2 were close to 100% with a H_2/CO ratio of 2. This catalyst is also suitable for the bireforming of natural gas that contains small amounts of ethane, propane, butane, and higher hydrocarbons. The conversions of CO_2 and natural gas (mainly methane) reached

~67% and ~70%, respectively, with a H_2/CO ratio of ~1.9. No other hydrocarbons were detected except for methane, which indicates that all higher hydrocarbons were converted to metgas and a little methane. Similar to dry or steam reforming, the bireforming process is also endothermic. Although the reaction can be heated by external energy input, it is advantageous to supply the required energy for the bireforming process in a self-sufficient way. This goal was achieved by the complete combustion of oxygen mixed with one-quarter of the methane or natural gas. As shown in Figure 8, the initial methane combustion provided a feed gas with the $\text{H}_2\text{O}/\text{CO}_2$ ratio of 2:1. Then the feed was mixed with three equivalents of methane to perform bireforming reaction, which produced a metgas with a H_2/CO ratio of 2:1 for subsequent methanol synthesis. Moreover, the methane combustion also provided the required heat for the endothermic bireforming process, thus the reaction is called "oxidative bireforming". The overall process is self-sufficient and exclusively converts natural gas or methane into metgas for the synthesis of methanol without any byproducts. Through this route, a long elusive but never reached goal for the highly selective oxidation of methane (or natural gas) using oxygen in the air to methanol without any oxidation byproducts was achieved.

The partial oxidation of methane with oxygen has also been industrialized for syngas production, in which the pure oxygen is introduced to meet the heating requirement of the reaction and to adjust the H_2/CO ratio of syngas to a desired value.³² However, this process is difficult to control because it potentially forms the local hot spots, which result in the catalyst deactivation because of sintering^{152,153} and further decreases the catalytic performance and induces safety concerns because of the highly exothermic reaction. The high-cost air-separation devices also impede the widespread deployment of these technologies.¹⁵⁴ Alternatively, the two-step chemical looping partial oxidation (CLPO) of methane has attracted both academic and industrial attention for syngas production. The process uses lattice oxygen from metal oxides, which can be regenerated by air and recycled back to the previous step by replenishing oxygen and releasing heat.^{155–157} Providing the optimum lattice oxygen for selective production of syngas remains a huge challenge in this process. Recently, Gong et al.¹⁵⁸ reported a Ni-modified WO_3 catalyst for the CLPO process through both rational design and controllable synthesis. The authors used WO_3 with a high melting point as the primary source of lattice oxygen and introduced NiO as promoter. The optimal $\text{Ni}_{0.5}\text{WO}_x/\text{Al}_2\text{O}_3$ achieved a CO yield of 0.95 mmol/g, which is about 2.7 times higher than that of the unmodified $\text{WO}_3/\text{Al}_2\text{O}_3$. The H_2/CO ratio in the produced syngas was 2.1, which is close to the theoretical value of 2.0. The total evolved CO amount of the 10th redox cycle reached 0.85 mmol/g, which was only slightly lower than that of the first redox cycle, displaying a good stability. The

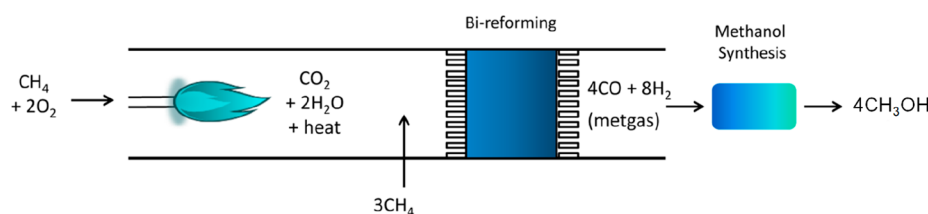


Figure 8. Oxidative bireforming.

incorporation of NiO strongly weaken the W–O bond strength in both bulk and surface regions and thus increase the availability of lattice oxygen. Surface-grafted Ni species effectively promoted the methane activation and subsequent partial oxidation, thus enhancing the syngas production. Furthermore, the WO_x species effectively improved the dispersion of Ni and resisted coking to improving the catalyst stability as compared to $\text{NiO}/\text{Al}_2\text{O}_3$.

3.2. Methane Pyrolysis to Hydrogen. As an alternative approach, H_2 can be produced via methane pyrolysis. Compared with SRM, only half of H_2 is produced per mole of methane; however, the process requires significantly less energy and produces solid carbon instead of CO_2 . This solid carbon can be stored safely and permanently; a subset can be used as the electrodes or additives to various materials (e.g., asphalt, concrete, and rubber). Furthermore, direct pyrolysis of methane can be conducted in a single step via a relatively simple and low-cost industrial process. Metallic methane activation catalysts (e.g., Pd, Ni, and Pt) can catalyze the methane pyrolysis into carbon and hydrogen under moderate conditions. However, these metallic catalysts have very high melting points and are rapidly deactivated by the solid carbon.^{159–161} Pure liquid Mg is the only reported molten metal catalyst for methane pyrolysis, and it achieved an equilibrium conversion of ~30% at 700 °C.¹⁶² Because of Mg evaporation, it is impossible to achieve higher conversions at higher temperatures. McFarland et al.¹⁶³ reported a series of liquid alloys of active metals (i.e., Ni, Pt, and Pd) in low melting point metal “solvents” (i.e., Pb, Sn, In, Bi, and Ga). A $\text{Ni}_{0.27}\text{Bi}_{0.73}$ catalyst showed the best performance, which achieved a methane conversion of 95% at 1065 °C in a 1.1-m bubble column and produced high-purity hydrogen without detectable CO_2 and other byproducts (Figure 9). Under these conditions, the achieved equilibrium conversion was 98%. In the molten alloy, the produced insoluble carbon during methane pyrolysis floats on the melt surface and can be easily removed. The catalyst activity remained stable over 170 h. During this period, the carbon dissolved into the melt and reached a steady state with the precipitation out of the melt. Calculation results indicated that the active metals in the molten alloys were atomically dispersed and negatively charged. There is a correlation between the amount of charge on the atoms and their catalytic performance.

3.3. Oxyhalogenation of Methane. The catalytic oxyhalogenation of methane, including its reaction with hydrogen halide (HCl or HBr) and oxygen, is an attractive approach to enable direct methane functionalization under moderate operating conditions (ca. 1 bar, <853 K).^{164–166} In methane oxyhalogenation, the reactive halogen generated via oxidation of hydrogen halide with O_2 can activate the C–H bond in methane. The thus formed methyl halides (CH_3Cl and CH_3Br) can serve as platform molecules for the production of olefins or aromatics via a coupling reaction. This technology faces significant issues: (i) low methane conversion, (ii) low methyl halides selectivity, and (iii) poor activity of the coupling reaction of methyl halides to higher hydrocarbons.¹⁶⁷ Noble-metal catalysts, such as the supported Ru or Rh catalysts, achieve good catalytic performance for methane oxyhalogenation, but the high cost obstructs their large-scale applications.^{167,168} Wang et al.¹⁶⁵ reported a new route to efficiently convert methane to propylene via CH_3Cl or CH_3Br , which consists of a two-step reaction, as expressed by eqs 1 and 2.

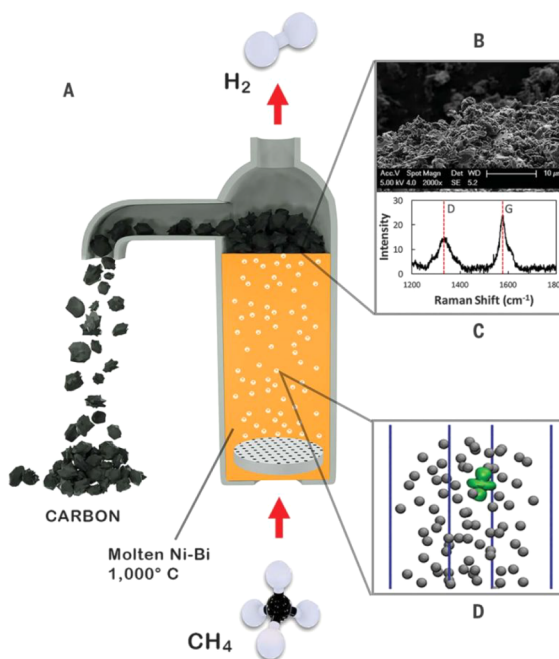
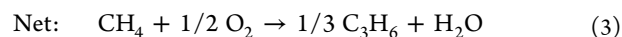
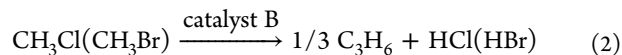
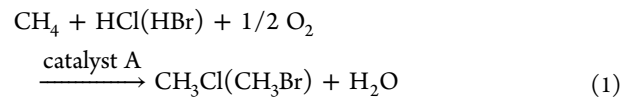


Figure 9. Hydrogen production with a Ni–Bi molten catalyst. (A) Reactor for CH_4 conversion to H_2 and carbon in a molten-metal bubble column under continuous carbon removal. (B) Scanning electron microscopic image of the obtained carbon. (C) Raman spectrum of surface carbon. The dashed line labeled “D” is at 1350 cm^{-1} , and the dashed line labeled “G” is at 1582 cm^{-1} . (D) Ab initio molecular dynamics simulation showing an orbital (green) of a Pt atom dissolved in molten Bi (gray) alloy.

The net reaction is the methane oxidation by O_2 to produce propylene and H_2O (eq 3).



After screening a variety of nonmetal catalysts, CeO_2 was identified as a highly active and stable catalyst for the oxyhalogenation of methane. The selectivity of CH_3Cl or CH_3Br product depended on the morphology of CeO_2 . The CeO_2 nanocubes with exposed {100} facets were a more selective catalyst and the modification with NiO or FeO_x can further enhance the selectivity toward CH_3Br or CH_3Cl . The 15 wt % $\text{FeO}_x/\text{CeO}_2$ nanorod and the 10 wt % $\text{NiO}_x/\text{CeO}_2$ nanocube achieved 74% and 82% selectivities of CH_3Cl and CH_3Br at CH_4 conversions of 23% and 22%, respectively. The catalytic performance remained unchanged over 100 h. The formed solid-solution phases between FeO_x or NiO with CeO_2 have been suggested to promote the adsorption and activation of HBr or HCl to produce Br or Cl active species. In the second step, an F-modified H-ZSM-5 ($\text{F/Si} = 0.063$) catalyst showed high selectivity and stability for the conversions of CH_3Cl or CH_3Br into propylene. The selectivity of C_3H_6 reached 64% and 56% at CH_3Cl and CH_3Br conversions of 76% and 94%, respectively. This C_3H_6 formation performance exceeds that of any previously reported catalysts for the conversion of halogenomethane. Catalyst stability was

maintained within 50 h reaction. Although HCl and HBr are not environmentally friendly, their net release could be avoided by the simple separation and recycling in this process. The estimated overall conversion efficiencies of HBr and HCl were 90–93% and 65–70%, respectively, without considering the uses of CH_2Cl_2 and CH_2Br_2 that formed in the first step.

If catalysts are used with mild oxidative methane oxohalogenation properties (e.g., LaOCl in oxychlorination and FePO_4 or VPO in oxybromination), the dominant oxidation product of methane oxohalogenation is CO, and only a trace amount of CO_2 is produced.^{166,169,170} These findings suggest additional potential for this route as an effective method for the conversion of natural gas for on-purpose production of CO. However, the commercial application of this oxyhalogenation reaction has not been considered to date because of the low CO selectivity (<50%).^{166,170} Ramirez et al.¹⁷¹ demonstrated the first example of a highly selective one-step CO production from methane via oxychlorination chemistry. In the process, HCl was added to a CH_4-O_2 to activate the C–H bond under mild reaction conditions while forming CH_3Cl , CH_2Cl_2 , and chloromethanes. The latter produces CO and recycles HCl via in situ oxidation over the same catalyst. An efficient catalyst should exhibit the essential chlorine evolution activity to facilitate the formation of chloromethanes and the ability to selectively oxidize the latter to produce CO. Following this design criteria, an outstanding vanadyl pyrophosphate (VPO) could be identified, which exhibited a CO yield of up to approximately 35% at 96% selectivities under ambient pressure and temperatures <835 K. The exceptional performance remained stable over 100 h on stream. The new route introduces a method for the development of a modular and decentralized process for the natural gas by exploiting CO as a versatile platform molecule for the manufacture of valuable chemicals.

3.4. Nonoxidative Methane Dehydroaromatization.

Nonoxidative methane dehydroaromatization (MDA) is a promising route for the direct conversion of natural gas into valued aromatics in a single step. The reaction is often operated at about 700 °C using catalysts with Mo nanoclusters supported on shape-selective zeolites such as MCM-22 and ZSM-5.¹⁷² Compared with other methane activation routes, this technique avoids the possibility of complete oxidation and explosion due to the absence of O_2 or other oxidants. The biggest obstacles in the commercialization of this process are low per-pass conversion (~10%) and rapid catalyst deactivation.^{173,174} The main challenge for catalyst development is to cleave the first C–H bond, while inhibiting further dehydrogenation to avoid carbon deposition. Lattice-confined single Fe atoms embedded in a silica (0.5% Fe@SiO_2) was reported by Bao et al.¹⁷⁵ and was found to be very active for the MDA. The catalyst achieved CH_4 conversion up to 48.1% with a selectivity to $\text{C}_2\text{H}_4 > 48.4\%$ (the remainder being aromatics) at 1363 K. The yields for ethylene, benzene, and naphthalene reached 91, 18, and 9 mol $\text{kg}_{\text{cat}}^{-1} \text{h}^{-1}$, respectively, with a total carbon selectivity to the three products >99% (Figure 10). In addition to the hydrocarbons, the byproduct is hydrogen and its concentration in the effluent ranged from 10.9 to 51.2% with varied reaction conditions. Deactivation was not observed even after 60 h reaction. This efficiency was attributed that the coordinated unsaturated Fe atoms showed a high activity for the activation of C–H bond in methane. The formed methyl radical on the single Fe site is released rather

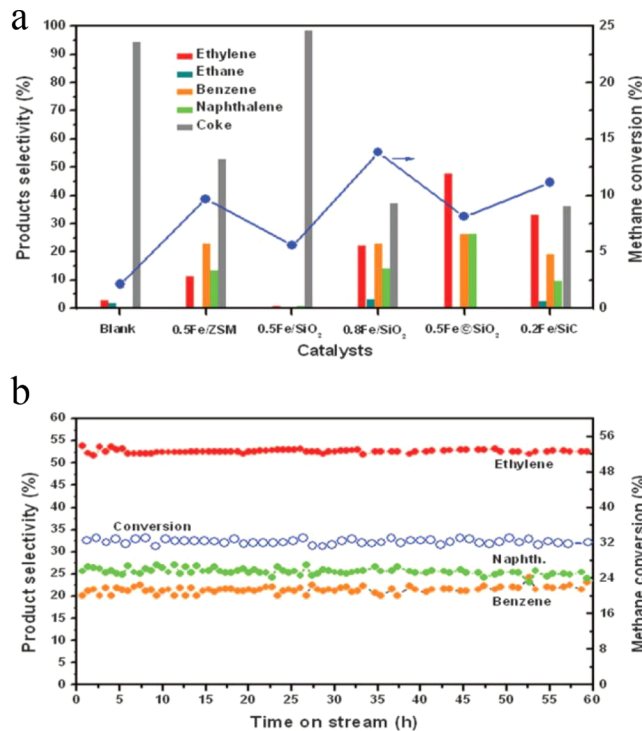


Figure 10. Reaction performance. (a) Comparison of different catalysts at 1223 K and 4.84 L $\text{g}_{\text{cat}}^{-1} \cdot \text{h}^{-1}$. (b) Long-term stability test of 0.5% Fe@SiO_2 at 1293 K and 14.5 L $\text{g}_{\text{cat}}^{-1} \cdot \text{h}^{-1}$.

than C–C coupling or further dehydrogenation. Subsequently, the exposed Fe site adsorbs the second methane molecule and thus generates another methyl radical. The isolated Fe atoms strongly interact with the silica support and are embedded in the support by bonding with C and Si atoms and thus become stable and persistent under harsh reaction conditions. These findings provide new insights into the fundamental understanding of direct, nonoxidative activation of CH_4 .

Kjolseth et al.¹⁷⁶ presented a novel approach to increase the aromatic yields and enhance catalyst stability for MDA reaction by integrating an ion-conducting membrane into the reactor. As shown in Figure 11, the tubular catalytic membrane reactor (CMR) consists of a dense $\text{BaZr}_{0.7}\text{Ce}_{0.2}\text{Y}_{0.1}\text{O}_{3-\delta}$ (BZCY72) electrolyte membrane (25 mm thickness) on a porous BZCY72-Ni cathode. The metallic Ni showed high activity for the reduction of H_2O and H_2 evolution. A Cu-based anode was coated on the electrolyte membrane on the other side, which catalyzed the electrocatalytic oxidation of H_2 to produce protons and prevented the secondary conversion of hydrocarbons to coke. During the reaction, CH_4 was first converted to H_2 and benzene over the Mo/zeolite catalyst. The produced H_2 was then transported to the sweep side. The oxide ions were transported to the reaction medium where they reacted with H_2 to produce H_2O . Then the H_2O reacted with coke and formed CO and H_2 . The CMR achieved an aromatic yield of 12% for the MDA, which is slightly higher than that of the conventional fixed-bed reactor (FBR, 10%). Interestingly, the selectivity for aromatics maintained a high level. Particularly, the benzene selectivity was more than 85% on a coke-free basis. More importantly, the catalyst in CMR exhibited improved stability. The decay rate was about 1 order of magnitude lower than that of conventional FBR. In situ extraction of H_2 shifted the reaction equilibrium and increased the aromatics yield, which would have significant impact on the

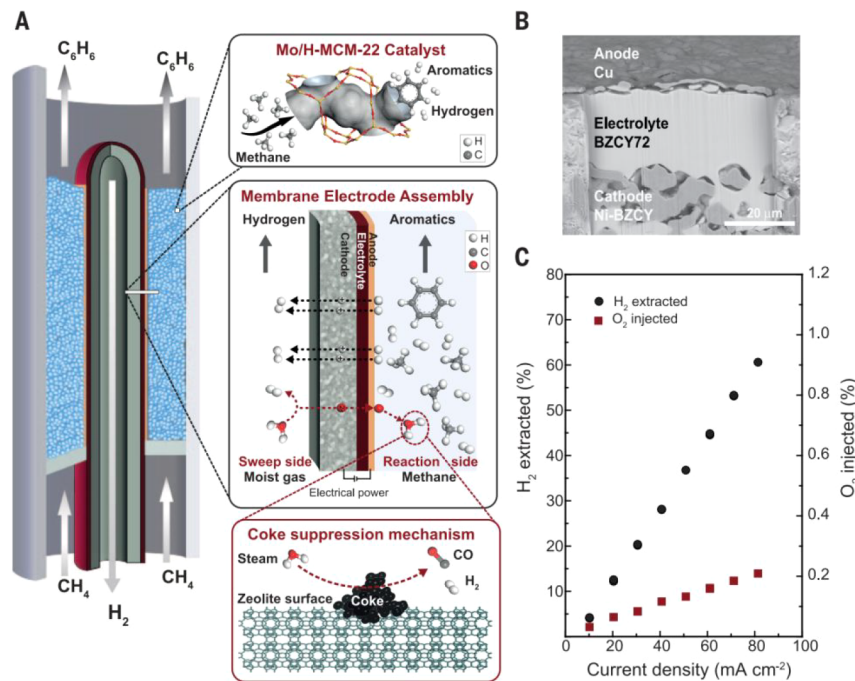
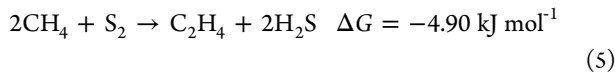
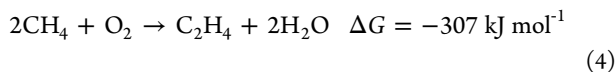


Figure 11. Current-controlled co-ionic membrane reactor. (A) CH₄ is converted to benzene and hydrogen via a Mo/zeolite catalyst. H₂ is transported as protons to the sweep side. Oxide ions are transported to the reaction medium where they react with H₂ and form steam as an intermediate before reacting with coke to form CO and H₂. (B) Scanning electron microscopic image of the membrane electrode assembly (focused ion beam section). Cathode porosity formed upon reduction of NiO can be observed beneath the dense electrolyte. (C) Percentage of H₂ extracted and O₂ injected versus current density at 700 °C. The anode is swept with a 10/90 mixture of H₂/CH₄ and the cathode with a 3/5/92 mixture of H₂O/H₂/Ar.

industrial application of the process. This excellent stability is due to the in situ-generated steam inhibiting the coke formation, indicating that the controlled and distributed oxygen injection is more effective for improving the stability of catalyst than the external addition of steam. Furthermore, the CMR system enabled a high carbon efficiency of up to 80%, similar to the results exhibited by large and optimized Fischer–Tropsch plants.¹⁷⁷

3.5. Oxidative Coupling of Methane. Oxidative coupling of methane (OCM) with O₂ is an attractive route for the synthesis of valuable chemicals and has been extensively studied over the past decades^{178–183} since the initial work of Keller and Bhasin.¹⁸⁴ Unfortunately, the presence of O₂ leads to severe overoxidation, which yields a large amount of thermodynamically stable H₂O and CO₂ and only a small amount of the desired products such as methanol, formaldehyde, and ethylene. Furthermore, the reactions with O₂ are highly exothermic, which can raise the local temperature by 150–300 °C, which presents major challenges for reactor design and heat management. In comparison to O₂, the thermodynamic driving force for methane overoxidation by S₂ is significantly reduced,^{185,186} making it a “softer” oxidant. The comparison of Gibbs enthalpy of the reaction for both processes (at 1073 K) clearly indicates this difference in the oxidizing power of oxygen and sulfur.^{185,186} The overoxidation of methane to CS₂ or other species is less favorable than the analogous overoxidation by O₂.



Marks et al.¹⁸⁷ demonstrated that the sulfur is a “soft” oxidant for the OCM to ethylene since the metal–sulfur (M–S) bond is significantly stronger than the metal–oxygen (M–O) bond in the corresponding O₂ oxidation. Sulfides with strong surface M–S bond exhibit a high selectivity for ethylene but a low conversion of methane. MoS₂, RuS₂, TiS₂, and PdS are effective catalysts for the OCM using sulfur as oxidant. The ZrO₂-supported Pd₁₆S₇ (10 wt % Pd) exhibited the highest ethylene selectivity of up to 20% at a CH₄ conversion >16% at 1323 K. Furthermore, the use of S₂ as the oxidant instead of O₂ can suppress the severe temperature drift that occurs in OCM with O₂, since the S₂ reaction is almost thermoneutral. Experiments and DFT showed that a catalyst with weak M–S bond enhanced the methane activation because it is easier to remove the first hydrogen atom from methane, which binds the resulting methyl groups more strongly. However, to enhance C–C coupling and increase ethylene selectivity, a strong M–S bond is required, which results in a weaker C–S bond. Despite the strong M–S bond, Pd₁₆S₇ was able to activate the initial CH₃–H bond on the Pd–S site with a relatively low barrier of 166 kJ mol⁻¹. Furthermore, the large Pd–S bond strength at these S–S sites can weaken the CH₂–S bonds, thus reducing the barrier for subsequent coupling. Based on the above, the same authors further examined the OCM by gaseous S₂ over Pd/Fe₃O₄ and bare Fe₃O₄, and they reported that a high selectivity of ethylene was achieved without noble metals.¹⁸⁸ Fe₃O₄ showed a high ethylene selectivity of 33% with a CH₄ conversion exceeding 4% at 950 °C. No deactivation was found over 48 h on-stream. The catalytic performance was much higher than that of the reported PdS_x and supported PdS_x. Furthermore, the C₂H₄/C₂H₆ ratios reached 9–12, which is significantly higher than

the reported values in previous OCM studies. The relationship between C_2H_6 , C_2H_4 , and C_2H_2 selectivities and WHSV indicated that the C_2H_4 and C_2H_2 were formed via dehydrogenation of C_2H_6 and C_2H_4 , respectively.

3.6. Methane to Methanol/Acetic Acid. For chemists, the direct partial oxidation of methane to methanol under moderate conditions is a very desired reaction, which circumvents the environmentally harmful and expensive syngas step and exhibits unique environmental and economic advantages. This reaction has not yet been solved satisfactorily because the desired methanol product is more reactive than methane, which is easily overoxidized to produce formic acid or CO_2 . In nature, methane monooxygenase (MMO) enzymes in the methanotrophic bacteria can effectively perform the desired reaction under ambient conditions.^{189–192} The enzymes contain di/tricopper or di-iron active clusters with intriguing structural motifs and can be used for the development of highly efficient biomimetic catalysts for methane activation.^{193,194} Inspired by these biocatalytic enzyme systems, transition-metal-exchanged zeolites (Fe or Cu exchanged-ZSM-5), with active sites similar to those in MMO, are the most widely studied catalysts for methane activation.^{169,195,196} The metal-oxo species in zeolite were proposed as active sites, and most researchers suggested that the species consist of more than one metal atoms. Lercher et al.¹⁹⁷ reported a Cu-MOR catalyst with uniform trinuclear Cu-oxo clusters ($[Cu_3(\mu-O)_3]^{2+}$), which is anchored to two Al atoms that are located at the pore mouth of the 8-MR side pockets. Mordenite micropores with a confined environment stabilized trinuclear Cu-oxo clusters. The material exhibited a high activity for methane conversion to methanol, which achieved a methanol yield ($160\text{ mmol g}_{\text{cat}}^{-1}$) at least 1 order of magnitude higher than the maximum value that were previously reported for this type of catalyst ($13\text{ mmol g}_{\text{cat}}^{-1}$). The trimeric Cu-oxo clusters were identified as active sites, which were highly stable under dry conditions. Even if the cluster is hydrolyzed by the reaction with methane followed by steam treatment, it can be regenerated by reactivation in O_2 without loss of activity. Similar to Cu-exchanged zeolites, Fe-exchanged zeolites have received considerable interest. Hutchings et al.¹⁹⁸ reported that Cu-promoted Fe-ZSM-5 zeolites are highly active for the methane oxidation to methanol in aqueous conditions using H_2O_2 . Under standard conditions ($50\text{ }^\circ C$, 30.5 bar), the normalized TOFs (mol (product) mol^{-1} (metal) h^{-1}) exceeded 2200 h^{-1} , which is about 3 orders of magnitude higher than any previously reported values. The methanol selectivity exceeded 90% at a methane conversion rate of 10%. The reaction mechanism differs from Fenton's chemistry,^{199,200} α -oxygen,^{201,202} and an MMO-type rebound mechanism.²⁰³ This suggested that H_2O_2 produced species that are capable of the methane activation at iron centers. Then, the formed methyl hydroperoxide underwent further conversion to methanol. This process is a low-energy pathway for methane oxidation. Copper has no direct effect on methane activation and improved the methanol selectivity by inhibiting the overoxidation to CO_2 and formic acid. The reaction process has been applied to ethane oxidation, for which a conversion of 56% with an oxygenate selectivity of 97% was obtained. This result suggests that hydrogen peroxide may be a viable oxidant with higher hydrocarbons, and a catalyst may have applicability in these reactions. More recently, Bao et al.²⁰⁴ reported that methane can be directly converted to C1 oxygenates (CH_3OH ,

CH_3OOH , $HOCH_2OOH$, and $HCOOH$) at $25\text{ }^\circ C$ over graphene-confined single Fe atoms using H_2O_2 as oxidant. The reported sum selectivity toward C1 oxygenates was 94%, with only 6% CO_2 selectivity after 10 h reaction. The unique O- FeN_4 -O structure activates the C-H bond to produce a methyl radical with a low barrier of 0.79 eV. The formed methyl radical is converted into CH_3OH and CH_3OOH ; then the CH_3OH is further catalyzed to form both $HOCH_2OOH$ and $HCOOH$ at room temperature.

If H_2O_2 is used as oxidant, the high degradation rate of H_2O_2 is generally harmful to the methane oxidation, either because of (i) the radical chains termination caused by high radical concentration or (ii) because the high consumption rate of H_2O_2 causes insufficient reaction with the low amount of solubilized methane. Investigating this issue, Hutchings et al.²⁰⁵ used colloidal Au-Pd nanoparticles, instead of the same nanoparticles supported on TiO_2 , to catalyze the methane oxidation to methanol. The colloidal catalyst decomposed H_2O_2 at a much slower rate than the supported catalyst, while producing more products. The productivity of the primary oxygenates (CH_3OOH and CH_3OH) was $29.4\text{ mol}\cdot kg_{\text{cat}}^{-1}\cdot h^{-1}$ at a selectivity of 90% at moderate temperature of $50\text{ }^\circ C$, which is much higher than that of the supported catalyst ($0.03\text{ mol}\cdot kg_{\text{cat}}^{-1}\cdot h^{-1}$; 26%). Furthermore, using oxygen as oxidant in the presence of H_2O_2 further increased the product yield to $39.4\text{ mol}\cdot kg_{\text{cat}}^{-1}\cdot h^{-1}$ while maintaining high selectivity (88%). This isotopically labeled experiment demonstrated that 70% of gaseous O_2 molecules were incorporated in the methanol product. The presence of the additional O_2 (in addition to that formed by H_2O_2 decomposition) facilitates the termination steps that produce primary products.

More recently, a significant breakthrough in methanol selectivity has been achieved by Bokhoven et al.²⁰⁶ The authors reported a direct stepwise route using water as oxidant for methane oxidation over the common Cu-MOR. The methanol productivity reached 0.202 mol per mole Cu at an ultrahigh selectivity of 97%. The water molecules played a central role, not only acting as the oxidant and regenerate the active sites of zeolite but also facilitating energetically favorable methanol desorption, as well as stabilizing reaction intermediates. The direct anaerobic methane oxidation to methanol is an attractive route for energy-and cost-efficient applications. The use of water instead of oxygen as oxidant is conducive to the development of an industrially feasible process.

The direct conversion of methane into methanol is a stepwise process, currently involving high-temperature activation, low-temperature reaction, and extraction with water. The repeated heating and cooling procedure limits the applicability of this technique and prolongs the required cycling time. Bokhoven et al.²⁰⁷ successfully developed an isothermal process to overcome this limitation. The authors reported that, in contrast to previous studies, the Cu-MOR catalyst activated at $200\text{ }^\circ C$ was able to convert methane to methanol if elevated methane pressure was employed. Based on this, catalyst activation with oxygen and reaction with methane, followed by methanol extraction were performed under the same temperature. After 13 h activation at 1 bar of oxygen at $200\text{ }^\circ C$, the methanol yield reached $56.2\text{ }\mu\text{mol}\cdot g^{-1}$ at a methane pressure of 37 bar. The activity remained stable over several cycles. The active sites were identified as small Cu clusters, which are neither di- or tricopper sites,^{197,208,209} nor m-oxo dicopper sites,²¹⁰ suggesting an unprecedented reaction mechanism. The isothermal and regenerable nature of this

process is a major breakthrough in the development of an applicable technology for the methane conversion into methanol. Sievers et al.²¹¹ also reported ceria–zirconia supported small nickel oxide clusters (2 wt % NiO/CZ) that can convert methane to alcohol at steady state and moderate temperature (723 K) with oxygen as oxidant in a single reactor. The methane conversion rate reached 15% and remained stable over 8 h on-stream. The ethanol and methanol yields reached 3.7% and 2.9%, respectively, corresponding to a total alcohol selectivity of 43%, and an ethanol selectivity of 24% on a C atom basis. This report by Sievers et al. is the first report of a single-reactor conversion of methane to ethanol. The unusual activity of the utilized catalyst can be attributed to the synergistic interaction between Lewis acidic NiO clusters and the redox active CZ support. The CZ support can also stabilize the small-sized NiO clusters. In the presence of steam, surface species can be hydrolyzed and desorbed as alcohols.

Acetic acid is one of the important intermediates in chemical industry, which is currently produced via methane reforming, methanol synthesis, and subsequent methanol carbonylation. The direct methane conversion into acetic acid through oxidative carbonylation has been proved to be feasible. However, improving the catalyst efficiency sufficiently to enable economical small-scale natural gas utilization (which is currently stranded or flared) remains the major challenge. Rh- or Pd-based noble metal catalysts have been widely studied for this reaction.^{212,213} Formation of single sites can achieve higher catalytic performance since the isolated cations exhibit a distinctly different coordination of metal atoms and also reduce the amount of noble metals.^{27,214,215} Recently, Li et al.²¹⁶ achieved a significant progress that addresses this issue. The authors prepared atomically dispersed Rh species on the ZSM-5 and TiO₂ support and applied the catalysts to the direct conversion of methane using CO and O₂ under mild conditions (150 °C). Three hours of reaction yielded approximately 22 000 mmol of acetic acid per gram of catalyst (0.5 wt % Rh/ZSM-5), or 230 mmol of methanol per gram of catalyst (0.6 wt % Rh/TiO₂), respectively, with selectivities of 60–100%. The reaction involves two steps: methane activation and subsequent M–CH₃ functionalization. Methane was first activated on isolated Rh⁺ cations to yield Rh–CH₃ in the presence of O₂, which was then functionalized through two independent reaction steps: O₂ insertion to form methanol, or CO insertion to form acetic acid. After hydrolysis, the isolated Rh⁺ species can be used for the next cycle. Tao et al.²¹⁷ reported a single-site Rh₁O₅ anchored in microporous aluminosilicates (0.10 wt % Rh/ZSM-5) via the vacuum pumping and incipient wetness impregnation. The catalyst activity for the synthesis of organic oxygenates (acetic acid, formic acid, and methanol) reached about 0.10 molecules per second on a Rh₁O₅ site, achieving ~70% selectivity toward acetic acid at ≤150 °C. This is more than 1000 times higher than that of the free Rh cations. DFT calculations have suggested that single-site Rh₁O₅ activates the first C–H bond in methane; then the formed CH₃ reacts with OH and CO to form acetic acid with a low activation barrier. Even though the efficiencies of the reported catalysts are still too low for industrial application, these pilot studies guide the development of efficient catalysts and processes for the direct methane conversion into high-value-added chemicals.

4. CO₂ CONVERSION

4.1. CO₂ to CO. CO₂ is considered as a cheap source of carbon rather than a waste product with negative impact on global warming. However, the direct conversion of CO₂ to valuable chemicals is very difficult because of its low reactivity and high stability. Clearly, an active catalyst for chemical processes involving CO₂ should be able to efficiently bind and activate CO₂. One attractive and potential route is to convert CO₂ to CO via reverse water gas shift (RWGS) reaction (CO₂ + H₂ → CO + H₂O). The resulting CO₂/CO/H₂ mixture after H₂O separation can be subsequently used as syngas in FT or methanol synthesis, which are both well-established chemical processes. Supported noble metals are the most commonly used catalysts for CO₂ hydrogenation.^{46,218–220} Metal sites facilitate the dissociation of hydrogen while the utilized oxide support assists with the cleavage of the C=O bond.^{221–223} The dispersion/chemical state of noble metal NPs critically impacts the adsorption behavior of the reactants and the subsequent conversion of reaction intermediates.^{224,225} However, the support can affect the chemical state of noble metal nanoparticles in a manner that differs from a substrate for metal dispersal.^{226,227} Controlling the metal size, especially the size uniformity, remains a major challenge for supported metal catalysts. Ma et al.²²⁸ developed a one-step ligand-free method to fabricate a monodispersed Ir/CeO₂ nanocatalyst. A strong metal–support interaction (SMSI) exists between Ir and CeO₂. The chemical state of Ir can be finely tuned by changing the metal loading. At 300 °C and 1.0 MPa, the Ir/CeO₂ catalyst exhibited a selectivity of up to 100% toward CO at a comparatively high CO₂ conversion activity of 81.1 mol_{CO₂}·mol_{Ir}⁻¹·h⁻¹. Characterization studies showed that the existence of isolated metal sites is not a prerequisite for inhibiting the methanation and producing solely CO in CO₂ hydrogenation. The modulation of chemical state of metal particles via the SMSI is more important. Due to the weak interaction between partially oxidized Ir species and CO, partially oxidized Ir/CeO₂ can catalyze the dissociative chemisorption and further reaction of CO₂. The resulting CO was more easily desorbed from the partially oxidized Ir, rather than requiring further dissociation/hydrogenation to obtain methane, thus leading to a very high selectivity for CO.

In addition to supported noble metal catalysts, the transition metal carbides (TMCs) have also attracted increasing attention for CO₂ conversion due to their similar properties to noble metal catalysts.^{229–231} The high activity of TMCs originates from a modification of their electronic properties caused by the addition of carbon.²³² This in turn affects the binding energy and the reactivity of adsorbate.²³³ Mo₂C is an active catalyst for CO₂ conversion via H₂ due to its ability of H₂ dissociation and C=O bond scission. In recent work, Mo₂C has been proposed as a more economical alternative to noble metal catalysts for RWGS reaction. A comparative study reported that orthorhombic β-Mo₂C is a highly efficient catalyst for RWGS.²³⁴ Furthermore, Mo₂C is also excellent substrate to disperse metal, and this strategy has also been successfully applied in RWGS reaction.²³⁵ Under the guidance of DFT results, Illas et al.²³⁶ experimentally proved that polycrystalline hexagonal α-Mo₂C has a high activity and selectivity for the conversion of CO₂ to CO at both mild temperatures and atmospheric pressures. From a feed gas of with CO₂/H₂ ratio of 1, the achieved conversion of CO₂ reached ~16% at 673 K, with a CO selectivity >99%. The modification of Co can

further improve the activity, selectivity, and stability of Mo_2C , as reported by Chen et al.²³⁷ The authors incorporated cobalt onto the Mo_2C via evaporation-deposition of cobalt nitrate and found that addition of 7.5 wt % Co to Mo_2C increased the CO_2 conversion from 8.7% to 9.5%; however, the $\text{CO}:\text{CH}_4$ ratio improved from 14.5 to 51.3 at 573 K, which is much higher than that of the noble bimetallic catalyst PtCo/CeO₂ (6.6%, 4.5, respectively). The catalytic performance remained stable over 36 h on-stream. The formed highly stable CoMoC_yO_z phase was identified as the critical active phase that dissociated CH_4 and was responsible for the improvement of $\text{CO}:\text{CH}_4$ selectivity by reacting with the CH_4 product or CH_x intermediate.

4.2. CO_2 to Methane. As an alternative route, CO_2 hydrogenation to methane via the Sabatier reaction ($4\text{H}_2 + \text{CO}_2 \rightarrow \text{CH}_4 + 2\text{H}_2\text{O}$) has recently received great attention, which fulfills the requirement of renewable carbon sources and a sustainable production process.^{238–240} The most employed catalysts include metals, such as Ru-, Pd-, Ni-based systems,²⁴¹ and metal oxides, such as CoO.²⁴² Similar to RWGS catalysts, these methanation catalysts also require bifunctional active sites, corresponding to CO_2 and H_2 dissociation, respectively. The surface hydrogen spillover between both active sites was generally proposed to be the rate-limiting mechanistic step.²⁴³ Benefiting from the rapidly developing nanoscience and nanotechnology, McIntosh et al.²⁴⁴ fabricated an active catalyst that consists of Co NPs on a perovskite-structured BaZrO₃. Both the Co and support surface are modified with highly dispersed Pt atoms. CO_2 preferentially dissociated on Co, while H_2 dissociation primarily on Pt. This catalyst achieved a 6-fold increase in the methane production rate with a methane selectivity of 80% as compared to when $\gamma\text{-Al}_2\text{O}_3$ is used as support (43% selectivity) at 325 °C. This enhancement is attributed to the strong interaction between Co particles and BaZrO₃. The atomic decoration of Pt enhanced the availability of hydrogen in close contact with the dissociated CO_2 on the surface of Co.

Ni-based catalysts are also considered as promising candidates for CO_2 hydrogenation due to their high activity, low cost, and earth abundance, which is an alternative to noble-metal catalysts.^{53,245–247} A bimetallic Ni₃Fe catalyst supported on $\gamma\text{-Al}_2\text{O}_3$ (17 wt % Ni₃Fe) was successfully applied for the methanation of CO_2 .²⁴⁸ High fractions of Ni and Fe formed the desired Ni₃Fe alloy, which has a uniform particle size of 4 nm and a relatively high dispersion of 24%. Under industrial conditions (358 °C and 6 bar), the alloy catalyst exhibited ultrahigh selectivity >98% toward CH_4 at a CO_2 conversion rate of 71%. Most remarkably, the catalyst remained highly stable above 350 °C after 45 h reaction. The enhanced activity may be attributed to a synergistic interaction between Ni and Fe, which enhances the CO_2 adsorption and activation at the Fe species and optimizes the CO dissociation energy of NiFe alloy.

More recently, Ajayan et al.²⁴⁹ reported a novel metal-free, nitrogen doped graphene quantum dots (NGQDs) catalyst for CO_2 methanation. The authors observed that the CO_2 conversion and CO/CH_4 selectivity over the catalyst had a turning point at ~300 °C. In a temperature range of 170–255 °C, the CO was predominant product with a selectivity of 60–65%. The initial CH_4 selectivity was ~30% at 170 °C, which decreased to 15% at 300 °C. With further increasing temperature, the CH_4 selectivity gradually increased to 55% above 380 °C. The rate-determining step (RDS) was proposed

to be changed at the turning point. The RDS for CO_2 hydrogenation switched from $^*\text{CH}_2\text{OH}$ hydrogenation to $^*\text{CH}_2$ at 170 °C to CO_2 activation to COOH^* at 300 °C. The pyridinic nitrogen at the edge sites of GQDs was considered as the catalytic active site. The increasing nitrogen content led to a lower onset temperature, and higher CO_2 conversion and CH_4 selectivity.

Two completely different reaction mechanisms have been proposed for CO_2 methanation:^{53,250,251} (i) CO_2 dissociates to CO (or carbonyl) and forms carboxylate species. The subsequent reaction route is the same as CO methanation. (ii) CO_2 and H_2 forms CH_4 by direct associative adsorption without forming CO (or carbonyl) as intermediate. To explore the reaction mechanism, Zeng et al.²⁵² designed and synthesized a mazelike nanoreactor by phase transformations of sandwich-structured ZIF-67@Pt@mSiO₂ nanocubes using a simple water-soaking method. The porous nanoreactor was highly active for gas-phase CO_2 methanation. Under conditions of 320 °C and 30 bar, the conversion of CO_2 reached 41.8% with a CH_4 selectivity up to 94%. Investigating the temperature-dependent performance indicated that the reaction pathway follows the first proposed mechanism, which involves (i) CO_2 dissociation to produce CO on the Pt site, followed by (ii) CO methanation over the nearby cobalt site. The overall retention time of feed gases on catalysts has a significantly effect on their catalytic performance. The TOFs of the nanoreactor with prolonged diffusion paths are about six times higher than that of the reference catalysts with shorter diffusion paths.

4.3. CO_2 to Liquid Fuels/Chemicals. Besides the various C_1 feedstocks, direct CO_2 conversion into C_{2+} products, such as lower olefins ($\text{C}_2=\text{C}_4=$) and gasoline-range hydrocarbons ($\text{C}_5\text{-C}_{11}$), is a more attractive route toward the provision of valuable fuels/chemicals as complementary alternatives to fossil-derived chemicals. However, the chemical inertness of CO_2 and high energy barrier of C–C coupling remain significant challenges.^{253,254} Moreover, improving the selectivity toward heavy hydrocarbons with a desired carbon number distribution and bonding pattern (branched, saturated, or unsaturated) remains very difficult. This is not only because of the limitation of ASF distribution but also because of the relatively low adsorption heat of CO_2 on the catalyst surface. This leads to a high H/C ratio, which improves the hydrogenation rate of surface-adsorbed intermediates, and thus results in the methane formation and a decrease in carbon chain growth.^{255,256} In contrast to CO hydrogenation, CO_2 requires the initial reduction to CO via the RWGS followed by subsequent C–C coupling. This requires an efficient catalyst that should contain bifunctional active sites to match both RWGS and C–C coupling.^{257,258} In this regard, various bifunctional catalysts, which are typically combinations of transition metal or metal oxide catalysts and zeolites, have been intensively studied for the production of desired products, such as lower olefins or gasoline-range hydrocarbons.^{67,219,259–263} Both kinetic and thermodynamic coupling between the tandem reactions and the precise control of the proximity of the two active sites are key factors for the design and preparation of such bifunctional catalysts.

Gasoline-range hydrocarbons ($\text{C}_5\text{-C}_{11}$) can be produced via direct CO_2 hydrogenation (CO_2 -FT) through a combination of RWGS and FTS reactions. Modified Fe-based catalysts remain the preferred candidate for this process because of their excellent catalytic ability for both RWGS and FTS reactions

and the highly olefinic nature of the products.²⁶¹ Despite considerable efforts directed toward the development of catalysts, the selectivity toward C₅–C₁₁ hydrocarbons is insufficient due to the poor proximity between the different components of catalysts. In response, Sun et al.²⁶⁴ developed a multifunctional Na-Fe₃O₄/HZSM-5 nanocatalyst, which efficiently converted CO₂ to C₅–C₁₁ hydrocarbons with a high selectivity of 78% and only 4% methane selectivity at a CO₂ conversion of 22% under industrial conditions (320 °C, 3 MPa). The stability was maintained over 1000 h on stream. The reaction route involved the intermediate formation of olefins. The synergy between the three types of components (Fe₃O₄, Fe₅C₂, and zeolite) catalyzed the tandem reactions, which consists of RWGS over Fe₃O₄, olefin formation over Fe₅C₂, and olefin oligomerization/aromatization/isomerization over the acid sites of zeolite. Furthermore, it was reported that the simple combination of partially reducible In₂O₃ and HZSM-5 zeolites showed a C₅₊ selectivity as high as 78.6% in a hydrocarbon distribution with only 1% CH₄ at a CO₂ conversion of 13.1% under 340 °C and 3.0 MPa.²⁶⁵ No obvious catalyst deactivation was reported after 150 h reaction. Industry-relevant tests using the pellet catalyst showed that tail-gas recycling further improved the catalytic performance, indicating a promising industrial application prospect. Unlike the olefin-mediated process over the Na-Fe₃O₄/HZSM-5, DFT calculations indicated that the production of hydrocarbons over the In₂O₃/HZSM-5 catalyst involved methanol intermediate formation. The oxygen vacancies on the In₂O₃ surface activate CO₂ and H₂ and produce methanol, which was transformed into gasoline hydrocarbons with high octane number at the acidic sites of zeolite via a hydrocarbon-pool mechanism. The proximity of the two components plays a central role in inhibiting the unwanted RWGS reaction and providing high selectivity for gasoline-range hydrocarbons.

Direct synthesis of lower olefins via CO₂ hydrogenation is also a promising route for the reduction of CO₂ emission, which can be accomplished via methanol- or dimethyl ether (DME)-mediated reaction. Li et al.²⁶⁶ fabricated a tandem catalyst by dispersing the ZnO-ZrO₂ solid solution onto the Zn-promoted SAPO-34 zeolite. This achieved a high selectivity toward lower olefins of 80–90% with only 3% methane selectivity among the hydrocarbon products at a CO₂ conversion of 12.6% under 380 °C and 2.0 MPa. No obvious deactivation was observed after 100 h reaction. The reaction was realized on the basis of the bifunctionality the catalyst: the CO₂ hydrogenation to methanol happened over the ZnO-ZrO₂ solid solution and lower olefins formation over the SAPO zeolite. In situ DRIFT demonstrated that the CH_xO species (mainly surface CHO*, CH₃O*, and CH₃OH) were first produced on the ZnZrO surface and then transferred onto SAPO zeolite for the further conversion to hydrocarbons. Furthermore, the use of In–Zr oxide as methanol synthesis catalyst combined with SAPO-34 also exhibited a superior performance with a C₂=–C₄= selectivity of 80% and a C₂–C₄ selectivity of ~93% at 400 °C and 3.0 MPa.²⁶⁷ Notably, the single-pass conversion of CO₂ exceeded 35%. No obvious catalyst deactivation could be observed during 150 h reaction, indicating a potential for industrial application. The role of Zr was to create new types of vacancies and prevent the sintering of oxide NPs. The defects on the surface of In₂O₃ increased the stability of the key intermediates involved in the methanol synthesis, which significantly suppresses the unwanted RWGS reaction.

Fe-based catalysts are active for both RWGS reaction^{2,86} and CO hydrogenation to lower olefins,⁹¹ and they are considered as a candidate for CO₂ hydrogenation to olefins. Wang et al.²⁶⁸ systematically investigated the effects of supports (Al₂O₃, SiO₂, ZrO₂, TiO₂, mesoporous carbon, and carbon nanotube) and alkali metal promoters (K⁺, Na⁺, and Cs⁺) on the performance of Fe-based catalysts for CO₂ hydrogenation to lower olefins. The best performance was obtained over a K⁺-promoted Fe/ZrO₂ catalyst with a K⁺ content of 0.5–1 wt %. The yield of C₂–C₄ olefins reached 13% with a selectivity of ~45% in the hydrocarbons under 613 K, 2.0 MPa, F = 20 mL/min and H₂/CO = 3. The modification of K⁺ accelerated the formation of χ -Fe₅C₂ active species, enhanced the adsorption of CO₂, and decreased the hydrogenation ability.

In nature, enzymes in biomass can efficiently convert CO₂ into carbohydrates through the photosynthesis. Biomass contains an abundance of mineral elements, such as Mg, K, Si, and Ca, which are involved in the carbohydrate synthesis from CO₂. These mineral elements in biomass have an ideal composition that matches plant evolution and improves the biocatalytic activity of enzymes.²⁶⁹ Informed by the synergistic catalysis of mineral elements in biomass enzymes, Sun et al.²⁷⁰ designed an enzyme-like composite catalyst, comprising Fe carbides and alkali promoters from calcined corncob ash. Under 320 °C and 1.0 MPa, the catalyst achieved a alkenes selectivity of 72% and C_{4–18} alkenes selectivity of 50.3%. The linear α -olefins accounted for 80% at a CO₂ conversion rate of 31%. The CH₄ selectivity decreased to 11.8%. The mineral elements of corncob were proposed to promote the enrichment of K on the surface, thus inhibiting the secondary hydrogenation of alkenes. Furthermore, carburization of Fe species could be enhanced to form more Fe₅C₂ species, thus promoting both RWGS reaction and subsequent C–C coupling.

Although gasoline and olefins can be successfully synthesized via CO₂ hydrogenation, the direct synthesis of aromatics from CO₂ hydrogenation still remains challenging because of the complex structures and high unsaturation degree of aromatics. In a very recent work, Liu et al.²⁷¹ reported a composite catalyst consisting of nanosized spinel structure ZnAlO_x oxide and H-ZSM-5 zeolite (ZnAlO_x and H-ZSM-5), which achieved a high aromatics selectivity of 73.9% with only 0.4% CH₄ selectivity in the carbon products without CO at 593 K, 3.0 MPa, H₂/CO₂/Ar = 3/1/0.2 and space velocity of 6000 mL g⁻¹ h⁻¹. The RWGS reaction can be inhibited to a large extent by increasing the H₂/CO₂ ratio or by introducing CO. The Zn²⁺ in ZnAlO_x is the active site for CO₂ hydrogenation. The shielding of the external Brønsted acid of H-ZSM-5 by ZnAlO_x is conductive for aromatization. Methanol and dimethyl ether are the key reaction intermediates, which are produced by the hydrogenation of the formate species formed on the surface of ZnAlO_x. Then, both methanol and dimethyl ether are transferred to H-ZSM-5 and further converted to olefins and finally aromatics.

The direct transformation of CO₂ with CH₄ (instead of H₂) into liquid fuels is a further promising route for both CO₂ and CH₄ utilization. CH₄ is an ideal H supplier with high H density and availability from a variety of sources. It is also a cheap carbon source, which can increase the atom utilization efficiency while reducing the formation of water. Generally, the process is an indirect route that consists of two steps: the conversion of CO₂ and CH₄ to syngas at high temperatures and subsequently, the conversion of syngas into liquid fuels

under high pressure.²⁷² The harsh reaction conditions and catalyst deactivation due to coke deposition impact the commercial application. Integrating both steps into a one-step process under mild conditions, bypassing the production of syngas, is a significant challenge. Tu et al.²⁷³ achieved a significant breakthrough on this issue. The authors successfully achieved the one-step conversion of CH₄ and CO₂ into valuable liquid chemicals (mainly acetic acid) under ambient conditions using a plasma dielectric barrier discharge (DBD) reactor with a groundwater electrode. Because of its non-equilibrium nature, nonthermal plasma (NTP) provides a unique method to enable thermodynamically unfavorable chemical reactions at comparatively low temperature. Although the gas temperature is low, the generated electrons have a high energy of 1–10 eV, which is sufficient to activate inert molecules (such as CO₂ and CH₄) into reactive species. The combination of plasma and Cu/γ-Al₂O₃ catalyst shows excellent catalytic ability for the direct conversion of CH₄ and CO₂. Under ambient conditions, the total selectivity toward oxygenates reached about 50–60%. Acetic acid was the dominant product with a selectivity of 40.2%, which is the highest value for acetic acid reported so far (Figure 12). Interestingly, the reaction has 100% atom economy, which is almost impossible to reach via thermal catalysis because of the significant thermodynamic barrier.

4.4. CO₂ to Alcohols. The direct conversion of CO₂ hydrogenation to methanol has also attracted strong interests because of its central role in CO₂ utilization. However, this process faces several significant challenges: (1) the required CO₂ activation, (2) the negative effect of the byproduct CO produced via the RWGS on the methanol formation, (3) the catalyst deactivation caused by the formed H₂O via the RWGS, and (4) the requirement for an effective low-pressure catalyst. Cu-based catalysts, which have been widely studied for CO hydrogenation, have also been intensively studied in the hydrogenation of CO₂ because of their high activity for the activation and conversion of CO₂.^{274–277} Small size Cu NPs typically exhibit high catalytic activity, but they are often unstable because Cu NPs easily sinter during the reaction process. Moreover, using the Cu-based catalyst for low-pressure methanol synthesis from CO₂ hydrogenation can lead to a significant CO production.²⁷⁸ Guo et al.²⁷⁹ prepared a common Cu/SiO₂ nanocatalyst via an ammonia-evaporation method without using any structure promoters. Here, the active Cu NPs with an average size of about 2.1 nm are uniformly dispersed on the surface of SiO₂. At 320 °C and 3.0 MPa, the CO₂ conversion reached 28%, which is close to the equilibrium conversion (30%). The methanol selectivity was 21.3%, far exceeding the equilibrium selectivity of 6.6%. The Cu⁺ species were identified as the active component for the activation and conversion of CO₂. The high performance of the nanocatalyst could be attributed to the high ratio of Cu⁺/(Cu⁰ + Cu⁺). The excellent thermal stability (over 120 h reaction) was mainly attributed to the interaction between the metal and support, as shown in Figure 13.

In addition to the Cu-based catalyst, other metals/oxides systems are explored to maximize performance. Colloidal Pd₂Ga has been demonstrated to efficiently catalyze the liquid-phase CO₂ hydrogenation to methanol.²⁸⁰ The intrinsic activity was 2-fold higher than that of the benchmark Cu-ZnO-Al₂O₃ (60.3 vs 37.2 × 10⁻⁹ mol_{MeOH} m⁻² s⁻¹) and 4-fold higher based on a Pd or Cu molar content (3330 μmol mmol_{Pd}⁻¹ h⁻¹ vs 910 μmol mmol_{Cu}⁻¹ h⁻¹) at 50 bar and 210

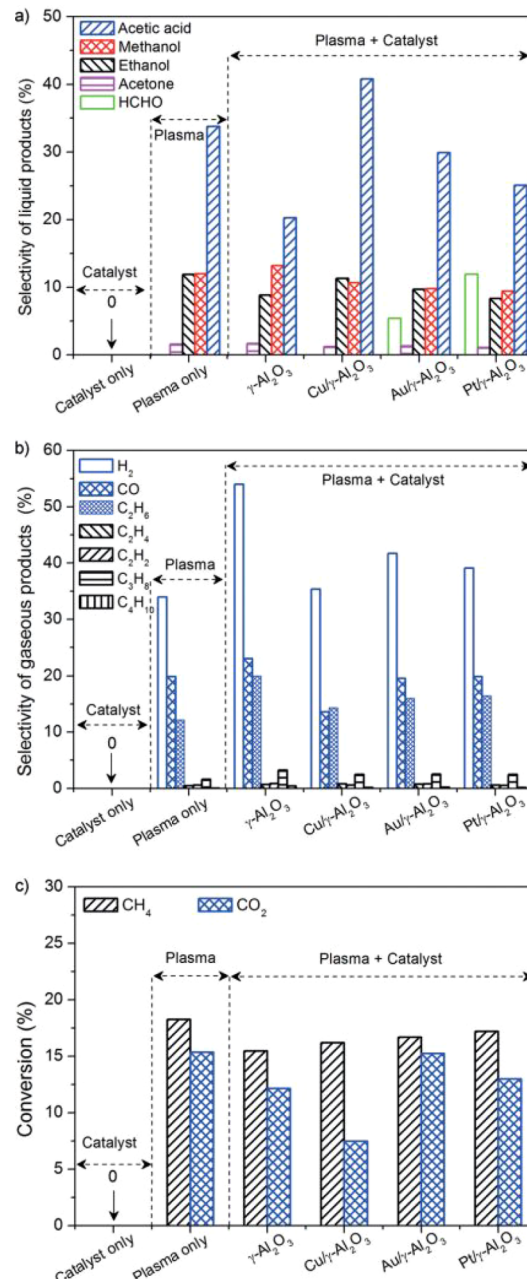


Figure 12. Effect of operating modes and catalysts on the reaction: (a) selectivities for oxygenates, (b) selectivities for gaseous products, and (c) conversion of CH₄ and CO₂ (total flow rate 40 mL·min⁻¹, discharge power 10 W, catalyst ca. 2 g).

°C. The activity increased with an increase of Ga₂O₃ content surrounding the Pd₂Ga NPs. The proposed reaction mechanism involves the formation of bi(carbonates) by CO₂ adsorption on Ga₂O₃ sites and subsequent hydrogenation of bi(carbonates) to produce formates, methylenebisoxo, methoxy species, and finally methanol. Ga₂O₃ can chemisorb and dissociate H₂ to obtain Ga–H species, which adsorbed CO₂ and hydrogenated the obtained carbonate groups. The Pd–Ga bimetallic crystallites provided atomic hydrogen for hydrogenation reaction and improving the concentration of carbonaceous intermediates that bond to Ga₂O₃.

Norskov et al.²⁷⁸ predicted a new class of Ni–Ga low-pressure catalysts using a computational descriptor-based approach and showed experimentally that it has the unique

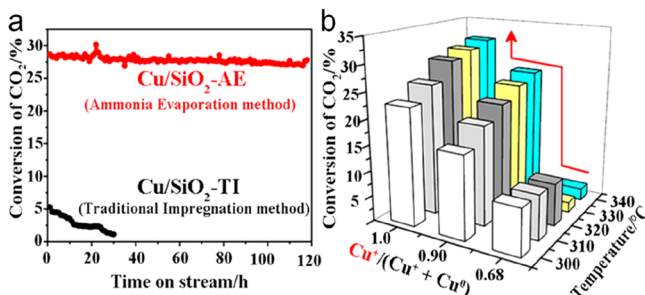


Figure 13. (a) Conversion of CO_2 as a function of time on-stream at $320\text{ }^\circ\text{C}$ and 3.0 MPa , (b) three-dimensional histogram of conversion of CO_2 , $\text{Cu}^+/\text{(Cu}^0 + \text{Cu}^+\text{)}$, and reaction temperature.

ability for methanol synthesis from CO_2 hydrogenation without significant CO production via RWGS. Above $220\text{ }^\circ\text{C}$ and under atmosphere pressure, the optimal Ni_5Ga_3 exhibited a higher methanol yield compared to the commercial $\text{Cu}/\text{ZnO}/\text{Al}_2\text{O}_3$ (0.20 vs $0.15\text{ mol/(active metal)\cdot h}$), with a selectivity of almost 100% including all products except CO. Notably, the Ni_5Ga_3 exhibited a significantly lower CO-to-methanol ratio than that of $\text{Cu}/\text{ZnO}/\text{Al}_2\text{O}_3$ (1.0 vs 10.0). These results provide a good start toward a new catalyst system. It is expected that this catalytic performance can be further improved after systematic optimization. A hybrid catalyst consisting of MnO_x NPs supported on mesoporous Co_3O_4 has also been reported to be highly active for CO_2 conversion to methanol under mild conditions.²⁸¹ This catalyst achieved a 30% selectivity and 0.18 s^{-1} yield for methanol synthesis, which is approximately 10 -fold higher compared with commercial Cu/ZnO catalysts (0.01 – 0.020 s^{-1}) under high pressure (10 – 50 atm). In addition to methanol, ethylene was also produced with a selectivity of 10% , indicating a C–C-bond-coupling reaction. The active phase consisted of MnO NPs that were dispersed on cobalt grains comprising a CoO shell with a metallic Co core. The formation of the MnO/CoO interface led to an enhanced activity for methanol production as compared with separate NPs and supports. Curtiss et al.²⁸² reported a very promising low-pressure catalyst (Al_2O_3 supported size-selected Cu_4 clusters), which exhibited the highest activity reported so far for CO_2 hydrogenation to methanol at a very low partial pressure of CO_2 (0.013 atm). Compared with the commercial $\text{Cu}/\text{ZnO}/\text{Al}_2\text{O}_3$ and recently developed $\text{Ni}_5\text{Ga}_3/\text{SiO}_2$ at ambient pressure, the Cu_4 cluster catalyst exhibited 1 order of magnitude higher activity at a slightly higher total pressure (1.25 atm), but with much lower partial pressures of CO_2 and H_2 (decreased by up to 2 orders of magnitude). DFT calculations indicated that Cu_4 clusters have a low activation barrier for the methanol synthesis from CO_2 hydrogenation. The unique coordination environment of Cu atoms in the size-selected Cu_4 clusters achieved superiority of active sites over larger Cu particles. The Cu_4 clusters catalyst displayed strong potential for the development of new generation of low-pressure catalysts for methanol synthesis from CO_2 hydrogenation, using alternative feed gas with low CO_2 concentration.

Compared with methanol synthesis, the direct synthesis of ethanol through CO_2 hydrogenation becomes more difficult since it requires an additional C–C coupling step. Homogeneous catalysts with air-sensitive organic ligands can effectively catalyze CO_2 hydrogenation to ethanol;^{283,284} however, these homogeneous catalysts are difficult to be regenerated or

separate from the reaction products. Over the past few years, noble-metal catalysts (Pt and Pd) have received considerable interest because of their ability to catalyze C–C coupling.²⁸⁵ However, achieving high ethanol selectivity remains the major challenge due to the coformation of methanol and other C_{2+} alcohols. Recently, Huang et al.²²⁰ reported highly ordered Pd–Cu NPs by using a wet-chemical approach. The optimized Pd_2Cu NPs/P25 achieved a high $\text{C}_2\text{H}_5\text{OH}$ selectivity of 92.0% and showed the highest TOF_{Pd} of 359.0 h^{-1} compared with all previously reported catalysts under $200\text{ }^\circ\text{C}$ and 3.2 MPa with a ratio of $\text{H}_2/\text{CO}_2 = 3:1$. The $\text{C}_2\text{H}_5\text{OH}$ yield was still as high as $38.3\text{ mmol g}^{-1}\text{ h}^{-1}$ (92.3% of the initial value) after six cycles. This improved selectivity was caused by the charge transfer between Pd and Cu, which enhanced the reducibility of the surface oxide. This high activity was attributed to the 3 -fold bridge-bonded *CO species with a low coverage over Pd atoms, which were more easily converted to ethanol than 2 -fold bridge-bonded *CO species.

Replacement of noble metals with inexpensive and abundant first-row transition metals, such as cobalt, has been proposed as a more economic and sustainable alternative, since these transition metals are well-known as efficient catalysts for the C–C coupling reaction (e.g., FTS).^{286,287} An abundant cobalt catalyst derived from the Co–Al layered double hydroxide (LDH) was reported to be highly selective for CO_2 hydrogenation to ethanol.²⁸⁸ After reduction at $600\text{ }^\circ\text{C}$, the catalyst showed an ethanol selectivity of 92.1% with the ethanol yield of $0.444\text{ mmol\cdot g}^{-1}\text{ h}^{-1}$ at $140\text{ }^\circ\text{C}$, 4.0 MPa . This catalytic performance outperformed all previously reported abundant-metal catalysts and also competes with the best Pt catalysts. The improved performance could be ascribed to the optimized presence of surface coexisting Co–CoO phases by optimizing the reduction temperature. This improved the production of $^{*}\text{CH}_x$ for the conversion of formate into acetate via insertion, which is an important intermediate for the ethanol production.

5. METHANOL CONVERSION

5.1. Methanol to Hydrogen. Methanol steam reforming (MSR; $\text{CH}_3\text{OH} + \text{H}_2\text{O} \rightarrow 3\text{H}_2 + \text{CO}_2$) has been considered as an important building block for the provision of clean hydrogen for the use in fuel cells. The main challenge is to suppress the CO formation, because the fuel cell catalysts only tolerate CO concentrations up to 50 ppm .²⁸⁹ Furthermore, low-temperature activity is highly desirable to optimize heat utilization between endothermic reforming process and exothermic fuel cell operation. The temperature limit for high-temperature proton exchange membrane (PEM) fuel cell is $180\text{ }^\circ\text{C}$,²⁹⁰ which is too low to operate an MSR reaction with high hydrogen yields.

Two different classes of heterogeneous catalysts dominate both research and industrial practice of MSR: Pd or Pt on different support types and Cu/ZnO systems.^{56,57} Iwasa et al.²⁹¹ were the first to describe the high catalytic performance of the Pd/ZnO catalyst for MSR and ascribed it to the formation of PdZn alloy. Interestingly, Dumesic et al.²⁹² developed a Pt/ Al_2O_3 catalyst that enables MSR at more acceptable temperatures (200 – $225\text{ }^\circ\text{C}$) and pressure (25 – 50 bar) levels. Inspired by homogeneous catalysts and metalloenzymes,^{293–295} efforts have been focused on dispersing active noble metals as isolated metal atoms to improve the catalytic efficiency while minimizing the amount of noble metal required.^{296–298} However, for a catalyst that contains only an

isolated metal site, it is difficult to effectively activate both water and methanol at the same time, which is the primary requirement for low-temperature MSR. To overcome these issues, Ma et al.²⁹⁹ developed a novel bifunctional Pt/ α -MoC catalyst. Driven by the strong interaction derived from α -MoC, Pt forms an atomic dispersion over α -MoC, thus producing an exceptionally high density of electron-deficient surface Pt sites for both the adsorption or activation of methanol. Moreover, the α -MoC support showed high water-dissociation activity and generated abundant surface hydroxyls, thus accelerating the MSR at the interface between Pt and α -MoC. This synergistic effect equips the catalyst with unprecedented activity and good stability for MSR at temperature ranges of 150–190 °C. The average TOF reached 18 046 mol H₂·mol_{Pt}⁻¹·h⁻¹, which is much higher than that of previous low-temperature MSR catalysts and meets the requirements for state-of-the-art PEMFC vehicle applications. Interestingly, no base was involved in the entire process, making this system both simple to operate and sustainable. It is further encouraging that the CO selectivity remained below 0.1%, indicating that it could be removed easily. In an 11-cycle test, the catalyst achieved a total turnover number of more than 132 000 for each platinum atom, generating about 1.68 mol hydrogen per gram of utilized catalyst. This new catalyst paves the way toward a commercially achievable hydrogen storage strategy.

In addition to working on the catalyst itself, a simple and efficient surface-modification strategy has been reported by Wasserscheid et al.,³⁰⁰ which significantly improved the catalytic performance of the Pt/Al₂O₃ catalyst for MSR. The strategy aimed to improve the mass transfer efficiency of reactants/products on the catalyst by coating a thin film of hygroscopic and basic inorganic salt Li/K/Cs acetate on the surface of Pt/Al₂O₃ catalyst. The coated catalyst showed a much higher CO₂ selectivity (99% vs 62%) and a significantly higher TOF based on the total Pt content (50 h⁻¹ vs 22 h⁻¹) at 230 °C compared with the catalyst without coating. The catalytic performance remained stable over a 500-h reaction. The reasons for this behavior include the fact that the coating of molten salt is very hygroscopic and basic, consequently increasing the availability of water at the active sites, while the very low solubility of H₂ in the salt leads to the effective H₂ removal from the surface. Furthermore, the basic acetate coating clearly enhanced the rate of WGS, causing a drastic shift in CO₂ selectivity. This surface-coating strategy is simple and universal, and therefore, it has the potential to be extended to other catalyst systems.

In addition to advanced noble-metal catalysts, particular attention also focused on the less expensive and more abundant Cu/ZnO systems; however, they require higher temperatures than the Pt catalyst.⁵⁷ A novel nonsyngas direct steam reforming (NSGDSR) route has been developed by Tsang et al.³⁰¹ for the methanol conversion to hydrogen using a CuZnGaO_x catalyst. This route is in clear contrast to the conventional complex route, which involves steam reforming to syngas at high temperature, followed by WGS and CO purification steps for hydrogen production. The CuZnGaO_x catalyst contains 3–4 nm Cu particles, along with extremely small Cu clusters that are stabilized on a defective surface of spinel ZnGa₂O₄. High-quality hydrogen can be produced over the catalyst at 150 °C and atmospheric pressure without detectable CO. The hydrogen production rate reached 393.6 mL·g⁻¹cat·h⁻¹ at a CH₃OH conversion of 22.5%. The energy is

sufficient to support the practical applications for small mobile devices using methanol and water as fuel without complex devices or pretreatment or postprocessing. Such catalytic performance has not been reported prior to this work and is clearly an important breakthrough. This route is technically feasible and can provide high-quality hydrogen for small mobile fuel cell devices. The outstanding MSR performance is caused by the presence of small-sized Cu islands under high isomeric strain on the support or catalyst structure, which provides optimal balance between Cu⁰ and Cu⁺. The catalyst remained stable for at least several days under the testing conditions. However, the long-term stability is not reported to date.

Spinel Cu-based catalysts (CuAl₂O₄, CuFe₂O₄, and CuCr₂O₄) are also candidate materials for MSR. The main advantage of this catalyst is that no prereduction is required before reaction, which not only avoids Cu sintering but also inhibits the Cu sintering during the reaction. Gao et al.³⁰² prepared a Cu-Al spinel oxide that contains a small amount of CuO phase via a green and simple solid-phase method. The catalyst calcined at 900 °C has a high CuAl₂O₄ content (91.8%), high BET surface area (33.1 m²g⁻¹), and small CuAl₂O₄ crystal size (8.5 nm). During the reaction, the CuO initiated MSR at a low temperature, and CuAl₂O₄ gradually released active Cu. Moreover, the catalytic performance could be further improved via addition of an appropriate amount of additional Al₂O₃ to increase the surface area and dispersion of CuAl₂O₄. The methanol conversion rate in MSR for the Cu-Al spinel oxide reached ~9.0 mmol s⁻¹ kg⁻¹ after 600 h on-stream at 240 °C and 1.0 MPa, which far exceeds the commercial Cu-Zn-Al catalyst (~5.0 mmol s⁻¹ kg⁻¹). The tested catalyst can be almost completely regenerated by calcination at 900 °C in air.

6. CONCLUSIONS, CHALLENGES, AND PERSPECTIVES

Induced by the gradual depletion of fossil fuels and the need to reduce greenhouse gas emissions, over the past decades, C1 catalysis has attracted widespread academic and industrial interest and became one of the most attractive research fields in heterogeneous catalysis. This Review focused on the latest developments (from 2012 to 2018) of highly efficient catalysts and new reaction processes in this field. For an overview, the details of these catalyst systems and their performance have been summarized in Table S1. These new catalyst systems and reaction processes are of great interest for both academia and industry and will require further studies to elucidate the mechanism, optimization of the catalysts, and practical processes. Furthermore, many challenges exist, as discussed in the following.

The synthesis of lower olefins from syngas has achieved a significant breakthrough. The OX-ZEO process shows promising potential for scale-up industrial application due to its unparalleled performance, requirement of relatively mild reaction conditions, and less expensive components; it has therefore become a strong competitor for other industrial processes such as MTO. The concept of a core–shell structured bifunctional catalyst provides a simple and effective approach for the tuning of the FTS product distribution, which may also be extended to other tandem catalytic reactions by varying the different compositions. Future work should focus on improving single-pass conversion, suppressing CH₄ and CO₂ selectivity, and enhancing catalyst stability. The HAS

reaction has received great attention in recent years. Despite remarkable improvements in improving the C₂₊ alcohols selectivity and suppressing the formation of methanol and CO₂, none of the catalysts or processes that have been developed to date feature a sufficient performance to justify their industrial commercialization. The exact nature of the active phase and insights into the reaction mechanism remain unclear. New efforts toward an improved understanding and the closure of these gaps are required to obtain superior HAS catalysts.

Methane conversion is currently the most active research area in C1 catalysis. Despite the achievement of many high-value-added products (e.g., aromatics, methanol, oxygenates, and olefins) that can be produced via direct conversion of CH₄, large-scale industrial applications have not achieved substantial progress to date. The unefficient activation of C—H in CH₄ under mild conditions, low selectivity of target products caused by overoxidation, and catalyst deactivation have been their greatest obstacles. New proposed catalytic reaction processes, such as the “super dry” reforming, the self-sufficient oxidative bireforming, or the CMR process, have been demonstrated to effectively circumvent the equilibrium limitation and increase product yields. In addition, atomic dispersed single site catalysts, such as the highly efficient Fe@SiO₂ for MDA, are also promising new catalyst system. However, the long-term stability of these catalysts systems and processes remains challenging. In addition, future studies aimed to identify the nature of the active sites and to understand the reaction mechanism in these advanced catalysts, especially in the zeolite catalysts, through a true reaction process would be an imperative step toward establishing the structure–performance relationship.

The direct conversion of CO₂ has often been regarded as a combination of CO₂ reduction to CO via the RWGS reaction and the subsequent CO hydrogenation to desired products, such as methanol, olefins, or hydrocarbons. This process faces several significant challenges, including CO₂ activation under mild conditions, the negative impact of CO produced via RWGS reaction, and the high H/C ratio obtained due to the relatively low adsorption heat of CO₂ on the catalyst surface. Active catalysts typically contain two or more different active sites, namely, bifunctional/multifunctional catalysts. Kinetic and thermodynamic coupling between tandem reactions and the precise control of the proximity between different active sites are key factors for the design and preparation of multifunctional catalysts. Several newly developed catalyst compositions, such as In-Zr/SAPO-34 for olefins synthesis, Na-Fe₃O₄/HZSM-5 for C₅–C₁₁ hydrocarbons, and Cu₄ clusters on Al₂O₃ for methanol synthesis, showed promising potential for industrial application. Although specific performance descriptors have been identified in these systems so far, the exact structure of the multiple active sites and the synergy between them remain unclear.

Of all known hydrogen storage materials, methanol represents a promising energy carrier for the provision of clear hydrogen through the MSR reaction. Two different classes of heterogeneous catalysts (Pd or Pt-based and Cu-based systems) dominate both research and industrial practice. Suppressing the CO formation, improving low-temperature activity, and enhancing catalyst stability are the main research targets. In general, Cu-based catalysts are more active while noble metals-based catalysts present improved thermal and long-term stability. The emerging Pt/α-MoC and CuZnGaO_x

are the latest and very promising catalysts in their respective systems. Both of them present superior MSR performance at low temperature. Long-term stability requires further investigation, especially with regard to the CuZnGaO_x. The exact nature and structure of active surface copper clusters during the reaction are still unclear.

In conclusion, the highly efficient conversion of C1 compounds into high-value-added fuels or chemicals remains a long-pursued target for C1 catalysis. Recent developments on advanced catalysts and new reaction processes in this field have provided important guidance for the design of next-generation catalysts and have stimulated intensive attention toward an improved understanding of the nature of active sites, reaction mechanisms, and the establishment of the structure–performance relationship.

ASSOCIATED CONTENT

Supporting Information

The Supporting Information is available free of charge on the ACS Publications website at DOI: [10.1021/acscatal.8b03924](https://doi.org/10.1021/acscatal.8b03924).

Details of these highly efficient catalyst systems and their performance ([PDF](#))

AUTHOR INFORMATION

Corresponding Authors

*E-mail: baoj@ustc.edu.cn.

*E-mail: tsubaki@eng.u-toyama.ac.jp.

ORCID

Jun Bao: [0000-0002-1812-8999](https://orcid.org/0000-0002-1812-8999)

Noritatsu Tsubaki: [0000-0001-6786-5058](https://orcid.org/0000-0001-6786-5058)

Notes

The authors declare no competing financial interest.

ACKNOWLEDGMENTS

The work is supported by the National Nature Science Foundation of China (21673214, U1732272), the National Key R&D Program of China (2017YFA0403402), the Japan Science and Technology Agency (MIRAI-JPMJMI17E2), and the JST-CREST project (Grant number: 17-141003297).

REFERENCES

- (1) Jahangiri, H.; Bennett, J.; Mahjoubi, P.; Wilson, K.; Gu, S. A review of advanced catalyst development for Fischer–Tropsch synthesis of hydrocarbons from biomass derived syn-gas. *Catal. Sci. Technol.* **2014**, *4*, 2210–2229.
- (2) Zhang, Q.; Kang, J.; Wang, Y. Development of Novel Catalysts for Fischer–Tropsch Synthesis: Tuning the Product Selectivity. *ChemCatChem* **2010**, *2*, 1030–1058.
- (3) Rofer-DePoorter, C. K. A Comprehensive Mechanism for the Fischer–Tropsch Synthesis. *Chem. Chem. Rev.* **1981**, *81*, 447–474.
- (4) Henrici-Olive, G.; Olive, S. The Fischer–Tropsch Synthesis: Molecular Weight Distribution of Primary Products and Reaction Mechanism. *Angew. Chem., Int. Ed. Engl.* **1976**, *15*, 136–141.
- (5) Van Der Laan, G. P.; Beenackers, A. A. C. M. Kinetics and Selectivity of the Fischer–Tropsch Synthesis: A Literature Review. *Catal. Rev.: Sci. Eng.* **1999**, *41*, 255–318.
- (6) Ojeda, M.; Nabar, R.; Nilekar, A. U.; Ishikawa, A.; Mavrikakis, M.; Iglesia, E. CO activation pathways and the mechanism of Fischer–Tropsch synthesis. *J. Catal.* **2010**, *272*, 287–297.
- (7) Peña, D.; Jensen, L.; Cognigni, A.; Myrstad, R.; Neumayer, T.; van Beek, W.; Ronning, M. The Effect of Copper Loading on Iron Carbide Formation and Surface Species in Iron-Based Fischer–Tropsch Synthesis Catalysts. *ChemCatChem* **2018**, *10*, 1300–1312.

- (8) Cheng, K.; Virginie, M.; Ordomsky, V. V.; Cordier, C.; Chernavskii, P. A.; Ivantsov, M. I.; Paul, S.; Wang, Y.; Khodakov, A. Y. Pore size effects in high-temperature Fischer–Tropsch synthesis over supported iron catalysts. *J. Catal.* **2015**, *328*, 139–150.
- (9) Li, S.; Krishnamoorthy, S.; Li, A.; Meitzner, G. D.; Iglesia, E. Promoted Iron-Based Catalysts for the Fischer–Tropsch Synthesis: Design, Synthesis, Site Densities, and Catalytic Properties. *J. Catal.* **2002**, *206*, 202–217.
- (10) Wezendonk, T. A.; Sun, X.; Dugulan, A. I.; van Hoof, A. J. F.; Hensen, E. J. M.; Kapteijn, F.; Gascon, J. Controlled formation of iron carbides and their performance in Fischer–Tropsch synthesis. *J. Catal.* **2018**, *362*, 106–117.
- (11) Iglesia, E. Design, synthesis, and use of cobalt-based Fischer–Tropsch synthesis catalysts. *Appl. Catal., A* **1997**, *161*, 59–78.
- (12) Lyu, S.; Wang, L.; Zhang, J.; Liu, C.; Sun, J.; Peng, B.; Wang, Y.; Rappé, K. G.; Zhang, Y.; Li, J.; Nie, L. Role of Active Phase in Fischer–Tropsch Synthesis: Experimental Evidence of CO Activation over Single-Phase Cobalt Catalysts. *ACS Catal.* **2018**, *8*, 7787–7798.
- (13) van Deelen, T. W.; Su, H.; Sommerdijk, N.; de Jong, K. P. Assembly and activation of supported cobalt nanocrystal catalysts for the Fischer–Tropsch synthesis. *Chem. Commun. (Cambridge, U. K.)* **2018**, *S4*, 2530–2533.
- (14) Dry, M. E. Fischer–Tropsch synthesis over iron catalysts. *Catal. Lett.* **1991**, *7*, 241–252.
- (15) Khodakov, A. Y.; Chu, W.; Fongarland, P. Advances in the Development of Novel Cobalt Fischer–Tropsch Catalysts for Synthesis of Long-Chain Hydrocarbons and Clean Fuels. *Chem. Rev.* **2007**, *107*, 1692–1744.
- (16) Luk, H. T.; Mondelli, C.; Ferre, D. C.; Stewart, J. A.; Perez-Ramirez, J. Status and prospects in higher alcohols synthesis from syngas. *Chem. Soc. Rev.* **2017**, *46*, 1358–1426.
- (17) Davies, P.; Snowdon, F. Production of oxygenated hydrocarbons. U.S. Patent No. 3326956. 1963.
- (18) Lu, Y.; Zhang, R.; Cao, B.; Ge, B.; Tao, F. F.; Shan, J.; Nguyen, L.; Bao, Z.; Wu, T.; Pote, J. W.; Wang, B.; Yu, F. Elucidating the Copper–Hägg Iron Carbide Synergistic Interactions for Selective CO Hydrogenation to Higher Alcohols. *ACS Catal.* **2017**, *7*, 5500–5512.
- (19) Liu, Y.; Liu, C.; Li, C.; Huang, W. CO hydrogenation to higher alcohols over Cu/Zn/Al catalysts without alkalis or Fischer–Tropsch elements: The effect of triethanolamine content. *Catal. Commun.* **2016**, *76*, 29–32.
- (20) Liu, Y.-J.; Zuo, Z.-J.; Liu, C.-B.; Li, C.; Deng, X.; Huang, W. Higher alcohols synthesis via CO hydrogenation on Cu/Zn/Al/Zr catalysts without alkalis and F-T elements. *Fuel Process. Technol.* **2016**, *144*, 186–190.
- (21) Anton, J.; Nebel, J.; Song, H.; Froese, C.; Weide, P.; Ruland, H.; Muhler, M.; Kaluza, S. The effect of sodium on the structure-activity relationships of cobalt-modified Cu/ZnO/Al₂O₃ catalysts applied in the hydrogenation of carbon monoxide to higher alcohols. *J. Catal.* **2016**, *335*, 175–186.
- (22) Pei, Y.-P.; Liu, J.-X.; Zhao, Y.-H.; Ding, Y.-J.; Liu, T.; Dong, W.-D.; Zhu, H.-J.; Su, H.-Y.; Yan, L.; Li, J.-L.; Li, W.-X. High Alcohols Synthesis via Fischer–Tropsch Reaction at Cobalt Metal/Carbide Interface. *ACS Catal.* **2015**, *5*, 3620–3624.
- (23) Zhang, R.; Wen, G.; Adidharma, H.; Russell, A. G.; Wang, B.; Radosz, M.; Fan, M. C₂ Oxygenate Synthesis via Fischer–Tropsch Synthesis on Co₂C and Co/Co₂C Interface Catalysts: How To Control the Catalyst Crystal Facet for Optimal Selectivity. *ACS Catal.* **2017**, *7*, 8285–8295.
- (24) Taborga Clauere, M.; Morrill, M. R.; Goh, J. W.; Chai, S.-H.; Dai, S.; Agrawal, P. K.; Jones, C. W. Insight into reaction pathways in CO hydrogenation reactions over K/MoS₂supported catalysts via alcohol/olefin co-feed experiments. *Catal. Sci. Technol.* **2016**, *6*, 1957–1966.
- (25) Morrill, M. R.; Thao, N. T.; Shou, H.; Davis, R. J.; Barton, D. G.; Ferrari, D.; Agrawal, P. K.; Jones, C. W. Origins of Unusual Alcohol Selectivities over Mixed MgAl Oxide-Supported K/MoS₂ Catalysts for Higher Alcohol Synthesis from Syngas. *ACS Catal.* **2013**, *3*, 1665–1675.
- (26) Liu, Y.; Göeltl, F.; Ro, I.; Ball, M. R.; Sener, C.; Aragão, I. B.; Zanchet, D.; Huber, G. W.; Mavrikakis, M.; Dumesic, J. A. Synthesis Gas Conversion over Rh-Based Catalysts Promoted by Fe and Mn. *ACS Catal.* **2017**, *7*, 4550–4563.
- (27) Huang, W.; Zhang, S.; Tang, Y.; Li, Y.; Nguyen, L.; Li, Y.; Shan, J.; Xiao, D.; Gagne, R.; Frenkel, A. I.; Tao, F. F. Low-Temperature Transformation of Methane to Methanol on Pd₁O₄ Single Sites Anchored on the Internal Surface of Microporous Silicate. *Angew. Chem., Int. Ed.* **2016**, *55*, 13441–13445.
- (28) Lee, E.; Cheng, Z.; Lo, C. S. Present and future prospects in heterogeneous catalysts for C1 chemistry. *Catalysis*; Royal Society of Chemistry: London, U.K., 2015; Vol. 27, pp 187–208. DOI: [10.1039/9781782622697-00187](https://doi.org/10.1039/9781782622697-00187)
- (29) Duarte, R. B.; Krumeich, F.; van Bokhoven, J. A. Structure, Activity, and Stability of Atomically Dispersed Rh in Methane Steam Reforming. *ACS Catal.* **2014**, *4*, 1279–1286.
- (30) Jones, G.; Jakobsen, J.; Shim, S.; Kleis, J.; Andersson, M.; Rossmeisl, J.; Abildpedersen, F.; Bligaard, T.; Helveg, S.; Hinnemann, B. First principles calculations and experimental insight into methane steam reforming over transition metal catalysts. *J. Catal.* **2008**, *259*, 147–160.
- (31) Besenbacher, F.; Chorkendorff, I.; Clausen, B. S.; Hammer, B.; Molenbroek, A. M.; Norskov, J. K.; Stensgaard, I. Design of a Surface Alloy Catalyst for Steam Reforming. *Science* **1998**, *279*, 1913–1915.
- (32) Mette, K.; Kühl, S.; Tarasov, A.; Willinger, M. G.; Kröhnert, J.; Wrabetz, S.; Trunschke, A.; Scherzer, M.; Girgsdies, F.; Düdder, H.; Kähler, K.; Ortega, K. F.; Muhler, M.; Schlögl, R.; Behrens, M.; Lunkenbein, T. High-Temperature Stable Ni Nanoparticles for the Dry Reforming of Methane. *ACS Catal.* **2016**, *6*, 7238–7248.
- (33) Verykios, X. Mechanistic aspects of the reaction of CO₂ reforming of methane over Rh/Al₂O₃ catalyst. *Appl. Catal., A* **2003**, *255*, 101–111.
- (34) Sepehri, S.; Rezaei, M.; Garbarino, G.; Busca, G. Preparation and characterization of mesoporous nanocrystalline La-, Ce-, Zr-, Sr-containing NiAl₂O₃ methane autothermal reforming catalysts. *Int. J. Hydrogen Energy* **2016**, *41*, 8855–8862.
- (35) Luneau, M.; Gianotti, E.; Guilhaume, N.; Landrivon, E.; Meunier, F. C.; Mirodatos, C.; Schuurman, Y. Experiments and Modeling of Methane Autothermal Reforming over Structured Ni–Rh-Based Si–SiC Foam Catalysts. *Ind. Eng. Chem. Res.* **2017**, *56*, 13165–13174.
- (36) Kondratenko, V. A.; Berger-Karin, C.; Kondratenko, E. V. Partial Oxidation of Methane to Syngas Over γ-Al₂O₃-Supported Rh Nanoparticles: Kinetic and Mechanistic Origins of Size Effect on Selectivity and Activity. *ACS Catal.* **2014**, *4*, 3136–3144.
- (37) Wang, F.; Li, W.-Z.; Lin, J.-D.; Chen, Z.-Q.; Wang, Y. Crucial support effect on the durability of Pt/MgAl₂O₄ for partial oxidation of methane to syngas. *Appl. Catal., B* **2018**, *231*, 292–298.
- (38) Pakhare, D.; Schwartz, V.; Abdelsayed, V.; Haynes, D.; Shekhawat, D.; Poston, J.; Spivey, J. Kinetic and mechanistic study of dry (CO₂) reforming of methane over Rh-substituted La₂Zr₂O₇ pyrochlores. *J. Catal.* **2014**, *316*, 78–92.
- (39) Iijima, T.; Yamaguchi, T. K₂CO₃-catalyzed direct synthesis of salicylic acid from phenol and supercritical CO₂. *Appl. Catal., A* **2008**, *345*, 12–17.
- (40) Pokrovski, K.; Bell, A. Effect of dopants on the activity of Cu/M0.3Zr0.7O₂ (M = Ce, Mn, and Pr) for CO hydrogenation to methanol. *J. Catal.* **2006**, *244*, 43–51.
- (41) Dai, W.-L.; Luo, S.-L.; Yin, S.-F.; Au, C.-T. The direct transformation of carbon dioxide to organic carbonates over heterogeneous catalysts. *Appl. Catal., A* **2009**, *366*, 2–12.
- (42) Guo, X.; Mao, D.; Lu, G.; Wang, S.; Wu, G. CO₂ hydrogenation to methanol over Cu/ZnO/ZrO₂ catalysts prepared via a route of solid-state reaction. *Catal. Commun.* **2011**, *12*, 1095–1098.
- (43) Gao, P.; Li, F.; Zhan, H.; Zhao, N.; Xiao, F.; Wei, W.; Zhong, L.; Wang, H.; Sun, Y. Influence of Zr on the performance of Cu/Zn/Al/Zr catalysts via hydrotalcite-like precursors for CO₂ hydrogenation to methanol. *J. Catal.* **2013**, *298*, 51–60.

- (44) Natesakhawat, S.; Lekse, J. W.; Baltrus, J. P.; Ohodnicki, P. R.; Howard, B. H.; Deng, X.; Matranga, C. Active Sites and Structure–Activity Relationships of Copper-Based Catalysts for Carbon Dioxide Hydrogenation to Methanol. *ACS Catal.* **2012**, *2*, 1667–1676.
- (45) Kattel, S.; Ramírez, P. J.; Chen, J. G.; Rodriguez, J. A.; Liu, P. Active sites for CO₂ hydrogenation to methanol on Cu/ZnO catalysts. *Science* **2017**, *355*, 1296–1299.
- (46) Jiang, X.; Koizumi, N.; Guo, X.; Song, C. Bimetallic Pd–Cu catalysts for selective CO₂ hydrogenation to methanol. *Appl. Catal., B* **2015**, *170–171*, 173–185.
- (47) Liang, X.-L.; Dong, X.; Lin, G.-D.; Zhang, H.-B. Carbon nanotube-supported Pd–ZnO catalyst for hydrogenation of CO₂ to methanol. *Appl. Catal., B* **2009**, *88*, 315–322.
- (48) Bahruji, H.; Bowker, M.; Hutchings, G.; Dimitratos, N.; Wells, P.; Gibson, E.; Jones, W.; Brookes, C.; Morgan, D.; Lalev, G. Pd/ZnO catalysts for direct CO₂ hydrogenation to methanol. *J. Catal.* **2016**, *343*, 133–146.
- (49) Jadhav, S. G.; Vaidya, P. D.; Bhanage, B. M.; Joshi, J. B. Catalytic carbon dioxide hydrogenation to methanol: A review of recent studies. *Chem. Eng. Res. Des.* **2014**, *92*, 2557–2567.
- (50) Zhu, H.; Razzaq, R.; Li, C.; Muhammad, Y.; Zhang, S. Catalytic Methanation of Carbon Dioxide by Active Oxygen Material Ce_xZr_{1-x}O₂ Supported Ni-Co Bimetallic Nanocatalysts. *AIChE J.* **2013**, *59*, 2567–2576.
- (51) Liu, J.; Li, C.; Wang, F.; He, S.; Chen, H.; Zhao, Y.; Wei, M.; Evans, D. G.; Duan, X. Enhanced low-temperature activity of CO₂ methanation over highly-dispersed Ni/TiO₂ catalyst. *Catal. Sci. Technol.* **2013**, *3*, 2627–2633.
- (52) He, S.; Li, C.; Chen, H.; Su, D.; Zhang, B.; Cao, X.; Wang, B.; Wei, M.; Evans, D. G.; Duan, X. A Surface Defect-Promoted Ni Nanocatalyst with Simultaneously Enhanced Activity and Stability. *Chem. Mater.* **2013**, *25*, 1040–1046.
- (53) Aziz, M. A. A.; Jalil, A. A.; Triwahyono, S.; Ahmad, A. CO₂ methanation over heterogeneous catalysts: recent progress and future prospects. *Green Chem.* **2015**, *17*, 2647–2663.
- (54) Chang, C. D.; Silvestri, A. J. *J. Catal.* **1977**, *47*, 249–259.
- (55) Tian, P.; Wei, Y.; Ye, M.; Liu, Z. Methanol to Olefins (MTO): From Fundamentals to Commercialization. *ACS Catal.* **2015**, *5*, 1922–1938.
- (56) Sá, S.; Silva, H.; Brandão, L.; Sousa, J. M.; Mendes, A. Catalysts for methanol steam reforming—A review. *Appl. Catal., B* **2010**, *99*, 43–57.
- (57) Palo, D. R.; Dagle, R. A.; Holladay, J. D. Methanol Steam Reforming for Hydrogen Production. *Chem. Rev.* **2007**, *107*, 3992–4021.
- (58) Mateos-Pedrero, C.; Silva, H.; Pacheco Tanaka, D. A.; Liguori, S.; Iulianelli, A.; Basile, A.; Mendes, A. CuO/ZnO catalysts for methanol steam reforming: The role of the support polarity ratio and surface area. *Appl. Catal., B* **2015**, *174–175*, 67–76.
- (59) Toyir, J.; Ramírez de la Piscina, P.; Homs, N. Ga-promoted copper-based catalysts highly selective for methanol steam reforming to hydrogen; relation with the hydrogenation of CO₂ to methanol. *Int. J. Hydrogen Energy* **2015**, *40*, 11261–11266.
- (60) Lytkina, A. A.; Zhilyaeva, N. A.; Ermilova, M. M.; Orekhova, N. V.; Yaroslavtsev, A. B. Influence of the support structure and composition of Ni–Cu-based catalysts on hydrogen production by methanol steam reforming. *Int. J. Hydrogen Energy* **2015**, *40*, 9677–9684.
- (61) Barrios, C. E.; Bosco, M. V.; Baltanás, M. A.; Bonivardi, A. L. Hydrogen production by methanol steam reforming: Catalytic performance of supported-Pd on zinc–cerium oxides’ nanocomposites. *Appl. Catal., B* **2015**, *179*, 262–275.
- (62) Zhang, H.; Sun, J.; Dagle, V. L.; Halevi, B.; Datye, A. K.; Wang, Y. Influence of ZnO Facets on Pd/ZnO Catalysts for Methanol Steam Reforming. *ACS Catal.* **2014**, *4*, 2379–2386.
- (63) Wichert, M.; Zapf, R.; Ziogas, A.; Kolb, G.; Klemm, E. Kinetic investigations of the steam reforming of methanol over a Pt/In₂O₃/Al₂O₃ catalyst in microchannels. *Chem. Eng. Sci.* **2016**, *155*, 201–209.
- (64) Gu, X.-K.; Qiao, B.; Huang, C.-Q.; Ding, W.-C.; Sun, K.; Zhan, E.; Zhang, T.; Liu, J.; Li, W.-X. Supported Single Pt₁/Au₁ Atoms for Methanol Steam Reforming. *ACS Catal.* **2014**, *4*, 3886–3890.
- (65) Kuld, S.; Thorhauge, M.; Falsig, H.; Elkjær, C. F.; Helveg, S.; Chorkendorff, I.; Sehested, J. Quantifying the promotion of Cu catalysts by ZnO for methanol synthesis. *Science* **2016**, *352*, 969–974.
- (66) van den Berg, R.; Prieto, G.; Korpershoek, G.; van der Wal, L. I.; van Bunningen, A. J.; Laegsgaard-Jorgensen, S.; de Jongh, P. E.; de Jong, K. P. Structure sensitivity of Cu and CuZn catalysts relevant to industrial methanol synthesis. *Nat. Commun.* **2016**, *7*, 13057.
- (67) Behrens, M.; Studt, F.; Kasatkina, I.; Kühl, S.; Hävecker, M.; Abild-Pedersen, F.; Zander, S.; Grgsdić, F.; Kurr, P.; Kniep, B.-L.; Tovar, M.; Fischer, R. W.; Nørskov, J. K.; Schlögl, R. The Active Site of Methanol Synthesis over Cu/ZnO/Al₂O₃ Industrial Catalysts. *Science* **2012**, *336*, 893–897.
- (68) Sun, Q.; Xie, Z.; Yu, J. The state-of-the-art synthetic strategies for SAPO-34 zeolite catalysts in methanol-to-olefin conversion. *Nat. Sci. Rev.* **2018**, *5*, 542–558.
- (69) Regalbuto, J. R. Cellulosic Biofuels—Got Gasoline? *Science* **2009**, *325*, 822–824.
- (70) Jiao, F.; Li, J.; Pan, X.; Xiao, J.; Li, H.; Ma, H.; Wei, M.; Pan, Y.; Zhou, Z.; Li, M.; Miao, S.; Li, J.; Zhu, Y.; Xiao, D.; He, T.; Yang, J.; Qi, F.; Fu, Q.; Bao, X. Selective conversion of syngas to light olefins. *Science* **2016**, *351*, 1065–1068.
- (71) Dry, M. E. The Fischer–Tropsch process: 1950–2000. *Catal. Today* **2002**, *71*, 227–241.
- (72) Marin, R. P.; Kondrat, S. A.; Gallagher, J. R.; Enache, D. I.; Smith, P.; Boldrin, P.; Davies, T. E.; Bartley, J. K.; Combes, G. B.; Williams, P. B.; Taylor, S. H.; Claridge, J. B.; Rosseinsky, M. J.; Hutchings, G. J. Preparation of Fischer–Tropsch Supported Cobalt Catalysts Using a New Gas Anti-Solvent Process. *ACS Catal.* **2013**, *3*, 764–772.
- (73) Liu, Z.-W.; Li, X.; Asami, K.; Fujimoto, K. High performance Pd/beta catalyst for the production of gasoline-range iso-paraffins via a modified Fischer–Tropsch reaction. *Appl. Catal., A* **2006**, *300*, 162–169.
- (74) Li, C.; Xu, H.; Kido, Y.; Yoneyama, Y.; Suehiro, Y.; Tsubaki, N. A capsule catalyst with a zeolite membrane prepared by direct liquid membrane crystallization. *ChemSusChem* **2012**, *5*, 862–866.
- (75) Subramanian, V.; Cheng, K.; Lancelot, C.; Heyte, S.; Paul, S.; Moldovan, S.; Ersen, O.; Marinova, M.; Ordovsky, V. V.; Khodakov, A. Y. Nanoreactors: An Efficient Tool To Control the Chain-Length Distribution in Fischer–Tropsch Synthesis. *ACS Catal.* **2016**, *6*, 1785–1792.
- (76) Kang, J.; Wang, X.; Peng, X.; Yang, Y.; Cheng, K.; Zhang, Q.; Wang, Y. Mesoporous Zeolite Y-Supported Co Nanoparticles as Efficient Fischer–Tropsch Catalysts for Selective Synthesis of Diesel Fuel. *Ind. Eng. Chem. Res.* **2016**, *55*, 13008–13019.
- (77) Kang, J.; Cheng, K.; Zhang, L.; Zhang, Q.; Ding, J.; Hua, W.; Lou, Y.; Zhai, Q.; Wang, Y. Mesoporous zeolite-supported ruthenium nanoparticles as highly selective Fischer–Tropsch catalysts for the production of C5–C11 isoparaffins. *Angew. Chem., Int. Ed.* **2011**, *50*, 5200–5203.
- (78) Cheng, K.; Kang, J.; Huang, S.; You, Z.; Zhang, Q.; Ding, J.; Hua, W.; Lou, Y.; Deng, W.; Wang, Y. Mesoporous Beta Zeolite-Supported Ruthenium Nanoparticles for Selective Conversion of Synthesis Gas to C5–C11 Isoparaffins. *ACS Catal.* **2012**, *2*, 441–449.
- (79) Cheng, K.; Zhang, L.; Kang, J.; Peng, X.; Zhang, Q.; Wang, Y. Selective transformation of syngas into gasoline-range hydrocarbons over mesoporous H-ZSM-5-supported cobalt nanoparticles. *Chem. - Eur. J.* **2015**, *21*, 1928–1937.
- (80) Cheng, Q.; Tian, Y.; Lyu, S.; Zhao, N.; Ma, K.; Ding, T.; Jiang, Z.; Wang, L.; Zhang, J.; Zheng, L.; Gao, F.; Dong, L.; Tsubaki, N.; Li, X. Confined small-sized cobalt catalysts stimulate carbon-chain growth reversely by modifying ASF law of Fischer–Tropsch synthesis. *Nat. Commun.* **2018**, *9*, 3250.
- (81) Bezemer, G. L.; Bitter, J. H.; Kuipers, H. P. C. E.; Oosterbeek, H.; Holewijn, J. E.; Xu, X.; Kapteijn, F.; van Dillen, A. J.; de Jong, K. P. Cobalt Particle Size Effects in the Fischer–Tropsch Reaction

- Studied with Carbon Nanofiber Supported Catalysts. *J. Am. Chem. Soc.* **2006**, *128*, 3956–3964.
- (82) den Breejen, J. P.; Radstake, P. B.; Bezemer, G. L.; Bitter, J. H.; Frøseth, V.; Holmen, A.; de Jong, K. P. On the Origin of the Cobalt Particle Size Effects in Fischer–Tropsch Catalysis. *J. Am. Chem. Soc.* **2009**, *131*, 7197–7203.
- (83) Li, J.; He, Y.; Tan, L.; Zhang, P.; Peng, X.; Oruganti, A.; Yang, G.; Abe, H.; Wang, Y.; Tsubaki, N. Integrated tuneable synthesis of liquid fuels via Fischer–Tropsch technology. *Nat. Catal.* **2018**, *1*, 787–793.
- (84) Abello, S.; Montane, D. Exploring iron-based multifunctional catalysts for Fischer–Tropsch synthesis: a review. *ChemSusChem* **2011**, *4*, 1538–56.
- (85) Sun, B.; Xu, K.; Nguyen, L.; Qiao, M.; Tao, F. F. Preparation and Catalysis of Carbon-Supported Iron Catalysts for Fischer–Tropsch Synthesis. *ChemCatChem* **2012**, *4*, 1498–1511.
- (86) de Smit, E.; Weckhuysen, B. M. The renaissance of iron-based Fischer–Tropsch synthesis: on the multifaceted catalyst deactivation behaviour. *Chem. Soc. Rev.* **2008**, *37*, 2758–2781.
- (87) Pendyala, V. R. R.; Graham, U. M.; Jacobs, G.; Hamdeh, H. H.; Davis, B. H. Fischer–Tropsch Synthesis: Morphology, Phase Transformation, and Carbon-Layer Growth of Iron-Based Catalysts. *ChemCatChem* **2014**, *6*, 1952–1960.
- (88) Büssemeier, B.; Frohning, C. D.; G. Horn, W. K. Process for the manufacture of unsaturated hydrocarbons. U.S. Patent No. 4564642 1986.
- (89) Shroff, M. D.; Kalakkad, D. S.; Coulter, K. E.; Kohler, S. D.; Harrington, M. S.; Jackson, N. B.; Sault, A. G.; Datye, A. K. Activation of precipitated iron Fischer–Tropsch synthesis catalysts. *J. Catal.* **1995**, *156*, 185–207.
- (90) Keyvanloo, K.; Mardkhe, M. K.; Alam, T. M.; Bartholomew, C. H.; Woodfield, B. F.; Hecker, W. C. Supported Iron Fischer–Tropsch Catalyst: Superior Activity and Stability Using a Thermally Stable Silica-Doped Alumina Support. *ACS Catal.* **2014**, *4*, 1071–1077.
- (91) Torres Galvis, H. M.; Bitter, J. H.; Khare, C. B.; Ruitenberg, M.; Dugulan, A. I.; de Jong, K. P. Supported Iron Nanoparticles as Catalysts for Sustainable Production of Lower Olefins. *Science* **2012**, *335*, 835–838.
- (92) Kang, S.-H.; Bae, J. W.; Woo, K.-J.; Sai Prasad, P. S.; Jun, K.-W. ZSM-5 supported iron catalysts for Fischer–Tropsch production of light olefin. *Fuel Process. Technol.* **2010**, *91*, 399–403.
- (93) Park, J.-Y.; Lee, Y.-J.; Khanna, P. K.; Jun, K.-W.; Bae, J. W.; Kim, Y. H. Alumina-supported iron oxide nanoparticles as Fischer–Tropsch catalysts: Effect of particle size of iron oxide. *J. Mol. Catal. A: Chem.* **2010**, *323*, 84–90.
- (94) Torres Galvis, H. M.; Bitter, J. H.; Davidian, T.; Ruitenberg, M.; Dugulan, A. I.; de Jong, K. P. Iron particle size effects for direct production of lower olefins from synthesis gas. *J. Am. Chem. Soc.* **2012**, *134*, 16207–15.
- (95) Santos, V. P.; Wezendonk, T. A.; Jaen, J. J.; Dugulan, A. I.; Nasalevich, M. A.; Islam, H. U.; Chojecki, A.; Sartipi, S.; Sun, X.; Hakeem, A. A.; Koeken, A. C.; Ruitenberg, M.; Davidian, T.; Meima, G. R.; Sankar, G.; Kapteijn, F.; Makkee, M.; Gascon, J. Metal organic framework-mediated synthesis of highly active and stable Fischer–Tropsch catalysts. *Nat. Commun.* **2015**, *6*, 6451.
- (96) Torres Galvis, H. M.; de Jong, K. P. Catalysts for Production of Lower Olefins from Synthesis Gas: A Review. *ACS Catal.* **2013**, *3*, 2130–2149.
- (97) Yang, Z.; Guo, S.; Pan, X.; Wang, J.; Bao, X. FeN nanoparticles confined in carbon nanotubes for CO hydrogenation. *Energy Environ. Sci.* **2011**, *4*, 4500.
- (98) Zecevic, J.; Vanbutsele, G.; de Jong, K. P.; Martens, J. A. Nanoscale intimacy in bifunctional catalysts for selective conversion of hydrocarbons. *Nature* **2015**, *528*, 245–248.
- (99) Jiao, F.; Pan, X.; Gong, K.; Chen, Y.; Li, G.; Bao, X. Shape-Selective Zeolites Promote Ethylene Formation from Syngas via a Ketene Intermediate. *Angew. Chem., Int. Ed.* **2018**, *57*, 4692–4696.
- (100) Yang, X.; Su, X.; Liang, B.; Zhang, Y.; Duan, H.; Ma, J.; Huang, Y.; Zhang, T. The influence of alkali-treated zeolite on the oxide–zeolite syngas conversion process. *Catal. Sci. Technol.* **2018**, *8*, 4338–4348.
- (101) Yang, J.; Pan, X.; Jiao, F.; Li, J.; Bao, X. Direct conversion of syngas to aromatics. *Chem. Commun.* **2017**, *53*, 11146–11149.
- (102) Cheng, K.; Gu, B.; Liu, X.; Kang, J.; Zhang, Q.; Wang, Y. Direct and Highly Selective Conversion of Synthesis Gas into Lower Olefins: Design of a Bifunctional Catalyst Combining Methanol Synthesis and Carbon–Carbon Coupling. *Angew. Chem., Int. Ed.* **2016**, *55*, 4725–4728.
- (103) Cheng, J.; Hu, P.; Ellis, P.; French, S.; Kelly, G.; Lok, C. M. Density Functional Theory Study of Iron and Cobalt Carbides for Fischer–Tropsch Synthesis. *J. Phys. Chem. C* **2010**, *114*, 1085–1093.
- (104) Claeys, M.; Dry, M. E.; van Steen, E.; du Plessis, E.; van Berge, P. J.; Saib, A. M.; Moodley, D. J. In situ magnetometer study on the formation and stability of cobalt carbide in Fischer–Tropsch synthesis. *J. Catal.* **2014**, *318*, 193–202.
- (105) Karaca, H.; Safanova, O. V.; Chambrey, S.; Fongarland, P.; Roussel, P.; Griboval-Constant, A.; Lacroix, M.; Khodakov, A. Y. Structure and catalytic performance of Pt-promoted alumina-supported cobalt catalysts under realistic conditions of Fischer–Tropsch synthesis. *J. Catal.* **2011**, *277*, 14–26.
- (106) Kwak, G.; Woo, M. H.; Kang, S. C.; Park, H.-G.; Lee, Y.-J.; Jun, K.-W.; Ha, K.-S. In situ monitoring during the transition of cobalt carbide to metal state and its application as Fischer–Tropsch catalyst in slurry phase. *J. Catal.* **2013**, *307*, 27–36.
- (107) Zhong, L.; Yu, F.; An, Y.; Zhao, Y.; Sun, Y.; Li, Z.; Lin, T.; Lin, Y.; Qi, X.; Dai, Y.; Gu, L.; Hu, J.; Jin, S.; Shen, Q.; Wang, H. Cobalt carbide nanoprisms for direct production of lower olefins from syngas. *Nature* **2016**, *538*, 84–87.
- (108) Barrault, J.; Forquy, C.; Menezo, J. C.; Maurel, R. Selective hydrocondensation of CO to light olefins with alumina-supported iron catalysts. *React. Kinet. Catal. Lett.* **1980**, *15*, 153–158.
- (109) Koeken, A. C.; Torres Galvis, H. M.; Davidian, T.; Ruitenberg, M.; de Jong, K. P. Suppression of carbon deposition in the iron-catalyzed production of lower olefins from synthesis gas. *Angew. Chem., Int. Ed.* **2012**, *51*, 7190–7193.
- (110) Gupta, M.; Smith, M. L.; Spivey, J. J. Heterogeneous Catalytic Conversion of Dry Syngas to Ethanol and Higher Alcohols on Cu-Based Catalysts. *ACS Catal.* **2011**, *1*, 641–656.
- (111) Pan, X.; Fan, Z.; Chen, W.; Ding, Y.; Luo, H.; Bao, X. Enhanced ethanol production inside carbon-nanotube reactors containing catalytic particles. *Nat. Mater.* **2007**, *6*, 507–11.
- (112) Spivey, J. J.; Egbebi, A. Heterogeneous catalytic synthesis of ethanol from biomass-derived syngas. *Chem. Soc. Rev.* **2007**, *36*, 1514–28.
- (113) Ao, M.; Pham, G. H.; Sunarso, J.; Tade, M. O.; Liu, S. Active Centers of Catalysts for Higher Alcohol Synthesis from Syngas: A Review. *ACS Catal.* **2018**, *8*, 7025–7050.
- (114) Zhao, Z.; Lu, W.; Yang, R.; Zhu, H.; Dong, W.; Sun, F.; Jiang, Z.; Lyu, Y.; Liu, T.; Du, H.; Ding, Y. Insight into the Formation of Co@Co₂C Catalysts for Direct Synthesis of Higher Alcohols and Olefins from Syngas. *ACS Catal.* **2018**, *8*, 228–241.
- (115) Yang, Y.; Lin, T.; Qi, X.; Yu, F.; An, Y.; Li, Z.; Dai, Y.; Zhong, L.; Wang, H.; Sun, Y. Direct synthesis of long-chain alcohols from syngas over CoMn catalysts. *Appl. Catal., A* **2018**, *S49*, 179–187.
- (116) Nguyen, T. T.; Zahedi-Niaki, M. H.; Alamdar, H.; Kaliaguine, S. Co–Cu Metal Alloys from LaCo_{1-x}Cu_xO₃ Perovskites as Catalysts for Higher Alcohol Synthesis from Syngas. *Int. J. Chem. React. Eng.* **2007**, *5*, ArticleA82.
- (117) Thao, N. T. Synthesis of Co–Cu/La₂O₃ Pervoskites for Hydrogenation of CO. *Asian J. Chem.* **2013**, *25*, 8082–8086.
- (118) Xiang, Y.; Barbosa, R.; Kruse, N. Higher Alcohols through CO Hydrogenation over CoCu Catalysts: Influence of Precursor Activation. *ACS Catal.* **2014**, *4*, 2792–2800.
- (119) Zhang, H. B.; Dong, X.; Lin, G. D.; Liang, X. L.; Li, H. Y. Carbon nanotube-promoted Co–Cu catalyst for highly efficient synthesis of higher alcohols from syngas. *Chem. Commun. (Cambridge, U. K.)* **2005**, 5094–5096.

- (120) Wu, X.-M.; Guo, Y.-Y.; Zhou, J.-M.; Lin, G.-D.; Dong, X.; Zhang, H.-B. Co-decorated carbon nanotubes as a promoter of Co-Mo-K oxide catalyst for synthesis of higher alcohols from syngas. *Appl. Catal., A* **2008**, *340*, 87–97.
- (121) Bao, J.; Fu, Y.-L.; Bian, G.-Z. Sol-gel Preparation of K-Co-Mo Catalyst and its Application in Mixed Alcohol Synthesis from CO Hydrogenation. *Catal. Lett.* **2008**, *121*, 151–157.
- (122) Lv, M.; Xie, W.; Sun, S.; Wu, G.; Zheng, L.; Chu, S.; Gao, C.; Bao, J. Activated-carbon-supported K-Co-Mo catalysts for synthesis of higher alcohols from syngas. *Catal. Sci. Technol.* **2015**, *5*, 2925–2934.
- (123) Bao, J.; Fu, Y.; Sun, Z.; Gao, C. A highly active K-Co-Mo/C catalyst for mixed alcohol synthesis from CO + H₂. *Chem. Commun.* **2003**, *746*–747.
- (124) Prieto, G.; Beijer, S.; Smith, M. L.; He, M.; Au, Y.; Wang, Z.; Bruce, D. A.; de Jong, K. P.; Spivey, J. J.; de Jongh, P. E. Design and synthesis of copper-cobalt catalysts for the selective conversion of synthesis gas to ethanol and higher alcohols. *Angew. Chem., Int. Ed.* **2014**, *53*, 6397–6401.
- (125) Xiang, Y.; Kruse, N. Tuning the catalytic CO hydrogenation to straight- and long-chain aldehydes/alcohols and olefins/paraffins. *Nat. Commun.* **2016**, *7*, 13058.
- (126) Surisetty, V. R.; Dalai, A. K.; Kozinski, J. Alkali-Promoted Trimetallic Co-Rh-Mo Sulfide Catalysts for Higher Alcohols Synthesis from Synthesis Gas: Comparison of MWCNT and Activated Carbon Supports. *Ind. Eng. Chem. Res.* **2010**, *49*, 6956–6963.
- (127) Wang, P.; Zhang, J.; Bai, Y.; Xiao, H.; Tian, S.; Xie, H.; Yang, G.; Tsubaki, N.; Han, Y.; Tan, Y. Ternary copper–cobalt–cerium catalyst for the production of ethanol and higher alcohols through CO hydrogenation. *Appl. Catal., A* **2016**, *514*, 14–23.
- (128) Guo, H.; Zhang, H.; Peng, F.; Yang, H.; Xiong, L.; Wang, C.; Huang, C.; Chen, X.; Ma, L. Effects of Cu/Fe ratio on structure and performance of attapulgite supported CuFeCo-based catalyst for mixed alcohols synthesis from syngas. *Appl. Catal., A* **2015**, *503*, 51–61.
- (129) Wang, P.; Bai, Y.; Xiao, H.; Tian, S.; Zhang, Z.; Wu, Y.; Xie, H.; Yang, G.; Han, Y.; Tan, Y. Effect of the dimensions of carbon nanotube channels on copper–cobalt–cerium catalysts for higher alcohols synthesis. *Catal. Commun.* **2016**, *75*, 92–97.
- (130) Yu, J.; Mao, D.; Han, L.; Guo, Q.; Lu, G. The effect of Fe on the catalytic performance of Rh–Mn–Li/SiO₂ catalyst: A DRIFTS study. *Catal. Commun.* **2012**, *27*, 1–4.
- (131) Surisetty, V. R.; Dalai, A. K.; Kozinski, J. Deactivation Studies of Alkali-Promoted Trimetallic Co-Rh-Mo Sulfide Catalysts for Higher Alcohols Synthesis from Synthesis Gas. *Energy Fuels* **2011**, *25*, 580–590.
- (132) Yu, J.; Mao, D.; Han, L.; Guo, Q.; Lu, G. Conversion of syngas to C₂₊ oxygenates over Rh-based/SiO₂ catalyst: The promoting effect of Fe. *J. Ind. Eng. Chem.* **2013**, *19*, 806–812.
- (133) Boahene, P. E.; Surisetty, V. R.; Sammynaiken, R.; Dalai, A. K. Higher Alcohol Synthesis Using K-Doped CoRhMoS₂/MWCNT Catalysts: Influence of Pelletization, Particle Size and Incorporation of Binders. *Top. Catal.* **2014**, *57*, 538–549.
- (134) Xiang, Y.; Barbosa, R.; Li, X.; Kruse, N. Ternary Cobalt–Copper–Niobium Catalysts for the Selective CO Hydrogenation to Higher Alcohols. *ACS Catal.* **2015**, *5*, 2929–2934.
- (135) Suárez París, R.; Boutonnet, M.; Järås, S. Effect of methanol addition on higher alcohol synthesis over modified molybdenum sulfide catalysts. *Catal. Commun.* **2015**, *67*, 103–107.
- (136) Tavasoli, A.; Karimi, S.; Davari, M.; Nasrollahi, N.; Nematian, T. Enhancement of MoO₃–K₂O/CNTs nanocatalyst activity and selectivity in higher alcohols synthesis using microemulsion technique. *J. Ind. Eng. Chem.* **2014**, *20*, 674–681.
- (137) Xie, W.; Zhou, J.; Ji, L.; Sun, S.; Pan, H.; Zhu, J.; Gao, C.; Bao, J. Targeted design and synthesis of a highly selective Mo-based catalyst for the synthesis of higher alcohols. *RSC Adv.* **2016**, *6*, 38741–38745.
- (138) Zhou, W.; Kang, J.; Cheng, K.; He, S.; Shi, J.; Zhou, C.; Zhang, Q.; Chen, J.; Peng, L.; Chen, M.; Wang, Y. Direct Conversion of Syngas into Methyl Acetate, Ethanol, and Ethylene by Relay Catalysis via the Intermediate Dimethyl Ether. *Angew. Chem., Int. Ed.* **2018**, *57*, 12012–12016.
- (139) Che, F.; Gray, J. T.; Ha, S.; McEwen, J.-S. Improving Ni Catalysts Using Electric Fields: A DFT and Experimental Study of the Methane Steam Reforming Reaction. *ACS Catal.* **2017**, *7*, 551–562.
- (140) Ray, K.; Sengupta, S.; Deo, G. Reforming and cracking of CH₄ over Al₂O₃ supported Ni, Ni-Fe and Ni-Co catalysts. *Fuel Process. Technol.* **2017**, *156*, 195–203.
- (141) Sehested, J. Four challenges for nickel steam-reforming catalysts. *Catal. Today* **2006**, *111*, 103–110.
- (142) Sehested, J. Sintering of nickel steam-reforming catalysts. *J. Catal.* **2003**, *217*, 417–426.
- (143) Gharibi, M.; Zangeneh, F. T.; Yaripour, F.; Sahebdelfar, S. Nanocatalysts for conversion of natural gas to liquid fuels and petrochemical feedstocks. *Appl. Catal., A* **2012**, *443*–444, 8–26.
- (144) Li, Z.; Mo, L.; Kathiraser, Y.; Kawi, S. Yolk–Satellite–Shell Structured Ni–Yolk@Ni@SiO₂ Nanocomposite: Superb Catalyst toward Methane CO₂ Reforming Reaction. *ACS Catal.* **2014**, *4*, 1526–1536.
- (145) Balasubramanian, B.; Ortiz, A. L.; Kaytakoglu, S.; Harrison, D. P. Hydrogen from methane in a single-step process. *Chem. Eng. Sci.* **1999**, *54*, 3543–3552.
- (146) Broda, M.; Kierzkowska, A. M.; Baudouin, D.; Imtiaz, Q.; Copéret, C.; Müller, C. R. Sorbent-Enhanced Methane Reforming over a Ni–Ca-Based, Bifunctional Catalyst Sorbent. *ACS Catal.* **2012**, *2*, 1635–1646.
- (147) Buelens, L. C.; Galvita, V. V.; Poelman, H.; Detavernier, C.; Marin, G. B. Super-dry reforming of methane intensifies CO₂ utilization via Le Chatelier’s principle. *Science* **2016**, *354*, 449.
- (148) Fan, M.-S.; Abdullah, A. Z.; Bhatia, S. Catalytic Technology for Carbon Dioxide Reforming of Methane to Synthesis Gas. *ChemCatChem* **2009**, *1*, 192–208.
- (149) Luo, S.; Zeng, L.; Xu, D.; Kathe, M.; Chung, E.; Deshpande, N.; Qin, L.; Majumder, A.; Hsieh, T.-L.; Tong, A.; Sun, Z.; Fan, L.-S. Shale gas-to-syngas chemical looping process for stable shale gas conversion to high purity syngas with a H₂ : CO ratio of 2 : 1. *Energy Environ. Sci.* **2014**, *7*, 4104–4117.
- (150) Rostrup-Nielsen, J.; Christiansen, L. *Concepts in Syngas Manufacture*; Imperial College Press: London, 2011.
- (151) Olah, G. A.; Goepert, A.; Czaun, M.; Mathew, T.; May, R. B.; Prakash, G. K. S. Single Step Bi-reforming and Oxidative Bi-reforming of Methane (Natural Gas) with Steam and Carbon Dioxide to Metgas (CO-2H₂) for Methanol Synthesis: Self-Sufficient Effective and Exclusive Oxygenation of Methane to Methanol with Oxygen. *J. Am. Chem. Soc.* **2015**, *137*, 8720–8729.
- (152) Yan, Q. Partial oxidation of methane to H₂ and CO over Rh/SiO₂ and Ru/SiO₂ catalysts. *J. Catal.* **2004**, *226*, 247–259.
- (153) Choudhary, T. V.; Choudhary, V. R. Energy-efficient syngas production through catalytic oxy-methane reforming reactions. *Angew. Chem., Int. Ed.* **2008**, *47*, 1828–1847.
- (154) Fan, L.-S.; Zeng, L.; Wang, W.; Luo, S. Chemical looping processes for CO₂ capture and carbonaceous fuel conversion – prospect and opportunity. *Energy Environ. Sci.* **2012**, *5*, 7254–7280.
- (155) Neal, L. M.; Shafiefarhood, A.; Li, F. Dynamic Methane Partial Oxidation Using a Fe₂O₃@La_{0.8}Sr_{0.2}FeO_{3-δ} Core–Shell Redox Catalyst in the Absence of Gaseous Oxygen. *ACS Catal.* **2014**, *4*, 3560–3569.
- (156) Li, K.; Wang, H.; Wei, Y.; Yan, D. Syngas production from methane and air via a redox process using Ce–Fe mixed oxides as oxygen carriers. *Appl. Catal., B* **2010**, *97*, 361–372.
- (157) Mihai, O.; Chen, D.; Holmen, A. Chemical looping methane partial oxidation: The effect of the crystal size and O content of LaFeO₃. *J. Catal.* **2012**, *293*, 175–185.
- (158) Chen, S.; Zeng, L.; Tian, H.; Li, X.; Gong, J. Enhanced Lattice Oxygen Reactivity over Ni-Modified WO₃-Based Redox Catalysts for Chemical Looping Partial Oxidation of Methane. *ACS Catal.* **2017**, *7*, 3548–3559.

- (159) Choudhary, T. V.; Aksoyulu, E.; Wayne Goodman, D. Nonoxidative Activation of Methane. *Catal. Rev.: Sci. Eng.* **2003**, *45*, 151–203.
- (160) Abánades, A.; Ruiz, E.; Ferruelo, E. M.; Hernández, F.; Cabanillas, A.; Martínez-Val, J. M.; Rubio, J. A.; López, C.; Gavela, R.; Barrera, G.; Rubbia, C.; Salmieri, D.; Rodilla, E.; Gutiérrez, D. Experimental analysis of direct thermal methane cracking. *Int. J. Hydrogen Energy* **2011**, *36*, 12877–12886.
- (161) Abbas, H. F.; Wan Daud, W. M. A. Hydrogen production by methane decomposition: A review. *Int. J. Hydrogen Energy* **2010**, *35*, 1160–1190.
- (162) Wang, K.; Li, W. S.; Zhou, X. P. Hydrogen generation by direct decomposition of hydrocarbons over molten magnesium. *J. Mol. Catal. A: Chem.* **2008**, *283*, 153–157.
- (163) Upham, D. C.; Agarwal, V.; Khechfe, A.; Snodgrass, Z. R.; Gordon, M. J.; Metiu, H.; McFarland, E. W. Catalytic molten metals for the direct conversion of methane to hydrogen and separable carbon. *Science* **2017**, *358*, 917–921.
- (164) Podkolzin, S. G.; Stangland, E. E.; Jones, M. E.; Peringer, E.; Lercher, J. A. Methyl Chloride Production from Methane over Lanthanum-Based Catalysts. *J. Am. Chem. Soc.* **2007**, *129*, 2569–2576.
- (165) He, J.; Xu, T.; Wang, Z.; Zhang, Q.; Deng, W.; Wang, Y. Transformation of methane to propylene: a two-step reaction route catalyzed by modified CeO₂ nanocrystals and zeolites. *Angew. Chem., Int. Ed.* **2012**, *51*, 2438–2442.
- (166) Paunovic, V.; Zichittella, G.; Moser, M.; Amrute, A. P.; Perez-Ramirez, J. Catalyst design for natural-gas upgrading through oxybromination chemistry. *Nat. Chem.* **2016**, *8*, 803–809.
- (167) Liu, Z.; Huang, L.; Li, W. S.; Yang, F.; Au, C. T.; Zhou, X. P. Higher hydrocarbons from methane condensation mediated by HBr. *J. Mol. Catal. A: Chem.* **2007**, *273*, 14–20.
- (168) Wang, K. X.; Xu, H. F.; Li, W. S.; Au, C. T.; Zhou, X. P. The synthesis of acetic acid from methane via oxidative bromination, carbonylation, and hydrolysis. *Appl. Catal., A* **2006**, *304*, 168–177.
- (169) Guo, Z.; Liu, B.; Zhang, Q.; Deng, W.; Wang, Y.; Yang, Y. Recent advances in heterogeneous selective oxidation catalysis for sustainable chemistry. *Chem. Soc. Rev.* **2014**, *43*, 3480–3524.
- (170) Lin, R.; Ding, Y.; Gong, L.; Dong, W.; Wang, J.; Zhang, T. Efficient and stable silica-supported iron phosphate catalysts for oxidative bromination of methane. *J. Catal.* **2010**, *272*, 65–73.
- (171) Paunovic, V.; Zichittella, G.; Verel, R.; Amrute, A. P.; Perez-Ramirez, J. Selective Production of Carbon Monoxide via Methane Oxychlorination over Vanadyl Pyrophosphate. *Angew. Chem., Int. Ed.* **2016**, *55*, 15619–15623.
- (172) Gao, J.; Zheng, Y.; Jehng, J.-M.; Tang, Y.; Wachs, I. E.; Podkolzin, S. G. Identification of molybdenum oxide nanostructures on zeolites for natural gas conversion. *Science* **2015**, *348*, 686–691.
- (173) Tempelman, C. H. L.; Hensen, E. J. M. On the deactivation of Mo/HZSM-5 in the methane dehydroaromatization reaction. *Appl. Catal., B* **2015**, *176–177*, 731–739.
- (174) Xu, Y.; Bao, X.; Lin, L. Direct conversion of methane under nonoxidative conditions. *J. Catal.* **2003**, *216*, 386–395.
- (175) Guo, X.; Fang, G.; Li, G.; Ma, H.; Fan, H.; Yu, L.; Ma, C.; Wu, X.; Deng, D.; Wei, M.; Tan, D.; Si, R.; Zhang, S.; Li, J.; Sun, L.; Tang, Z.; Pan, X.; Bao, X. Direct, Nonoxidative Conversion of Methane to Ethylene, Aromatics, and Hydrogen. *Science* **2014**, *344*, 616–619.
- (176) Morejudo, S. H.; Zanón, R.; Escolástico, S.; Yuste-Tirados, I.; Malerod-Fjeld, H.; Vestre, P. K.; Coors, W. G.; Martínez, A.; Norby, T.; Serra, J. M.; Kjølseth, C. Direct conversion of methane to aromatics in a catalytic co-ionic membrane reactor. *Science* **2016**, *353*, 563–566.
- (177) National Energy Technology Laboratory (NETL). *Analysis of natural gas-to liquid transportation fuels via Fischer-Tropsch*. U.S. Department of Energy, DOE/NETL-2013/1597; NETL, 2013.
- (178) Farrell, B. L.; Linic, S. Oxidative coupling of methane over mixed oxide catalysts designed for solid oxide membrane reactors. *Catal. Sci. Technol.* **2016**, *6*, 4370–4376.
- (179) Czuprat, O.; Schiestel, T.; Voss, H.; Caro, J. r. Oxidative Coupling of Methane in a BCFZ Perovskite Hollow Fiber Membrane Reactor. *Ind. Eng. Chem. Res.* **2010**, *49*, 10230–10236.
- (180) Schwach, P.; Willinger, M. G.; Trunschke, A.; Schlogl, R. Methane Coupling over Magnesium Oxide: How Doping Can Work. *Angew. Chem., Int. Ed.* **2013**, *52*, 11381–11384.
- (181) Luo, L.; Tang, X.; Wang, W.; Wang, Y.; Sun, S.; Qi, F.; Huang, W. Methyl radicals in oxidative coupling of methane directly confirmed by synchrotron VUV photoionization mass spectroscopy. *Sci. Rep.* **2013**, *3*, 1625.
- (182) Farrell, B. L.; Igenegbai, V. O.; Linic, S. A Viewpoint on Direct Methane Conversion to Ethane and Ethylene Using Oxidative Coupling on Solid Catalysts. *ACS Catal.* **2016**, *6*, 4340–4346.
- (183) Hou, Y.-H.; Han, W.-C.; Xia, W.-S.; Wan, H.-L. Structure Sensitivity of La₂O₂CO₃ Catalysts in the Oxidative Coupling of Methane. *ACS Catal.* **2015**, *5*, 1663–1674.
- (184) Keller, G. E.; Bhasin, M. M. Synthesis of ethylene via oxidative coupling of methane: I. Determination of active catalysts. *J. Catal.* **1982**, *73*, 9–19.
- (185) Linstrom, P. J. M., W. G. (eds) *NIST Chemistry WebBook*; NIST Standard Reference Database Number 69 (National Institute of Standards and Technology, 2011). Available at <http://webbook.nist.gov>.
- (186) Stull, D. R.; Westrum, E. F.; Sinke, G. C. *The Chemical Thermodynamics of Organic Compounds*; Wiley, 1969; pp 243–244.
- (187) Zhu, Q.; Wegener, S. L.; Xie, C.; Uche, O.; Neurock, M.; Marks, T. J. Sulfur as a selective ‘soft’ oxidant for catalytic methane conversion probed by experiment and theory. *Nat. Chem.* **2013**, *5*, 104–109.
- (188) Peter, M.; Marks, T. J. Platinum Metal-Free Catalysts for Selective Soft Oxidative Methane→ Ethylene Coupling. Scope and Mechanistic Observations. *J. Am. Chem. Soc.* **2015**, *137*, 15234–15240.
- (189) Lieberman, R. L.; Rosenzweig, A. C. Crystal structure of a membrane-bound metalloenzyme that catalyses the biological oxidation of methane. *Nature* **2005**, *434*, 177–181.
- (190) Hakemian, A. S.; Rosenzweig, A. C. The biochemistry of methane oxidation. *Annu. Rev. Biochem.* **2007**, *76*, 223–41.
- (191) Balasubramanian, R.; Smith, S. M.; Rawat, S.; Yatsunyk, L. A.; Stemmler, T. L.; Rosenzweig, A. C. Oxidation of methane by a biological dicopper centre. *Nature* **2010**, *465*, 115–119.
- (192) Baik, M.-H.; Newcomb, M.; Friesner, R. A.; Lippard, S. J. Mechanistic Studies on the Hydroxylation of Methane by Methane Monoxygenase. *Chem. Rev.* **2003**, *103*, 2385–2419.
- (193) Bordeaux, M.; Galarneau, A.; Drone, J. Catalytic, mild, and selective oxyfunctionalization of linear alkanes: current challenges. *Angew. Chem., Int. Ed.* **2012**, *51*, 10712–10723.
- (194) Rosenzweig, A. C.; Frederick, C. A.; Lippard, S. J.; Nordlund, P. Crystal structure of a bacterial non-haem iron hydroxylase that catalyses the biological oxidation of methane. *Nature* **1993**, *366*, 537–543.
- (195) Hammond, C.; Conrad, S.; Hermans, I. Oxidative methane upgrading. *ChemSusChem* **2012**, *5*, 1668–1686.
- (196) Olivos-Suarez, A. I.; Szécsényi, Á.; Hensen, E. J. M.; Ruiz-Martinez, J.; Pidko, E. A.; Gascon, J. Strategies for the Direct Catalytic Valorization of Methane Using Heterogeneous Catalysis: Challenges and Opportunities. *ACS Catal.* **2016**, *6*, 2965–2981.
- (197) Grundner, S.; Markovits, M. A.; Li, G.; Tromp, M.; Pidko, E. A.; Hensen, E. J.; Jentys, A.; Sanchez-Sanchez, M.; Lercher, J. A. Single-site trinuclear copper oxygen clusters in mordenite for selective conversion of methane to methanol. *Nat. Commun.* **2015**, *6*, 7546.
- (198) Hammond, C.; Forde, M. M.; Ab Rahim, M. H.; Thetford, A.; He, Q.; Jenkins, R. L.; Dimitratos, N.; Lopez-Sánchez, J. A.; Dummer, N. F.; Murphy, D. M.; Carley, A. F.; Taylor, S. H.; Wilcock, D. J.; Stangland, E. E.; Kang, J.; Hagen, H.; Kiely, C. J.; Hutchings, G. J. Direct catalytic conversion of methane to methanol in an aqueous medium by using copper-promoted Fe-ZSM-5. *Angew. Chem., Int. Ed.* **2012**, *51*, 5129–33.

- (199) Ensing, B.; Buda, F.; Blöchl, P. E.; Baerends, E. J. A Car-Parrinello study of the formation of oxidizing intermediates from Fenton's reagent in aqueous solution. *Phys. Chem. Chem. Phys.* **2002**, *4*, 3619–3627.
- (200) Yuan, Q.; Deng, W.; Zhang, Q.; Wang, Y. Osmium-Catalyzed Selective Oxidations of Methane and Ethane with Hydrogen Peroxide in Aqueous Medium. *Adv. Synth. Catal.* **2007**, *349*, 1199–1209.
- (201) Knops-Gerrits, P. P.; Goddard, W. A., III Methane partial oxidation in iron zeolites: theory versus experiment. *J. Mol. Catal. A: Chem.* **2001**, *166*, 135–145.
- (202) Wood, B. Methanol formation on Fe/Al-MFI via the oxidation of methane by nitrous oxide. *J. Catal.* **2004**, *225*, 300–306.
- (203) Bosnjakovic, A.; Schlick, S. Spin Trapping by 5,5-Dimethylpyrroline-N-oxide in Fenton Media in the Presence of Nafion Perfluorinated Membranes: Limitations and Potential. *J. Phys. Chem. B* **2006**, *110*, 10720–10728.
- (204) Cui, X.; Li, H.; Wang, Y.; Hu, Y.; Hua, L.; Li, H.; Han, X.; Liu, Q.; Yang, F.; He, L.; Chen, X.; Li, Q.; Xiao, J.; Deng, D.; Bao, X. Room-Temperature Methane Conversion by Graphene-Confined Single Iron Atoms. *Chem.* **2018**, *4*, 1902–1910.
- (205) Agarwal, N.; Freakley, S. J.; McMicker, R. U.; Althahban, S. M.; Dimitratos, N.; He, Q.; Morgan, D. J.; Jenkins, R. L.; Willock, D. J.; Taylor, S. H.; Kiely, C. J.; Hutchings, G. J. Aqueous Au-Pd colloids catalyze selective CH₄ oxidation to CH₃OH with O₂ under mild conditions. *Science* **2017**, *358*, 223–227.
- (206) Sushkevich, V. L.; Palagin, D.; Ranocchiari, M.; van Bokhoven, J. A. Selective anaerobic oxidation of methane enables direct synthesis of methanol. *Science* **2017**, *356*, 523–527.
- (207) Tomkins, P.; Mansouri, A.; Bozbag, S. E.; Krumeich, F.; Park, M. B.; Alayon, E. M.; Ranocchiari, M.; van Bokhoven, J. A. Isothermal Cyclic Conversion of Methane into Methanol over Copper-Exchanged Zeolite at Low Temperature. *Angew. Chem., Int. Ed.* **2016**, *55*, 5467–5471.
- (208) Alayon, E. M.; Nachtegaal, M.; Ranocchiari, M.; van Bokhoven, J. A. Catalytic conversion of methane to methanol over Cu-mordenite. *Chem. Commun. (Cambridge, U. K.)* **2012**, *48*, 404–406.
- (209) Smeets, P. J.; Groothaert, M. H.; Schoonheydt, R. A. Cu based zeolites: A UV-vis study of the active site in the selective methane oxidation at low temperatures. *Catal. Today* **2005**, *110*, 303–309.
- (210) Vanelderen, P.; Vancauwenbergh, J.; Tsai, M. L.; Hadt, R. G.; Solomon, E. I.; Schoonheydt, R. A.; Sels, B. F. Spectroscopy and redox chemistry of copper in mordenite. *ChemPhysChem* **2014**, *15*, 91–99.
- (211) Okolie, C.; Belhseine, Y. F.; Lyu, Y.; Yung, M. M.; Engelhard, M. H.; Kovarik, L.; Stavitski, E.; Sievers, C. Conversion of Methane into Methanol and Ethanol over Nickel Oxide on Ceria-Zirconia Catalysts in a Single Reactor. *Angew. Chem., Int. Ed.* **2017**, *56*, 13876–13881.
- (212) Lin, M.; Hogan, T. E.; Sen, A. Catalytic Carbon-Carbon and Carbon-Hydrogen Bond Cleavage in Lower Alkanes. Low-Temperature Hydroxylations and Hydroxycarbonylations with Dioxygen as the Oxidant. *J. Am. Chem. Soc.* **1996**, *118*, 4574–4580.
- (213) Kinnunen, N. M.; Suvanto, M.; Moreno, M. A.; Savimäki, A.; Kallinen, K.; Kinnunen, T. J. J.; Pakkanen, T. A. Methane oxidation on alumina supported palladium catalysts: Effect of Pd precursor and solvent. *Appl. Catal., A* **2009**, *370*, 78–87.
- (214) Pelletier, J. D.; Basset, J. M. Catalysis by Design: Well-Defined Single-Site Heterogeneous Catalysts. *Acc. Chem. Res.* **2016**, *49*, 664–77.
- (215) Serna, P.; Gates, B. C. Molecular metal catalysts on supports: organometallic chemistry meets surface science. *Acc. Chem. Res.* **2014**, *47*, 2612–2620.
- (216) Shan, J.; Li, M.; Allard, L. F.; Lee, S.; Flytzani-Stephanopoulos, M. Mild oxidation of methane to methanol or acetic acid on supported isolated rhodium catalysts. *Nature* **2017**, *551*, 605–608.
- (217) Tang, Y.; Li, Y.; Fung, V.; Jiang, D. E.; Huang, W.; Zhang, S.; Iwasawa, Y.; Sakata, T.; Nguyen, L.; Zhang, X.; Frenkel, A. I.; Tao, F. F. Single rhodium atoms anchored in micropores for efficient transformation of methane under mild conditions. *Nat. Commun.* **2018**, *9*, 1231.
- (218) Panagiotopoulou, P. Hydrogenation of CO₂ over supported noble metal catalysts. *Appl. Catal., A* **2017**, *542*, 63–70.
- (219) Yang, X.; Kattel, S.; Senanayake, S. D.; Boscoboinik, J. A.; Nie, X.; Graciani, J.; Rodriguez, J. A.; Liu, P.; Stacchiola, D. J.; Chen, J. G. Low Pressure CO₂ Hydrogenation to Methanol over Gold Nanoparticles Activated on a CeO(x)/TiO₂ Interface. *J. Am. Chem. Soc.* **2015**, *137*, 10104–10107.
- (220) Bai, S.; Shao, Q.; Wang, P.; Dai, Q.; Wang, X.; Huang, X. Highly Active and Selective Hydrogenation of CO₂ to Ethanol by Ordered Pd-Cu Nanoparticles. *J. Am. Chem. Soc.* **2017**, *139*, 6827–6830.
- (221) Chen, C.-S.; Cheng, W.-H.; Lin, S.-S. Mechanism of CO formation in reverse water–gas shift reaction over Cu/Al₂O₃ catalyst. *Catal. Lett.* **2000**, *68*, 45–48.
- (222) Conner, W. C.; Falconer, J. L. Spillover in Heterogeneous Catalysis. *Chem. Rev.* **1995**, *95*, 759–788.
- (223) Porosoff, M. D.; Chen, J. G. Trends in the catalytic reduction of CO₂ by hydrogen over supported monometallic and bimetallic catalysts. *J. Catal.* **2013**, *301*, 30–37.
- (224) Marimuthu, A.; Zhang, J.; Linic, S. Tuning Selectivity in Propylene Epoxidation by Plasmon Mediated Photo-Switching of Cu Oxidation State. *Science* **2013**, *339*, 1590–1593.
- (225) Che, F.; Ha, S.; McEwen, J. S. Catalytic Reaction Rates Controlled by Metal Oxidation State: C-H Bond Cleavage in Methane over Nickel-Based Catalysts. *Angew. Chem., Int. Ed.* **2017**, *56*, 3557–3561.
- (226) Kattel, S.; Yu, W.; Yang, X.; Yan, B.; Huang, Y.; Wan, W.; Liu, P.; Chen, J. G. CO₂ Hydrogenation over Oxide-Supported PtCo Catalysts: The Role of the Oxide Support in Determining the Product Selectivity. *Angew. Chem., Int. Ed.* **2016**, *55*, 7968–7973.
- (227) Rodriguez, J. A.; Grinter, D. C.; Liu, Z.; Palomino, R. M.; Senanayake, S. D. Ceria-based model catalysts: fundamental studies on the importance of the metal-ceria interface in CO oxidation, the water-gas shift, CO₂ hydrogenation, and methane and alcohol reforming. *Chem. Soc. Rev.* **2017**, *46*, 1824–1841.
- (228) Li, S.; Xu, Y.; Chen, Y.; Li, W.; Lin, L.; Li, M.; Deng, Y.; Wang, X.; Ge, B.; Yang, C.; Yao, S.; Xie, J.; Li, Y.; Liu, X.; Ma, D. Tuning the Selectivity of Catalytic Carbon Dioxide Hydrogenation over Iridium/Cerium Oxide Catalysts with a Strong Metal-Support Interaction. *Angew. Chem., Int. Ed.* **2017**, *56*, 10761–10765.
- (229) Hwu, H. H.; Chen, J. G. Surface Chemistry of Transition Metal Carbides. *Chem. Rev.* **2005**, *105*, 185–212.
- (230) Kunkel, C.; Viñes, F.; Illas, F. Transition metal carbides as novel materials for CO₂ capture, storage, and activation. *Energy Environ. Sci.* **2016**, *9*, 141–144.
- (231) Viñes, F.; Rodriguez, J. A.; Liu, P.; Illas, F. Catalyst size matters: Tuning the molecular mechanism of the water–gas shift reaction on titanium carbide based compounds. *J. Catal.* **2008**, *260*, 103–112.
- (232) Liu, P.; Rodriguez, J. A. Effects of carbon on the stability and chemical performance of transition metal carbides: a density functional study. *J. Chem. Phys.* **2004**, *120*, 5414–5423.
- (233) Chen, J. G. Carbide and Nitride Overlays on Early Transition Metal Surfaces: Preparation, Characterization, and Reactivities. *Chem. Rev.* **1996**, *96*, 1477–1498.
- (234) Porosoff, M. D.; Kattel, S.; Li, W.; Liu, P.; Chen, J. G. Identifying trends and descriptors for selective CO₂ conversion to CO over transition metal carbides. *Chem. Commun. (Cambridge, U. K.)* **2015**, *51*, 6988–6991.
- (235) Zhang, X.; Zhu, X.; Lin, L.; Yao, S.; Zhang, M.; Liu, X.; Wang, X.; Li, Y.-W.; Shi, C.; Ma, D. Highly Dispersed Copper over β -Mo₂C as an Efficient and Stable Catalyst for the Reverse Water Gas Shift (RWGS) Reaction. *ACS Catal.* **2017**, *7*, 912–918.
- (236) Liu, X.; Kunkel, C.; Ramírez de la Piscina, P.; Homs, N.; Viñes, F.; Illas, F. Effective and Highly Selective CO Generation from CO₂ Using a Polycrystalline α -Mo₂C Catalyst. *ACS Catal.* **2017**, *7*, 4323–4335.

- (237) Porosoff, M. D.; Yang, X.; Boscoboinik, J. A.; Chen, J. G. Molybdenum Carbide as Alternative Catalysts to Precious Metals for Highly Selective Reduction of CO₂ to CO. *Angew. Chem., Int. Ed.* **2014**, *53*, 6705–6709.
- (238) Zhen, W.; Gao, F.; Tian, B.; Ding, P.; Deng, Y.; Li, Z.; Gao, H.; Lu, G. Enhancing activity for carbon dioxide methanation by encapsulating (1 1 1) facet Ni particle in metal–organic frameworks at low temperature. *J. Catal.* **2017**, *348*, 200–211.
- (239) Rodriguez, J. A.; Evans, J.; Feria, L.; Vidal, A. B.; Liu, P.; Nakamura, K.; Illas, F. CO₂ hydrogenation on Au/TiC, Cu/TiC, and Ni/TiC catalysts: Production of CO, methanol, and methane. *J. Catal.* **2013**, *307*, 162–169.
- (240) Martin, N. M.; Velin, P.; Skoglundh, M.; Bauer, M.; Carlsson, P.-A. Catalytic hydrogenation of CO₂ to methane over supported Pd, Rh and Ni catalysts. *Catal. Sci. Technol.* **2017**, *7*, 1086–1094.
- (241) Porosoff, M. D.; Yan, B.; Chen, J. G. Catalytic reduction of CO₂ by H₂ for synthesis of CO, methanol and hydrocarbons: challenges and opportunities. *Energy Environ. Sci.* **2016**, *9*, 62–73.
- (242) Melaet, G.; Ralston, W. T.; Li, C. S.; Alayoglu, S.; An, K.; Musselwhite, N.; Kalkan, B.; Somorjai, G. A. Evidence of highly active cobalt oxide catalyst for the Fischer–Tropsch synthesis and CO₂ hydrogenation. *J. Am. Chem. Soc.* **2014**, *136*, 2260–2263.
- (243) Beaumont, S. K.; Alayoglu, S.; Specht, C.; Kruse, N.; Somorjai, G. A. A nanoscale demonstration of hydrogen atom spillover and surface diffusion across silica using the kinetics of CO₂ methanation catalyzed on spatially separate Pt and Co nanoparticles. *Nano Lett.* **2014**, *14*, 4792–6.
- (244) Shin, H. H.; Lu, L.; Yang, Z.; Kiely, C. J.; McIntosh, S. Cobalt Catalysts Decorated with Platinum Atoms Supported on Barium Zirconate Provide Enhanced Activity and Selectivity for CO₂Methanation. *ACS Catal.* **2016**, *6*, 2811–2818.
- (245) Yan, Y.; Dai, Y.; He, H.; Yu, Y.; Yang, Y. A novel W-doped Ni-Mg mixed oxide catalyst for CO₂ methanation. *Appl. Catal., B* **2016**, *196*, 108–116.
- (246) Liu, J.; Bing, W.; Xue, X.; Wang, F.; Wang, B.; He, S.; Zhang, Y.; Wei, M. Alkaline-assisted Ni nanocatalysts with largely enhanced low-temperature activity toward CO₂ methanation. *Catal. Sci. Technol.* **2016**, *6*, 3976–3983.
- (247) Bette, N.; Thielemann, J.; Schreiner, M.; Mertens, F. Methanation of CO₂ over a (Mg,Al)Ox Supported Nickel Catalyst Derived from a (Ni,Mg,Al)-Hydrotalcite-like Precursor. *ChemCatChem* **2016**, *8*, 2903–2906.
- (248) Mutz, B.; Belimov, M.; Wang, W.; Sprenger, P.; Serrer, M.-A.; Wang, D.; Pfeifer, P.; Kleist, W.; Grunwaldt, J.-D. Potential of an Alumina-Supported Ni₃Fe Catalyst in the Methanation of CO₂: Impact of Alloy Formation on Activity and Stability. *ACS Catal.* **2017**, *7*, 6802–6814.
- (249) Wu, J.; Wen, C.; Zou, X.; Jimenez, J.; Sun, J.; Xia, Y.; Fonseca Rodrigues, M.-T.; Vinod, S.; Zhong, J.; Chopra, N.; Odeh, I. N.; Ding, G.; Lauterbach, J.; Ajayan, P. M. Carbon Dioxide Hydrogenation over a Metal-Free Carbon-Based Catalyst. *ACS Catal.* **2017**, *7*, 4497–4503.
- (250) Miao, B.; Ma, S. S. K.; Wang, X.; Su, H.; Chan, S. H. Catalysis mechanisms of CO₂ and CO methanation. *Catal. Sci. Technol.* **2016**, *6*, 4048–4058.
- (251) Peebles, D. E.; Goodman, D. W.; White, J. M. Methanation of Carbon Dioxide on Ni(100) and the Effects of Surface Modifiers. *J. Phys. Chem.* **1983**, *87*, 4378–4387.
- (252) Zhan, G.; Zeng, H. C. ZIF-67-Derived Nanoreactors for Controlling Product Selectivity in CO₂ Hydrogenation. *ACS Catal.* **2017**, *7*, 7509–7519.
- (253) Sakakura, T.; Choi, J.-C.; Yasuda, H. Transformation of Carbon Dioxide. *Chem. Rev.* **2007**, *107*, 2365–2387.
- (254) Montoya, J. H.; Peterson, A. A.; Nørskov, J. K. Insights into C–C Coupling in CO₂ Electroreduction on Copper Electrodes. *ChemCatChem* **2013**, *5*, 737–742.
- (255) Wang, W.; Wang, S.; Ma, X.; Gong, J. Recent advances in catalytic hydrogenation of carbon dioxide. *Chem. Soc. Rev.* **2011**, *40*, 3703–27.
- (256) Saeidi, S.; Amin, N. A. S.; Rahimpour, M. R. Hydrogenation of CO₂ to value-added products—A review and potential future developments. *J. CO₂ Util.* **2014**, *5*, 66–81.
- (257) Gnanamani, M. K.; Jacobs, G.; Hamdeh, H. H.; Shafer, W. D.; Liu, F.; Hopps, S. D.; Thomas, G. A.; Davis, B. H. Hydrogenation of Carbon Dioxide over Co–Fe Bimetallic Catalysts. *ACS Catal.* **2016**, *6*, 913–927.
- (258) Centi, G.; Quadrelli, E. A.; Perathoner, S. Catalysis for CO₂ conversion: a key technology for rapid introduction of renewable energy in the value chain of chemical industries. *Energy Environ. Sci.* **2013**, *6*, 1711–1731.
- (259) Kattel, S.; Ramirez, P. J.; Chen, J. G.; Rodriguez, J. A.; Liu, P. Active sites for CO₂ hydrogenation to methanol on Cu/ZnO catalysts. *Science* **2017**, *355*, 1296–1299.
- (260) Khan, M. U.; Wang, L.; Liu, Z.; Gao, Z.; Wang, S.; Li, H.; Zhang, W.; Wang, M.; Wang, Z.; Ma, C.; Zeng, J. Pt3 Co Octapods as Superior Catalysts of CO₂ Hydrogenation. *Angew. Chem., Int. Ed.* **2016**, *55*, 9548–9552.
- (261) Dorner, R. W.; Hardy, D. R.; Williams, F. W.; Willauer, H. D. Heterogeneous catalytic CO₂ conversion to value-added hydrocarbons. *Energy Environ. Sci.* **2010**, *3*, 884–890.
- (262) Dang, S.; Gao, P.; Liu, Z.; Chen, X.; Yang, C.; Wang, H.; Zhong, L.; Li, S.; Sun, Y. Role of zirconium in direct CO₂ hydrogenation to lower olefins on oxide/zeolite bifunctional catalysts. *J. Catal.* **2018**, *364*, 382–393.
- (263) Rungtaweevoranit, B.; Baek, J.; Araujo, J. R.; Archanjo, B. S.; Choi, K. M.; Yaghi, O. M.; Somorjai, G. A. Copper Nanocrystals Encapsulated in Zr-based Metal–Organic Frameworks for Highly Selective CO₂ Hydrogenation to Methanol. *Nano Lett.* **2016**, *16*, 7645–7649.
- (264) Wei, J.; Ge, Q.; Yao, R.; Wen, Z.; Fang, C.; Guo, L.; Xu, H.; Sun, J. Directly converting CO₂ into a gasoline fuel. *Nat. Commun.* **2017**, *8*, 15174.
- (265) Gao, P.; Li, S.; Bu, X.; Dang, S.; Liu, Z.; Wang, H.; Zhong, L.; Qiu, M.; Yang, C.; Cai, J.; Wei, W.; Sun, Y. Direct conversion of CO₂ into liquid fuels with high selectivity over a bifunctional catalyst. *Nat. Chem.* **2017**, *9*, 1019–1024.
- (266) Li, Z.; Wang, J.; Qu, Y.; Liu, H.; Tang, C.; Miao, S.; Feng, Z.; An, H.; Li, C. Highly Selective Conversion of Carbon Dioxide to Lower Olefins. *ACS Catal.* **2017**, *7*, 8544–8548.
- (267) Gao, P.; Dang, S.; Li, S.; Bu, X.; Liu, Z.; Qiu, M.; Yang, C.; Wang, H.; Zhong, L.; Han, Y.; Liu, Q.; Wei, W.; Sun, Y. Direct Production of Lower Olefins from CO₂ Conversion via Bifunctional Catalysis. *ACS Catal.* **2018**, *8*, 571–578.
- (268) Wang, J.; You, Z.; Zhang, Q.; Deng, W.; Wang, Y. Synthesis of lower olefins by hydrogenation of carbon dioxide over supported iron catalysts. *Catal. Today* **2013**, *215*, 186–193.
- (269) Sun, J.; Xu, H.; Liu, G.; Zhu, P.; Fan, R.; Yoneyama, Y.; Tsubaki, N. Green Synthesis of Rice Bran Microsphere Catalysts Containing Natural Biopromoters. *ChemCatChem* **2015**, *7*, 1642–1645.
- (270) Guo, L.; Sun, J.; Ji, X.; Wei, J.; Wen, Z.; Yao, R.; Xu, H.; Ge, Q. Directly converting carbon dioxide to linear α -olefins on bio-promoted catalysts. *Commun. Chem.* **2018**, *1*, 11.
- (271) Ni, Y.; Chen, Z.; Fu, Y.; Liu, Y.; Zhu, W.; Liu, Z. Selective conversion of CO₂ and H₂ into aromatics. *Nat. Commun.* **2018**, *9*, 3457.
- (272) Shi, L.; Yang, G.; Tao, K.; Yoneyama, Y.; Tan, Y.; Tsubaki, N. An Introduction of CO₂ Conversion by Dry Reforming with Methane and New Route of Low-Temperature Methanol Synthesis. *Acc. Chem. Res.* **2013**, *46*, 1838–1847.
- (273) Wang, L.; Yi, Y.; Wu, C.; Guo, H.; Tu, X. One-Step Reforming of CO₂ and CH₄ into High-Value Liquid Chemicals and Fuels at Room Temperature by Plasma-Driven Catalysis. *Angew. Chem., Int. Ed.* **2017**, *56*, 13679–13683.
- (274) Liao, F.; Huang, Y.; Ge, J.; Zheng, W.; Tedsree, K.; Collier, P.; Hong, X.; Tsang, S. C. Morphology-dependent interactions of ZnO with Cu nanoparticles at the materials' interface in selective

- hydrogenation of CO₂ to CH₃OH. *Angew. Chem., Int. Ed.* **2011**, *50*, 2162–2165.
- (275) Arena, F.; Mezzatesta, G.; Zafarana, G.; Trunfio, G.; Frusteri, F.; Spadaro, L. Effects of oxide carriers on surface functionality and process performance of the Cu–ZnO system in the synthesis of methanol via CO₂ hydrogenation. *J. Catal.* **2013**, *300*, 141–151.
- (276) Meunier, F. C. Mixing Copper Nanoparticles and ZnO Nanocrystals: A Route towards Understanding the Hydrogenation of CO₂ to Methanol? *Angew. Chem., Int. Ed.* **2011**, *50*, 4053–4054.
- (277) Graciani, J.; Mudiyanselage, K.; Xu, F.; Baber, A. E.; Evans, J.; Senanayake, S. D.; Stacchiola, D. J.; Liu, P.; Hrbek, J.; Sanz, J. F.; Rodriguez, J. A. Highly active copper-ceria and copper-ceria-titania catalysts for methanol synthesis from CO₂. *Science* **2014**, *345*, S46–S50.
- (278) Studt, F.; Sharafutdinov, I.; Abild-Pedersen, F.; Elkjaer, C. F.; Hummelshøj, J. S.; Dahl, S.; Chorkendorff, I.; Norskov, J. K. Discovery of a Ni-Ga catalyst for carbon dioxide reduction to methanol. *Nat. Chem.* **2014**, *6*, 320–324.
- (279) Wang, Z.-Q.; Xu, Z.-N.; Peng, S.-Y.; Zhang, M.-J.; Lu, G.; Chen, Q.-S.; Chen, Y.; Guo, G.-C. High-Performance and Long-Lived Cu/SiO₂ Nanocatalyst for CO₂ Hydrogenation. *ACS Catal.* **2015**, *5*, 4255–4259.
- (280) García-Trenco, A.; White, E. R.; Regoutz, A.; Payne, D. J.; Shaffer, M. S. P.; Williams, C. K. Pd₂Ga-Based Colloids as Highly Active Catalysts for the Hydrogenation of CO₂ to Methanol. *ACS Catal.* **2017**, *7*, 1186–1196.
- (281) Li, C.-S.; Melaet, G.; Ralston, W. T.; An, K.; Brooks, C.; Ye, Y.; Liu, Y.-S.; Zhu, J.; Guo, J.; Alayoglu, S.; Somorjai, G. A. High-performance hybrid oxide catalyst of manganese and cobalt for low-pressure methanol synthesis. *Nat. Commun.* **2015**, *6*, 6538.
- (282) Liu, C.; Yang, B.; Tyo, E.; Seifert, S.; DeBartolo, J.; von Issendorff, B.; Zapol, P.; Vajda, S.; Curtiss, L. A. Carbon Dioxide Conversion to Methanol over Size-Selected Cu₄ Clusters at Low Pressures. *J. Am. Chem. Soc.* **2015**, *137*, 8676–8679.
- (283) Qian, Q.; Cui, M.; He, Z.; Wu, C.; Zhu, Q.; Zhang, Z.; Ma, J.; Yang, G.; Zhang, J.; Han, B. Highly selective hydrogenation of CO₂ into C₂+ alcohols by homogeneous catalysis. *Chem. Sci.* **2015**, *6*, 5685–5689.
- (284) Cui, M.; Qian, Q.; He, Z.; Zhang, Z.; Ma, J.; Wu, T.; Yang, G.; Han, B. Bromide promoted hydrogenation of CO₂ to higher alcohols using Ru-Co homogeneous catalyst. *Chem. Sci.* **2016**, *7*, 5200–5205.
- (285) He, Z.; Qian, Q.; Ma, J.; Meng, Q.; Zhou, H.; Song, J.; Liu, Z.; Han, B. Water-Enhanced Synthesis of Higher Alcohols from CO₂ Hydrogenation over a Pt/Co₃O₄ Catalyst under Milder Conditions. *Angew. Chem., Int. Ed.* **2016**, *55*, 737–41.
- (286) Wang, H.; Zhou, W.; Liu, J. X.; Si, R.; Sun, G.; Zhong, M. Q.; Su, H. Y.; Zhao, H. B.; Rodriguez, J. A.; Pennycook, S. J.; Idrobo, J. C.; Li, W. X.; Kou, Y.; Ma, D. Platinum-modulated cobalt nanocatalysts for low-temperature aqueous-phase Fischer–Tropsch synthesis. *J. Am. Chem. Soc.* **2013**, *135*, 4149–4158.
- (287) Peng, X.; Cheng, K.; Kang, J.; Gu, B.; Yu, X.; Zhang, Q.; Wang, Y. Impact of Hydrogenolysis on the Selectivity of the Fischer–Tropsch Synthesis: Diesel Fuel Production over Mesoporous Zeolite-Y-Supported Cobalt Nanoparticles. *Angew. Chem., Int. Ed.* **2015**, *54*, 4553–4556.
- (288) Wang, L.; Wang, L.; Zhang, J.; Liu, X.; Wang, H.; Zhang, W.; Yang, Q.; Ma, J.; Dong, X.; Yoo, S. J.; Kim, J. G.; Meng, X.; Xiao, F. S. Selective Hydrogenation of CO₂ to Ethanol over Cobalt Catalysts. *Angew. Chem., Int. Ed.* **2018**, *57*, 6104–6108.
- (289) Oetjen, H.-F.; Schmidt, V. M.; Stimming, U.; Trila, F. Performance Data of a Proton Exchange Membrane Fuel Cell Using H₂/CO as Fuel Gas. *J. Electrochem. Soc.* **1996**, *143*, 3838–3842.
- (290) Wannek, C. In *Hydrogenenergy*; Stoltzen, D., Ed.; Wiley-VCH: Weinheim, 2010; pp 17–40.
- (291) Iwasa, N.; Mayanagi, T.; Ogawa, N.; Sakata, K.; Takezawa, N. New catalytic functions of Pd–Zn, Pd–Ga, Pd–In, Pt–Zn, Pt–Ga and Pt–In alloys in the conversions of methanol. *Catal. Lett.* **1998**, *54*, 119–123.
- (292) Shabaker, J. Aqueous-phase reforming of methanol and ethylene glycol over alumina-supported platinum catalysts. *J. Catal.* **2003**, *215*, 344–352.
- (293) Nielsen, M.; Alberico, E.; Baumann, W.; Drexler, H. J.; Junge, H.; Gladiali, S.; Beller, M. Low-temperature aqueous-phase methanol dehydrogenation to hydrogen and carbon dioxide. *Nature* **2013**, *495*, 85–89.
- (294) Denard, C. A.; Huang, H.; Bartlett, M. J.; Lu, L.; Tan, Y.; Zhao, H.; Hartwig, J. F. Cooperative tandem catalysis by an organometallic complex and a metalloenzyme. *Angew. Chem., Int. Ed.* **2014**, *53*, 465–469.
- (295) Gunanathan, C.; Milstein, D. Bond activation and catalysis by ruthenium pincer complexes. *Chem. Rev.* **2014**, *114*, 12024–12087.
- (296) Zhai, Y.; Pierre, D.; Si, R.; Deng, W.; Ferrin, P.; Nilekar, A. U.; Peng, G.; Herron, J. A.; Bell, D. C.; Saltsburg, H.; Mavrakakis, M.; Flytzani-Stephanopoulos, M. Alkali-Stabilized Pt-OH_x Species Catalyze Low-Temperature Water-Gas Shift Reactions. *Science* **2010**, *329*, 1633–1636.
- (297) Zhao, D.; Xu, B. Q. Enhancement of Pt utilization in electrocatalysts by using gold nanoparticles. *Angew. Chem., Int. Ed.* **2006**, *45*, 4955–4959.
- (298) Qiao, B.; Wang, A.; Yang, X.; Allard, L. F.; Jiang, Z.; Cui, Y.; Liu, J.; Li, J.; Zhang, T. Single-atom catalysis of CO oxidation using Pt₁/FeO_x. *Nat. Chem.* **2011**, *3*, 634–641.
- (299) Lin, L.; Zhou, W.; Gao, R.; Yao, S.; Zhang, X.; Xu, W.; Zheng, S.; Jiang, Z.; Yu, Q.; Li, Y. W.; Shi, C.; Wen, X. D.; Ma, D. Low-temperature hydrogen production from water and methanol using Pt/alpha-MoC catalysts. *Nature* **2017**, *544*, 80–83.
- (300) Kusche, M.; Enzenberger, F.; Bajus, S.; Niedermeyer, H.; Bosmann, A.; Kaftan, A.; Laurin, M.; Libuda, J.; Wasserscheid, P. Enhanced activity and selectivity in catalytic methanol steam reforming by basic alkali metal salt coatings. *Angew. Chem., Int. Ed.* **2013**, *52*, 5028–5032.
- (301) Yu, K. M.; Tong, W.; West, A.; Cheung, K.; Li, T.; Smith, G.; Guo, Y.; Tsang, S. C. Non-syngas direct steam reforming of methanol to hydrogen and carbon dioxide at low temperature. *Nat. Commun.* **2012**, *3*, 1230.
- (302) Xi, H.; Hou, X.; Liu, Y.; Qing, S.; Gao, Z. Cu-Al spinel oxide as an efficient catalyst for methanol steam reforming. *Angew. Chem., Int. Ed.* **2014**, *53*, 11886–11889.